Aus dem Institut für Klinische Neuroimmunologie

Institut der Ludwig-Maximilians-Universität München

Vorstand: Prof. Dr. Martin Kerschensteiner

The Role of Cytokine-producing B cells in Initiation and Regulation of EAE

Dissertation

zum Erwerb des Doktorgrades der Naturwissenschaften

an der Medizinischen Fakultät der

Ludwig-Maximilians-Universität zu München

vorgelegt von

Anna Sophie Thomann

aus

Ulm

2021

Mit Genehmigung der Medizinischen Fakultät

der Universität München

Betreuerin:	Dr. Anneli Peters
Zweitgutachterin:	Prof. Dr. Susanna Zierler
Dekan:	Prof. Dr. med. Thomas Gudermann
Tag der mündlichen Prüfung:	23.05.2022

“Above all, don’t fear difficult moments. The best comes from them”

Rita Levi-Montalcini (1909–2012)

Acknowledgments

First and foremost, I would like to thank my supervisor Dr. Anneli Peters for giving me the opportunity to do my PhD in her lab. Thank you, Anneli, for your advice, patience and support even during challenging times. Thank you for your guidance but also for the freedom to follow up on my own ideas and for letting this project be my own. I could not have chosen a better supervisor and I always enjoyed being part of your lab.

In addition, I would like to thank Prof. Reinhard Hohlfeld for being my official IMPRS mentor and for making it possible to meet Anneli and be part of this lab and institute.

I especially want to thank my TAC members Prof. Thomas Korn, Prof. Marc Schmidt-Supprian and Prof. Dirk Baumjohann for their time, support and valuable discussions.

I would like to thank Lisa Richter and Pardis Khosravani from the BMC Core Facility Flow Cytometry, Andreas Thomae and Steffen Dietzel from the Core Facility Bioimaging and all staff members from the Core Facility Animal Models for their technical support.

Special thanks go to all current and former members of the Peters lab for the good time and friendly atmosphere both inside and outside the lab. Importantly, I want to thank Anna for going on this PhD journey with me right from the beginning and for being a great colleague and friend during the last four years. Many thanks also to all members of the Institute of Clinical Neuroimmunology, especially everyone from the Kawakami lab, for the fun lab meetings, nice chats and sometimes urgently needed coffee and cake breaks.

Furthermore, I would like to thank my fellow PhD students from the IMPRS program. Although being in different labs, we went on this journey together. Johanna, Andi, Laura, Stephan, Jasmin and Kerstin, thank you for the coffee breaks, fun nights and activities in and around Munich, thank you for being my friends.

Most importantly, Daniel, I am grateful to have you in my life. Thank you for the survival packages on long Saturdays in the lab, for your shoulder to lean and cry on, for your understanding, love and support. Ich liebe dich! Finally, I want to thank my family, especially my parents and Stephanie for their endless love and support throughout my whole life, for always being there for me. Vielen Dank für alles!

Attributions

ES cell culture and blastocyst injections for the generation of IL-23p19.LacZ mice as described in section 3.2 were performed by Dr. Soo Jin Min-Weißenhorn at the Transgenic Core Facility of the of the Max Planck Institutes of Biochemistry and Neurobiology in Martinsried.

sgRNA design and cloning of CRISPR KO plasmids described in sections 3.3 and 3.4.2 was performed together with Courtney McQuade. The data shown in Figure 22C, D was generated by Courtney McQuade.

Primer design and cloning of pMSCV vectors for the overexpression of different cytokines (section 3.4.1) was performed by Katarina Pinjusic and Dr. Anneli Peters.

The 40LB-CD8-21 feeder cell line was generated by Katarina Pinjusic and Dr. Anneli Peters.

The Th17 culture shown in Figure 24 was performed with the help of Anna Kolz.

The Western Blot shown in Figure 31B was performed together with Michelle Biljecki.

Abbreviations

(e)GFP	(Enhanced) Green fluorescent protein
AF	Alexa Fluor®
APC	Antigen-presenting cell
APRIL	A proliferation-inducing ligand
ASC	Antibody-secreting cell
BAFF	B cell-activating factor
BCR	B cell receptor
Blimp-1	B lymphocyte-induced maturation protein-1
BM	Bone marrow
BMDC	Bone marrow-derived dendritic cell
BSA	Bovine serum albumin
BV	Brilliant Violet™
Cas9	CRISPR associated protein 9
CD	Cluster of differentiation
CD40L	CD40 ligand
CFA	Complete Freund's adjuvant
CIA	Collagen-induced arthritis
cLN	Cervical lymph node
CNS	Central nervous system
CRISPR	Clustered regularly interspaced short palindromic repeats
CSF	Cerebrospinal fluid
CTLA	Cytotoxic T lymphocyte-associated protein
Cy	Cyanine
DAMPs	Damage-associated molecular patterns
DAPI	4’,6-diamidino-2-phenylindole
DC	Dendritic cell
DMEM	Dulbecco’s Modified Eagle’s Medium
EAE	Experimental autoimmune encephalomyelitis
Ebi	Epstein-Barr virus induced gene
EDTA	Ethylendiamintetraacetat

eLFs	Ectopic lymphoid follicles
ELISA	Enzyme-linked immunosorbent assay
ES cells	Embryonic stem cells
FACS	Fluorescence-activated cell sorting
FBS	Fetal bovine serum
FDC	Follicular dendritic cell
FDG	Fluorescein di(β-D-galactopyranoside)
FITC	Fluorescein isothiocyanate
Flp	Flippase
Fol B cells	Follicular B cells
FoxP3	Forkhead-Box-Protein P3
FRT	Flippase Recognition Target
GC	Germinal center
GM-CSF	Granulocyte macrophage-colony stimulating factor
HBSS	Hanks' Balanced Salt Solution
HEPES	2-(4-(2-Hydroxyethyl)-1-piperazinyl)-ethansulfonsäure
HRP	Horseradish peroxidase
i.p.	Intraperitoneally
i.v.	Intravenously
ICAM-1	Intracellular adhesion molecule-1
IFN	Interferon
Ig	Immunoglobulin
iGB cell	Induced germinal center B cell
IHC	Immunohistochemistry
IL	Interleukin
ILC	Innate lymphoid cell
iLN	Inguinal lymph node
iPBs	Induced plasmablasts
iPCs	Induced plasma cells
IRES	Internal ribosome entry sequence
KO	Knock-out

LAG3	Lymphocyte-activation gene 3
LN	Lymph node
LPS	Lipopolysaccharide
LT	Lymphotoxin
MAdCAM-1	Mucosal addressin cell adhesion molecule 1
MAG	Myelin-associated glycoprotein
MBP	Myelin basic protein
MCS	Multiple cloning site
MHC	Major histocompatibility complex
mLN	Mesenteric lymph node
MOG	Myelin oligodendrocyte glycoprotein
MS	Multiple sclerosis
MSCV	Murine stem cell virus
MZ	Marginal zone
NK cell	Natural killer cell
PAMPs	Pathogen-associated molecular patterns
PBS	Phosphate-buffered saline
PD	Programmed cell death protein
PD-L1	Programmed cell death 1 ligand 1
PE	Phycoerythrin
PerCP	Peridinin chlorophyll protein
PFA	Paraformaldehyde
PKC	Protein kinase C
PLP	Proteolipid protein
PMA	Phorbol 12-myristate 13-acetate
PTX	Pertussis toxin
RA	Rheumatoid arthritis
Rag	Recombination activating gene
ROR	RAR-related orphan receptor
RR	Relapsing-remitting
RT	Room temperature

s.c.	Subcutaneously
SLE	Systemic lupus erythematosus
SP	Secondary progressive
SS	Sjörgen's syndrome
T-bet	T-box expressed in T cells
TCR	T cell receptor
T_{FH} cell	Follicular T helper cell
TGF	Transforming growth factor
Th cell	T helper cell
TLR	Toll-like receptor
TNF	Tumor necrosis factor
Tr1 cells	Type 1 regulatory T cells
Tregs	Regulatory T cells
VCAM-1	Vascular cell adhesion molecule-1
VEGF	Vascular endothelial growth factor
WT	Wild type

List of figures

List of tables

Contents

Summary

Multiple sclerosis (MS) is a common disease of the central nervous system with almost 2.5 million patients worldwide. It is characterized by chronic autoimmune inflammation targeting the myelin sheath and resulting in tissue inflammation, demyelination, axonal damage and loss. Traditionally, research efforts in MS and its animal model experimental autoimmune encephalomyelitis (EAE) focused on autoreactive T cells specific for myelin antigens such as myelin oligodendrocyte glycoprotein (MOG). These autoreactive T cells are thought to be primed in the periphery before they enter the CNS where they drive inflammatory processes that lead to lesion formation and tissue damage. However, in the last years, clinical data suggested an additional important role of B cells in MS pathogenesis. Increasing evidence supports the hypothesis that among the B cell effector functions, antigen presentation and cytokine production rather than secretion of antibodies are crucial for disease initiation and progression. Thereby, B cells may promote differentiation of autoreactive T helper (Th) cells into pathogenic subsets such as Th1 and Th17 cells. To test by which mechanisms antigen-specific B cells could cooperate with antigen-specific T cells to induce EAE, B cells isolated from Th mice, which harbor B cells specific for the CNS antigen MOG, were characterized. In this thesis it was demonstrated that Th B cells have an expanded compartment of marginal zone B cells, a B cell subset often associated with different autoimmune diseases. Furthermore, Th B cells produced significantly more pro-inflammatory cytokines such as IL-6 and TNFα, and less anti-inflammatory IL-10 indicating a more pathogenic potential of MOG-specific B cells.

To investigate how cytokine production by antigen-specific B cells in the context of antigen-presentation can shape T cell responses *in vivo*, a novel adoptive co-transfer system was developed, in which activated MOG-specific B cells stimulate MOG-specific $CD4^+$ T cells to induce EAE. Using an *in vitro* culture system, different cytokines were overexpressed in MOG-specific B cells before adoptive transfer to evaluate the role of these cytokines in initiation of EAE. It could be shown that overexpression of IL-6 and IL-23p19 leads to an accelerated EAE onset mediated by different mechanisms. In contrast, overexpression of anti-inflammatory IL-10 in plasmablasts could contribute to

disease regulation in a Th17 adoptive transfer EAE model by increasing the frequency of anti-inflammatory T cells directly in the CNS.

Lastly, a novel IL-23p19 reporter mouse was developed to identify the cellular sources of IL-23p19, a cytokine crucial for differentiation and stabilization of pathogenic Th17 cells. It was discovered that activated T cells express and secrete high levels of IL-23p19, but that T cell-derived IL-23p19 is dispensable for EAE.

Overall, the role of different B cell-derived cytokines was investigated in this thesis, and it was shown that B cells can contribute to both the initiation but also the regulation of EAE depending on the cytokines they produce. Furthermore, the sources of the cytokine IL-23p19, which is crucial for Th17 differentiation, and its role in T cell biology during EAE were investigated. These findings shed light on the role of different B cell subsets, effector functions, and cytokines during EAE and MS, whose understanding is crucial to develop novel, more specific therapies for MS.

Zusammenfassung

Multiple Sklerose (MS) ist eine chronisch-entzündliche Autoimmunerkrankung, bei der die Myelinscheiden im zentralen Nervensystem (ZNS) von Immunzellen angegriffen werden. Dies führt zu lokalen Entzündungen und Demyelinisierung sowie zur Schädigung und zum Verlust von Nervenzellen. Obwohl MS eine häufige Erkrankung ist, von der weltweit fast 2,5 Millionen Menschen betroffen sind, ist die Pathogenese noch nicht abschließend verstanden. Traditionell fokussierte sich die Forschung an MS und seinem Tiermodell, der experimentellen autoimmunen Enzephalomyelitis (EAE), auf autoreaktive T-Zellen, die spezifisch auf Myelin-Antigene wie beispielsweise das Myelin-Oligodendrozyten-Glykoprotein (MOG) reagieren. Man geht davon aus, dass diese autoreaktiven T-Zellen in der Peripherie aktiviert werden und dann ins ZNS einwandern, wo sie Entzündungsreaktionen auslösen, die zu Läsionen und Gewebsschädigung führen. In den letzten Jahren verdichteten sich jedoch die Hinweise auf eine zusätzliche wichtige Beteiligung von B-Zellen an der MS-Pathogenese. Besonders klinische Daten deuten darauf hin, dass B-Zellen zum Krankheitsbeginn und -verlauf beitragen, indem sie Antigene präsentieren und Zytokine sezernieren, die möglicherweise die Differenzierung von pathogenen T-Helfer (Th-)Zellen wie Th1- oder Th17-Zellen fördern. Um zu testen, durch welche Mechanismen antigen-spezifische B-Zellen mit antigen-spezifischen T-Zellen kooperieren und EAE induzieren können, wurden B-Zellen von Th Mäusen, die MOG-spezifische B-Zellen besitzen, isoliert und charakterisiert. In dieser Dissertation konnte gezeigt werden, dass Th B-Zellen einen erhöhten Anteil an Marginalzonen B-Zellen besitzen, eine B-Zell-Population, die im Zusammenhang mit verschiedenen Autoimmunkrankheiten steht. Des Weiteren produzierten die Th B-Zellen deutlich mehr entzündungsfördernde Zytokine wie IL-6 oder TNFα und weniger entzündungshemmendes IL-10, was auf ein pathogenes Potenzial der MOG-spezifischen B-Zellen hindeutet.

Um zu untersuchen, ob antigen-spezifische B-Zellen die T-Zellantwort *in vivo* durch die Produktion von Zytokinen im Kontext der Antigen-Präsentation beeinflussen können, wurde ein neues Ko-Transfermodell entwickelt, in dem aktivierte MOG-spezifische B-Zellen MOG-spezifische $CD4^+$ T-Zellen stimulieren und so EAE induzieren können. In einem *in vitro* Zellkultursystem wurden vor dem Transfer verschiedene Zytokine in

MOG-spezifischen B-Zellen überexprimiert und so die Rolle dieser Zytokine für die Initiierung der Krankheit bewertet. Es konnte gezeigt werden, dass die Überexpression von IL-6 und IL-23p19 zu einem beschleunigten Krankheitsbeginn führt; ein Effekt, der je nach Zytokin durch unterschiedliche Mechanismen vermittelt wird. Im Gegensatz dazu trägt die Überexpression von entzündungshemmendem IL-10 in Plasmablasten zur Krankheitsregulation bei, indem sie den Anteil entzündungshemmender T-Zellen im ZNS erhöht.

Außerdem wurde in dieser Dissertation eine neuartige IL-23p19 Reportermaus entwickelt, um die zellulären Quellen des Zytokins IL-23p19 zu untersuchen, das für die Differenzierung und Stabilisierung pathogener Th17-Zellen von entscheidender Bedeutung ist. Es konnte gezeigt werden, dass aktivierte T-Zellen IL-23p19 exprimieren und sezernieren, dass aber das von T-Zellen stammende IL-23p19 unwesentlich für die Entwicklung der EAE ist.

Zusammenfassend wurde in dieser Arbeit die Rolle von verschiedenen B-Zell-Zytokinen untersucht und es konnte gezeigt werden, dass B-Zellen, abhängig von den produzierten Zytokinen, sowohl zur Krankheitsauslösung als auch zur -regulation beitragen können. Außerdem wurden die zelluläre Herkunft des Zytokins IL-23p19 sowie seine Rolle in der T-Zellbiologie im Zusammenhang mit Entzündungsprozessen in der EAE untersucht. Diese Erkenntnisse geben Aufschluss über die Rolle von verschiedenen B-Zellpopulationen, Effektor-Funktionen und Zytokinen während der EAE. Dieses Verständnis ist ausschlaggebend für die Entwicklung neuer, gezielterer Therapien für MS.

1. Introduction

1.1 The immune system

The immune system is crucial for defending all parts of the body against any kind of pathogen that threatens our health frequently in our daily life. Depending on the speed and specificity of the immune reaction, immunity can be divided into two parts. Innate immunity is the first and fastest line of defense and includes physical and chemical barriers, as well as innate immune cells, complement and acute phase proteins. In contrast, adaptive immunity is mediated by lymphocytes and provides highly specific protection but takes days to weeks to develop. The functionality and efficacy of both parts as well as their interplay is crucial to prevent severe infections, but also the uncontrolled division of cells leading to the development of tumors.

1.1.1 Innate immunity

The initial response to pathogens is mediated by innate immune cells such as macrophages, dendritic cells (DCs) and neutrophils. These cells recognize microbial structures, so called pathogen-associated molecular patterns (PAMPs) or molecules released by damaged or dying cells (damage-associated molecular patterns, DAMPs) [1]. For this, they use several pattern recognition receptors, most importantly toll-like receptors (TLRs)[2]. In addition, the more recently described innate lymphoid cells (ILCs) contribute to multiple immune pathways. ILCs can be divided into five subgroups, which correspond in their effector function to the adaptive T cell response that is induced by a particular pathogen: for example, pathogens that lead to activation of group 1 ILCs will later elicit a specific Th1/cytotoxic T cell response (described in section 1.4.1). Natural killer (NK) cells are the best described ILC subset and are equipped with different types of receptors that determine NK cell reactivity [3]. Activating receptors recognize ligands expressed on stressed, infected or transformed cells, whereas inhibitory receptors recognize healthy nucleated cells. The balance of activating and inhibitory receptor stimulation determines whether a NK cell will be fully activated and perform its effector function through secretion of cytokines and cytolytic proteins that induce killing of the infected or abnormal cell [4]. Identification of a pathogen by innate immune cells ultimately leads to phagocytosis and elimination of the microbe or infected cell,

initiation of the complement cascade and/or activation of the adaptive immune system to create a more specific response [5].

1.1.2 Adaptive immunity

T and B cells are the most important components of the adaptive immune system and mediate cellular and humoral immunity, respectively. In contrast to innate immune cells, T and B cells have an almost unlimited repertoire of receptors, which are produced by random rearrangement and splicing of multiple DNA segments in the antigen-binding areas of the receptors. This leads to the production of over 10^8 T cell receptors (TCRs) and 10^{10} B cell receptors (BCRs), which allows the cells to fight any individual pathogen to be encountered in life [6]. Recognition of antigen by cells of the adaptive immune system leads to cell activation, expansion and differentiation of antigen-specific B and T cells, which contribute to pathogen elimination by different mechanisms.

While the BCR can bind soluble antigen, T cells require antigen presentation on major histocompatibility complex (MHC) molecules as linear peptides. Recognition of the antigen in association with the MHC molecule and proper activation of the T cell requires additional binding and stimulation of the co-receptor CD4 or CD8 [7]. $CD8^+$ T cells recognize antigens bound to MHC class I molecules. Since MHC-I molecules are expressed by all nucleated cells, they are loaded with cytosolic antigens in cells infected with intracellular pathogens or tumor antigens in abnormal cells. Activation of $CD8^+$ T cells induces the secretion of cytotoxic molecules, which leads to lysis and removal of the infected cell [8].

$CD4^+$ T cells, also called T helper (Th) cells, recognize antigens bound to MHC-II molecules, which are expressed exclusively by specialized antigen-presenting cells (APCs) such as macrophages, DCs and B cells. Since antigens loaded on MHC-II molecules are derived from pathogens that have been taken up by phagocytosis, $CD4^+$ T cells are crucial for the defense against extracellular pathogens. In addition to the first activation signal mediated by the antigen:MHC-II complex, APCs also provide costimulation via molecules such as CD80, CD86 and CD40 that bind CD28 and CD40 ligand (CD40L) on the T cell (signal 2), which is required for full activation of the T cell [9]. Additionally,

cytokines produced by APCs determine the fate of the T cells and the direction of the immune response (signal 3) (section 1.4.1).

Naïve B cells can be divided into three subsets, which respond to different types of antigens: B-1 cells, marginal zone (MZ) B cells and follicular B cells. B-1 cells are localized in mucosal tissues and the peritoneal cavity and are activated by lipopolysaccharide (LPS) and other TLR ligands. This leads to proliferation of B-1 cells as well as to T cell-independent differentiation into short-lived IgM-secreting plasma cells and IgA-secreting cells [10, 11]. Similarly, MZ B cells are considered innate-like cells that express high levels of TLRs and respond rapidly to blood-borne microorganisms to produce low-affinity IgM antibodies [12]. In addition to this fast, T cell-independent response, MZ B cells are also able to generate long-lived plasma cells in T cell-dependent immune responses. Indeed, MZ B cells express high levels of MHC-II, CD80 and CD86 molecules, which are crucial for the interaction with $CD4^+$ T cells [13, 14]. Most mature naïve B cells, however, are follicular B cells that recirculate in the blood and the B cell areas of secondary lymphoid organs such as spleen, lymph nodes (LNs) and Peyer's patches. In contrast to MZ B cells and B-1 cells, follicular B cells are unable to differentiate into antibody-secreting cells (ASCs) in response to TLR stimulation alone but require BCR activation [15]. Activation of antigen-specific follicular B cells is initiated by binding of antigen in 3D structure to membrane-bound IgM or IgD immunoglobulins (Igs), which leads to receptor internalization, antigen processing and presentation on MHC-II molecules on the cell surface. Furthermore, activated follicular B cells migrate to the T cell zones in spleen and LNs where they interact with antigen-specific T helper cells [16]. Activated T helper cells express CD40L which binds to CD40 on the B cells and induces B cell proliferation and differentiation [17, 18]. Some B cells leave the follicle and differentiate into short-lived plasma cells that stay in secondary lymphoid organs and non-lymphoid tissues [19]. Other B cells migrate back to the follicle and form germinal centers (GCs). Here, the B cells proliferate extensively and undergo somatic hypermutation of Ig genes and isotype switching to diversify the affinity of their BCR. B cell clones with increased affinity are selected by their interaction with follicular dendritic cells (FDCs) and follicular T helper (T_{FH}) cells. FDCs do not express MHC-II molecules but bind unprocessed antigen through Fc receptors [20]. Only high-affinity B cells are able to take up antigen provided by FDCs, load it on MHC-II and present it to

T_{FH} cells. Upon recognition of the antigen, T_{FH} cells provide help in the form of CD40L and interleukin (IL-)21, which are crucial for the survival of the GC B cells [21]. Depending on the type of microbial stimulus that induced the GC, T_{FH} cells can also secrete other cytokines such as interferon (IFN)γ and IL-4, which support isotype class switching to IgG1 or IgG2a respectively [22, 23]. Upon T_{FH} cell help, selected GC B cells undergo further rounds of affinity maturation, whereas low-affinity B cells die from apoptosis [24]. Eventually, the GC reaction produces high-affinity memory B cells and ASCs that home to the bone marrow (BM) where they differentiate into long-lived plasma cells that persist for years [25].

1.1.3 Tolerance mechanisms

The immune system is very effective and eliminates pathogens often even before any clinical symptoms are noticed. However, such strong immune reactions must be thoroughly regulated in order to prevent exaggerated inflammation and tissue damage. Furthermore, tolerance against self-structures and harmless environmental factors such as cosmetics and food are essential and dysregulation in immune tolerance leads to severe autoimmunity or allergies. Therefore, different tolerance mechanisms exist, which can be divided into central and peripheral tolerance and have been best characterized in $CD4^+$ T cells. Central tolerance is induced during T cell development in the thymus, when T cells that recognize self-antigens are deleted by negative selection or develop into regulatory T cells (Tregs) [26]. However, some autoreactive T cells escape these mechanisms and enter peripheral tissues. Therefore, peripheral tolerance mechanisms are required to allow for tolerance against tissue-specific self-antigens and harmless foreign antigens. Peripheral tolerance by T cells consists of three basic mechanisms which include the deletion of autoreactive T cells, the differentiation of peripheral Tregs and T cell anergy [27]. Chronic stimulation of the TCR with self-antigens leads to apoptosis of autoreactive T cells mediated by Fas receptor engagement or a Bcl-2 and Bcl-xL-regulated intrinsic mechanisms [28]. In contrast, lack of costimulation or strong co-inhibitory signals mediated by cytotoxic T-lymphocyte-associated protein (CTLA)-4 and programmed cell death protein (PD)-1 on tolerogenic APCs can induce anergy, which describes a state of functional unresponsiveness, in which T cell clones are unable to proliferate and perform effector functions in response to antigen

encounter [29]. Anergic T cells persist for long time *in vivo* but whether or to which extent they fulfill an active role in immune tolerance is still controversial. In addition, continuous stimulation with low dose antigen, which is presented by tolerogenic DCs in the presence of transforming growth factor (TGF)β can induce Treg differentiation in the periphery [30-32].

Tregs can actively suppress immune responses. Both thymus-derived natural Tregs (nTregs) and peripherally induced Tregs (iTregs) can be identified by the expression of CD25 and the transcription factor FoxP3. Tregs suppress effector T cells by expression of inhibitory receptors such as CTLA-4 and PD-1 which bind to CD80/86 and programmed cell death 1 ligand 1 (PD-L1) on APCs respectively, thereby inhibiting costimulation and complete T cell activation [33, 34]. Furthermore, Tregs fulfill their regulatory function by the secretion of suppressive cytokines such as IL-10 and TGFβ. Type 1 regulatory T cells (Tr1 cells) represent a distinct subset of regulatory T cells. Although not expressing the characteristic transcription factor FoxP3, Tr1 cells have been shown to have similar regulatory capability as classical $CD4^+$ $CD25^+$ Tregs [35]. They produce high levels of IL-10 and contribute to immune tolerance by their suppressive activity [36-38].

Similar to T cell tolerance, different mechanisms exist to control autoreactive B cells and prevent the production of autoreactive antibodies. A very important mechanism to ensure central B cell tolerance, is receptor editing. During their development in the bone marrow, B cells express recombination-activating genes (Rag-1 and Rag-2), which ensure rearrangement of Ig genes crucial for BCR diversity. Rag expression is lost during development, however, immature B cells that strongly interact with self-antigens reactivate Rag expression to enter a new round of antibody light chain recombination. This leads to an altered specificity of the BCR, which may then not recognize self-antigen anymore [39]. However, if receptor editing fails, the autoreactive B cells are deleted by apoptosis. If developing B cells recognize self-antigen only weakly, they become anergic and exit the bone marrow [39]. In the periphery, mature B cells that are repeatedly stimulated by self-antigens in the absence of T cell help also become anergic. Since anergic B cells require high levels of B cell-activating factor (BAFF) for survival, they cannot compete with less BAFF-dependent non-autoreactive B cells, which leads to their gradual deletion over time [40, 41].

Despite these various mechanisms, self-reactive immune cells sometimes escape immune tolerance and induce tissue inflammation and autoimmunity. Autoimmune diseases can be systemic like in systemic lupus erythematosus (SLE), when the autoantigen is present throughout the whole body, or restricted to a specific organ or tissue like in type 1 diabetes or multiple sclerosis.

1.2 Multiple Sclerosis

Multiple sclerosis (MS) is characterized by chronic autoimmune inflammation targeting the myelin sheath and resulting in tissue inflammation, demyelination, axonal damage and loss. Typical symptoms include visual loss or double vision, limb weakness, sensory loss, ataxia and paralysis [42]. In the majority of patients, episodes of neurological impairment – also called relapses – are fully or partially reversible resulting in the typical relapsing-remitting (RR)MS disease course. After 10–20 years, some patients develop a secondary progressive disease course characterized by a progressive worsening of neurological function leading to increasing disability over time. About 15 % of patients have a progressive disease course without relapses or remissions from the onset of symptoms (primary progressive MS)[43].

1.2.1 Neuropathology

MS is a heterogeneous disease, not only clinically but also pathologically. MS lesions can appear throughout the CNS and are characterized as areas of focal inflammation, demyelination and reactive gliosis. The heterogeneity in early stage acute white matter lesions suggests that different immunological mechanisms play a role, which may even be different among individual patients [44]. Histologically, MS lesions can be divided into four subtypes with different patterns of demyelination: while patterns I and II are mainly immune cell mediated with infiltrates of macrophages and deposition of immunoglobulins, respectively, patterns III and IV are characterized by the damage of oligodendrocytes [45]. Whether an individual lesion with a given demyelination pattern becomes remyelinated or evolves into a chronic lesion, remains poorly understood. Furthermore, the size or load of focal white matter lesions does not necessarily correlate with clinical disability [46, 47]. In contrast, neurodegeneration and progressive atrophy

are not limited to individual lesions but can be observed as diffuse injury of both white and grey matter in cortex and spinal cord.

1.2.2 Etiology and Pathogenesis

Although MS is a common neurological disorder with almost 2.5 million patients worldwide and was first described approximately 150 years ago, the cause of the disease remains elusive. Nevertheless, various genetic and environmental risk factors have been identified. Since people with an affected first-degree relative have a 20–40 times higher risk to develop the disease themselves [48, 49], a genetic predisposition is likely and has been studied extensively. Genome-wide association studies have identified over 200 risk alleles, most of them associated with pathways directly involved in immune regulation such as the HLA DRB1*1501 haplotype [50]. Although genetic variation accounts for approximately 20 % of the overall risk to develop the disease, MS is not considered a pure genetic but rather a multifactorial disease. Several environmental factors have been discussed such as viral infections in early life, vitamin D deficiency, smoking or obesity [51]. Recent studies have identified changes in the gut microbiota of MS patients compared to controls [52-54], and the role of the microbiome and microbial products in MS pathogenesis is subject of ongoing research.

1.3 Experimental autoimmune encephalomyelitis

To decipher the cellular and molecular mechanisms of MS pathogenesis, the animal model experimental autoimmune encephalomyelitis (EAE) was developed. EAE was first described over 85 years ago when the virologist Thomas M. Rivers observed that monkeys immunized with CNS homogenate from rabbits developed paralysis caused by acute disseminated encephalomyelitis and perivascular demyelination [55]. Addition of adjuvant further accelerated the disease process [56] and is used until today with mice being the most frequently used animals for EAE research.

1.3.1 Active EAE

Nowadays, mice are immunized with a single myelin protein or peptides emulsified in complete Freund's adjuvant (CFA). Myelin contains different proteins, of which myelin oligodendrocyte glycoprotein (MOG), proteolipid protein (PLP) and myelin basic protein (MBP) are mostly used to induce EAE. Although MOG represents only 0.05–0.1 % of the total myelin protein content, its localization at the outer surface of the myelin sheath, as well as its structure with a single extracellular Ig-domain makes it easily accessible to immune cells or antibodies [57] (Figure 1). MOG, specifically the $MOG_{35–55}$ peptide, is commonly used to induce EAE in C57BL/6 mice. 10–14 days after immunization, the mice develop ascending paralysis affecting tail, hind limbs and sometimes even fore limbs. The model is characterized by a monophasic disease course with a peak of neurological disability three days after onset and a subsequent recovery phase [58]. In contrast, SJL mice immunized with the encephalitogenic peptide $PLP_{139–151}$, derived from proteolipid protein, develop a relapsing-remitting disease course [59].

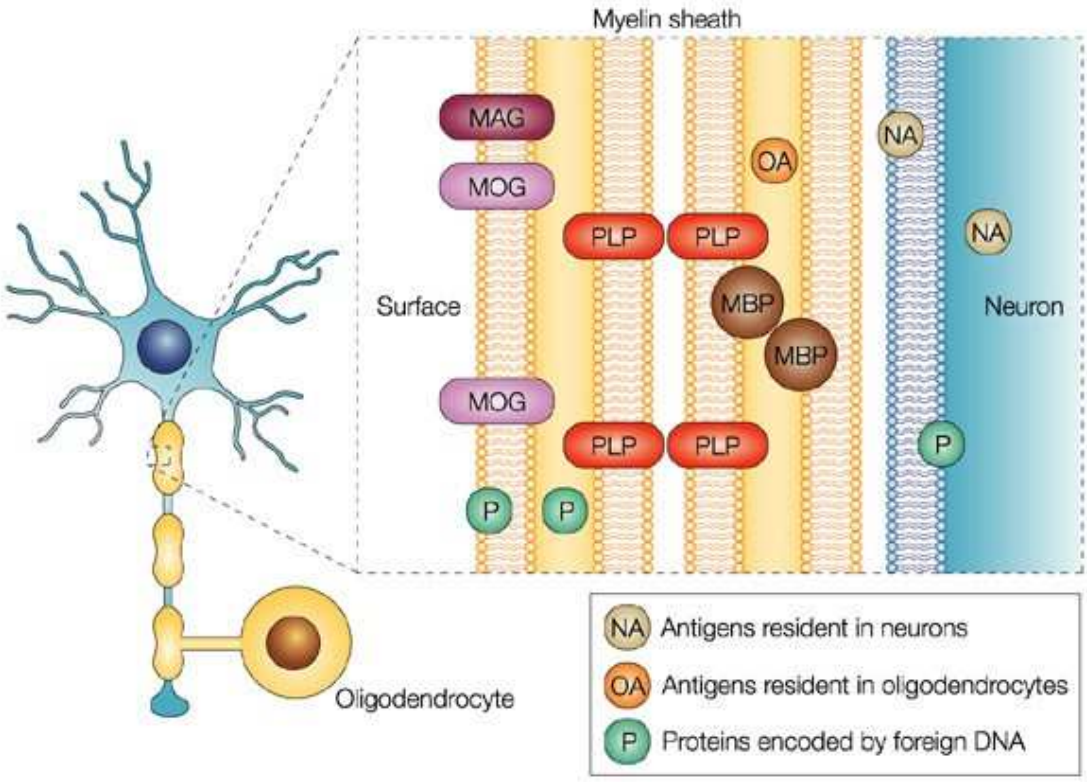

Figure 1: Localization of myelin proteins in the myelin sheath of the CNS. *MAG, myelin-associated glycoprotein; MBP, myelin basic protein; MOG, myelin oligodendrocyte glycoprotein; PLP, proteolipid protein. Adapted by permission from [60].*

1.3.2 Passive EAE

Another way to induce EAE in mice is the adoptive transfer of encephalitogenic T cells. This was first demonstrated when bulk LN cells isolated from previously immunized rats induced EAE upon transfer into naïve animals [61]. Later, it was shown that transfer of $CD4^+$ T cells was sufficient to induce EAE [62, 63]. In addition, encephalitogenic T cells can be isolated from transgenic mice with a myelin-specific TCR. 2D2 mice with a TCR specific for the $MOG_{35–55}$ peptide have been developed on the C57BL/6 background and transgenic T cells isolated from 2D2 mice have been used sucessfully to induce EAE after adoptive transfer [64].

1.3.3 Spontaneous EAE models

In both active and passive EAE, $CD4^+$ T cells are the main drivers of the disease. Furthermore, immunization of B cell-deficient mice with the $MOG_{35–55}$ peptide suggests that B cells may not be essential for EAE development [65]. In contrast, immunization with whole MOG protein is dependent on the presence of B cells indicating a pathogenic role of antigen-specific B cells in the disease [66, 67]. Therefore, different B cell-dependent EAE mouse models were developed. First, Litzenburger et al. generated the IgH^{MOG} mouse (hereinafter referred to as Th), a knock-in mouse carrying the rearranged $V_HD_HJ_H$ sequence of a MOG-specific monoclonal antibody leading to the development of MOG-specific B cells, which secrete MOG-specific antibodies [68]. These mice show no signs of spontaneous disease; however, when crossed with 2D2 mice, about 60 % of animals spontaneously develop severe EAE with a progressive disease course indicating that antigen-specific B and T cells cooperate to induce autoimmunity [69, 70]. In contrast, in another spontaneous EAE model created on the SJL/J background, the TCR^{1640} model, transgenic MOG-specific T cells recruit endogenous B cells, which leads to the production of MOG-specific antibodies that contribute to spontaneous disease with a relapsing-remitting course [71]. T cell responses in those models involve both pathogenic Th1 and Th17 cells, however, whether both subsets or rather only one of them interacts with B cells remains unclear.

1.4 Immune cells and their role in MS and EAE

1.4.1 T helper cells

Self-reactive $CD4^+$ T helper cells are the main drivers of tissue inflammation in many autoimmune diseases. According to the current understanding, in CNS autoimmunity autoreactive T cells are primed in the periphery before they cross the blood-brain barrier and enter the CNS. Depending on the cytokine milieu present during activation, naïve T cells differentiate into different T helper cell subsets.

Traditionally, $CD4^+$ T cells were classified as Th1 or Th2 cells based on transcription factor expression and cytokine production [72]. Th1 cells express the transcription factor T-box expressed in T cells (T-bet) and secrete IFNγ leading to macrophage activation, which is important for cell-mediated immunity against intracellular pathogens. In contrast, Th2 cells with their signature cytokines IL-4, IL-5 and IL-13, promote clearance of extracellular pathogens such as parasites and helminths. While Th2 cells are associated with IgE-mediated allergy and asthma, uncontrolled Th1 responses can lead to autoimmunity [73]. Th1 cells were studied extensively in the context of EAE, since CNS-infiltrating cells were originally found to have a Th1 phenotype [74, 75]. Consistent with that, mice lacking the transcription factor T-bet are completely resistant to EAE further suggesting that Th1 cells may be crucial for EAE induction [76]. Evidence for this hypothesis was found in human disease, as IFNγ was detected in CNS lesions of MS patients and IFNγ administration exacerbated MS symptoms [77, 78]. Moreover, elevated levels of IL-12, the key differentiation cytokine for Th1 cells, were found in the CNS of MS patients [79] further supporting the long-standing theory of Th1 cells as the pathogenic entity in CNS autoimmunity.

The Th1 paradigm, however, was challenged when it was shown that mice lacking the IL-12p35 subunit were highly susceptible to EAE, whereas IL-12p40-deficient mice were completely resistant [80]. In 2000, Oppmann et al. found that the IL-12p40 subunit can also pair with the newly-identified protein p19 to form the cytokine IL-23 [81] indicating that IL-23 rather than IL-12 is the critical cytokine for CNS autoimmunity. This hypothesis was confirmed when mice lacking IL-23p19 (encoded by the *Il23a* gene) were found to be resistant to EAE [82]. Later it was shown that IL-23 drives differentiation of a novel T helper cell subset, so called Th17 cells, from *in vivo* activated T cell populations [83].

In contrast, differentiation of Th17 cells from naïve T cells requires a combination of TGFβ and IL-6 but does not depend on IL-23 [84-86]. This can be explained by the fact that the IL-23 receptor is not expressed on naïve T cells but is upregulated during Th17 differentiation [87]. Polarized Th17 cells express the transcription factor RAR-related orphan receptor (ROR)γt and secrete the cytokines IL-17A, IL-17F, IL-21 and IL-22 [83]. Since their discovery, the role of the IL-23-Th17 axis in MS and EAE has been studied extensively: monocyte-derived DCs from MS patients produce more IL-23 than DCs from healthy controls and *Il17* mRNA levels were elevated in blood and cerebrospinal fluid (CSF) of MS patients [88, 89]. Furthermore, lack of IL-17A leads to attenuated EAE and IL-17A neutralization ameliorates clinical symptoms [90, 91]. Using MOG-specific transgenic 2D2 T cells, it was shown that both Th1 and Th17 cells are able to induce EAE independently of each other [92]. However, due to T helper cell plasticity and the abundance of several cytokines and other differentiation factors *in vivo*, probably a mixed population of Th1, Th17 and even other T helper cells subsets are generated in MS patients which may contribute to the heterogeneity of MS lesions.

1.4.2 B cells

Traditionally, research efforts focused on autoreactive T cells, which were thought to be the orchestrators of autoimmunity and inflammation in MS. However, in the last years, B cells entered the stage in MS research since increasing evidence suggested a role of B cells in MS pathogenesis: B cells are primarily known by their ability to produce antibodies and the presence of antibodies (oligoclonal bands) in the CSF of MS patients was one of the first biomarkers used for diagnosis of MS [93]. Many of these intrathecal antibodies do not recognize CNS antigens [94]. However, antibodies specific for MOG can be found in a subgroup of MS patients, although the role of these antibodies in MS pathogenesis remains controversial [95-97]. Nevertheless, the fact that antibodies and complement are present in active MS lesions and some patients benefit from plasmapheresis suggests an involvement of autoantibodies in the disease [98, 99].

Additionally, ectopic lymphoid follicle-like structures (eLFs) have been observed in the CNS of patients who suffer from a secondary progressive (SP)MS disease course, as well as in some EAE animal models [100-102]. Among other immune cells, eLFs contain

clusters of B cells and plasma cells indicating that they are recruited to the sites of inflammation and demyelination during EAE and may contribute to disease pathogenesis.

The most striking evidence for the role of B cells in MS pathogenesis, however, was provided by clinical studies showing that MS patients benefit enormously from B cell depletion therapy using anti-CD20 antibodies such as rituximab or ocrelizumab [103]. However, antibody-producing plasma cells do not express CD20 and are thereby not affected by treatment with anti-CD20 antibodies. This indicates that B cells fulfill an alternative, antibody-independent role in MS pathogenesis e.g. by acting as APCs and/or by the production of cytokines. Through their specific BCR, B cells are able to capture and process their cognate antigen and present it on MHC class II molecules, thereby providing highly efficient antigen-specific stimulation to T cells with the same specificity [104]. In CNS autoimmunity, antigen presentation by B cells was sufficient to induce disease by reactivation of mainly Th1 cells, but also Th17 cells in the CNS [105, 106].

Additionally, B cells are important cytokine producers and different cytokines were found to be expressed by B cells in the context of autoimmunity and MS: on the one hand, B cells from MS patients produce increased amounts of the pro-inflammatory cytokines IL-6, tumor necrosis factor (TNF)α and lymphotoxin (LT) but lower levels of anti-inflammatory IL-10 [107-109]. Furthermore, IL-6 secretion by B cells was shown to be crucial for differentiation of pathogenic Th17 cells and disease induction in EAE [106, 110]. In addition, B cells are able to produce IFNγ thereby amplifying Th1 responses and promoting autoimmunity in an animal model of arthritis [111, 112]. Furthermore, B cells of MS patients produce pro-inflammatory granulocyte macrophage-colony stimulating factor (GM-CSF) suggesting an additional role in the stimulation of pro-inflammatory myeloid cell responses [113]. In contrast, it is not clear whether B cells can also secrete IL-12, which is important for differentation of Th1 cells, and IL-23, which is crucial for terminal differentiation and stability of pathogenic Th17 cells.

On the other hand, B cells are also able to fulfill regulatory functions by secretion of anti-inflammatory cytokines such as IL-10 and IL-35, and both IL-10 and IL-35-producing B cells and plasma cells can ameliorate and even suppress EAE [114, 115]. In addition, B cell-specific TGFβ deficiency leads to earlier disease onset and was associated with an

enhanced pro-inflammatory Th1 and Th17 response and increased activation of APCs indicating that TGFβ contributes to the anti-inflammatory potential of B cells in EAE [116]. Which cytokines are produced by B cells is determined by the type of stimulus and the environment, in which the B cell is activated. For example, human B cells stimulated by BCR signaling and CD40L secrete TNFα, LT and IL-6, whereas TLR4 stimulation via LPS induces the secretion of IFNγ, IL-6 but also IL-10 [117, 118]. Furthermore, T cell-derived cytokines can influence the B cell cytokine profile as B cells activated in the presence of Th1-associated cytokines produce IFNγ while B cells activated in the presence of Th2 cells produce IL-2 and IL-4 [119]. Thus, via cytokines, B cells can amplify but also regulate T cell responses and may therefore have multiple implications in MS and EAE. An overview of the different B cell effector functions is depicted in Figure 2.

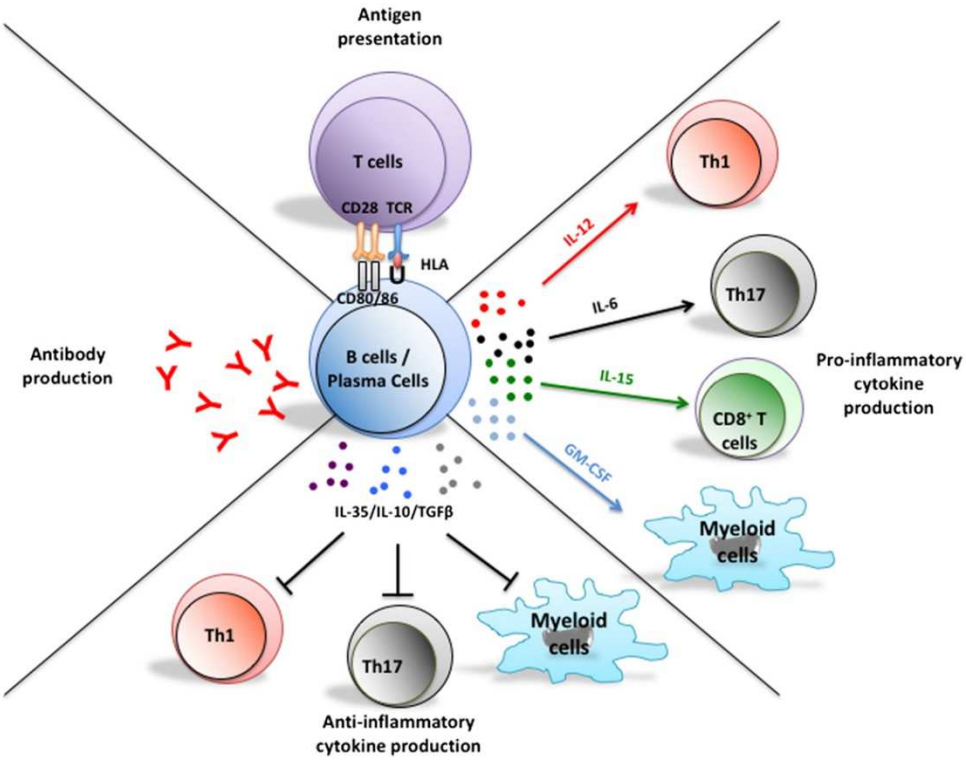

Figure 2: The many faces of B cells. *In addition to the production of antibodies, B cells fulfill other important functions. B cells can act as APCs by presenting their cognate antigen to T cells with the same specificity. Furthermore, B cells can express both pro-inflammatory and anti-inflammatory cytokines, which can modulate T cell and myeloid cell responses. Adapted by permission from [120].*

1.5 The role of IL-23p19 in autoimmunity and neuroinflammation

After the discovery of IL-23 and its role in Th17 differentiation (section 1.4.1), the IL-12 family of cytokines was studied extensively. Soon, other members of this family such as IL-27 and IL-35 were identified. All of these heterodimeric cytokines are composed of an α-chain (p19, p28 or p35) and a β-chain (p40 or Ebi3) (Figure 3). The p40 subunit can pair with p35 and p19 to form IL-12 and IL-23, respectively [81, 121]. IL-27, which consists of p28 and Epstein-Barr virus induced gene (Ebi)3, was first described as another pro-inflammatory cytokine inducing activation, expansion and IFNγ secretion in naïve T cells [122]. On the other hand, IL-27 is also capable of inducing IL-10 production in T cells and differentiation into Tr1 cells, thereby fulfilling a rather regulatory, anti-inflammatory function [123-125]. Furthermore, by inhibiting Th17 differentiation IL-27 is able to suppress CNS autoimmunity [126, 127]. Another potent inhibitory member of the IL-12 family is IL-35, which consists of p35 and Ebi3 [128]. IL-35 can be produced by Tregs and contributes to their anti-inflammatory function [129]. It is further able to suppress T cell proliferation and can promote the differentiation of a peripheral Treg population called Tr35 cells [130]. Later, it was shown that IL-35 can also be produced by B cells, which can thereby regulate autoimmunity [115].

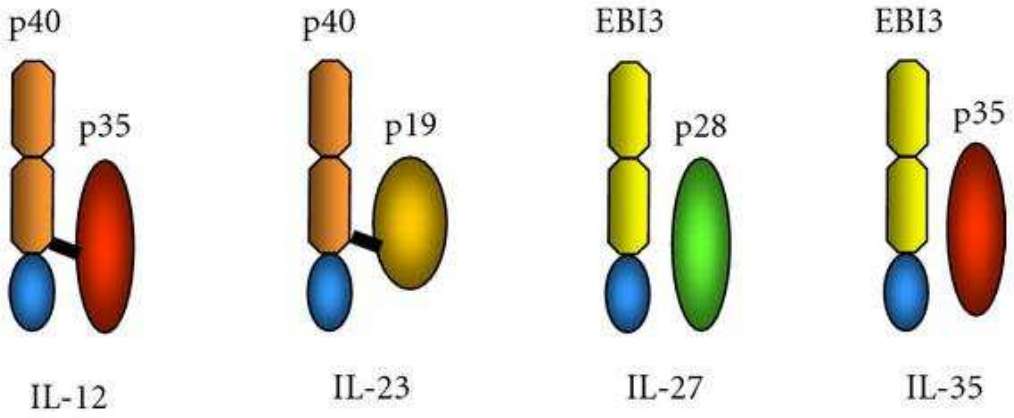

Figure 3: The IL-12 family of cytokines. *The heterodimeric cytokines are composed of an α-chain (p19, p28 or p35) and a β-chain (p40 or Ebi3). The p40 β -subunit is shared between IL-12 and IL-23, whereas IL-27 and IL-35 share the Ebi3 β-subunit. Adapted by permission from [131].*

Recently, the novel cytokine IL-39 was described, which is composed of p19 and Ebi3 [132]. IL-39 is secreted by activated B cells and mediates inflammation by neutrophil expansion in a mouse model of SLE [132, 133]. Additionally, p19 was found to act by itself intracellularly in human endothelial cells, where it led to an upregulation of intracellular adhesion molecule-1 (ICAM-1) and vascular cell adhesion molecule-1 (VCAM-1), and thereby supported leukocyte adhesion and transendothelial migration [134]. These novel findings support the hypothesis that the p19 subunit of IL-23 and IL-39 drives the pathogenicity of these two cytokines and may even fulfill individual functions.

Cytokines of the IL-12 family are produced by APCs to shape the T cell response during antigen presentation. However, due to the lack of reliable reagents, tools to thoroughly study cellular sources and stimuli of the IL-23p19 subunit are limited. In addition, it is unclear, whether B cells can also contribute to IL-23 secretion during EAE.

2. Objectives

Pathogenic T cell responses have been thought to be the only important drivers of autoimmune inflammation in MS for decades; however, recent studies reveal the additional importance of B cells. Increasing evidence supports the hypothesis that antigen presentation and cytokine production rather than secretion of antibodies are crucial for disease pathogenesis. Thereby, B cells may promote differentiation of autoreactive T helper cells into pathogenic subsets such as Th1 and Th17 cells. The aim of this thesis was to investigate how cytokine production by antigen-specific B cells can shape the T cell response in EAE. To address this, first, a novel B cell adoptive transfer system was established, in which activated antigen-specific B cells stimulate T cells of the same antigen specificity to induce EAE. Second, to investigate whether the expression of pro-inflammatory cytokines by antigen-specific B cells can support differentiation of pathogenic Th1 or Th17 cells, different cytokines were retrovirally overexpressed in MOG-specific B cells in an *in vitro* system prior to transfer. Additionally, the role of MOG-specific IgG1 antibodies in this system was investigated (section 4.2).

Besides secretion of pro-inflammatory cytokines, B cells are also able to secrete regulatory cytokines such as IL-10 and IL-35 and can thereby control T cell responses in the periphery and even suppress EAE. However, it is not yet clear whether these regulatory B cells can suppress B and T effector cell responses directly in the CNS. To test this, injection of IL-10-overexpressing plasmablasts was combined with Th17 transfer EAE, a model in which high numbers of B cells and plasma cells are recruited to the CNS. The ability of IL-10-overexpressing plasmablasts to contribute to the regulation of Th17-mediated EAE was investigated in section 4.3.

Th17 differentiation and stability depends on the cytokine IL-23, and IL-23 is essential for the development of EAE. IL-23 can be produced by APCs such as dendritic cells and macrophages; however, due to a lack of reliable reagents, tools to thoroughly study cellular sources and stimuli of the IL-23p19 subunit are limited. Further, it is not known whether B cells can also contribute to IL-23 secretion during EAE. Therefore, an IL-23p19 reporter mouse was generated to identify the cellular sources of IL-23p19 during EAE. Further, the requirement of T cells to produce IL-23p19 was investigated by generating T cell-specific IL-23p19 knock-out (KO) mice (section 4.4).

3. Material and Methods

3.1 Mice

2D2 mice with a transgenic TCR specific for the $MOG_{35–55}$ peptide on a C57BL/6 background have been described previously [64] and were purchased from The Jackson Laboratory. IgH^{MOG} mice on a C57BL/6 background (hereinafter called Th mice) carrying a rearranged $V_HD_HJ_H$ sequence of the MOG-specific monoclonal antibody 8.18C5 replacing the endogenous IgH-D and IgH-J elements and therefore harboring MOG-specific B cells were generously provided by Prof. Hartmut Wekerle [68]. Th mice were crossed to 2D2 mice to generate 2D2 x Th mice that spontaneously develop EAE [69, 70]. In addition, Th mice were crossed to the C57BL/6 congenic CD45.1 strain [135] (The Jackson Laboratory) to allow for tracing of the cells after injection into C57BL/6 hosts that carry the CD45.2 allele. Rag1-KO mice on the C57BL/6 background, which lack Rag1 and are therefore not able to develop mature T and B cells [136] were purchased from The Jackson Laboratory. R26-Cas9 mice, which constitutively express the CRISPR associated protein 9 (Cas9) endonuclease and an enhanced green fluorescent protein (eGFP) under the control of the CAG promoter [137] were purchased from The Jackson Laboratory on a mixed background, backcrossed onto the C57BL/6 background for at least five generations and crossed to Th.CD45.1 mice to generate R26-Cas9 x Th.CD45.1 mice.

R26-Flpe mice on C57BL/6 background express the FLPe variant of the *Saccharomyces cerevisiae* FLP1 recombinase gene driven by the Gt(ROSA)26Sor promotor [138] and were purchased from The Jackson Laboratory. CD4-Cre mice on C57BL/6 background, which express a Cre recombinase gene under the control of the CD4 promoter, were purchased from The Jackson Laboratory and were crossed to IL-23p19.fl mice (section 3.2) to generate CD4-Cre x IL-23p19.fl mice.

All mice were housed and bred under specific pathogen-free conditions in the Core Facility Animal Models at the Biomedical Center of the Ludwig-Maximilians-Universität München. Animal experiments were designed and performed according to regulations of the animal welfare acts and approved by the animal ethics committee of the state of Bavaria (Regierung von Oberbayern) in accordance with European guidelines.

3.2 Generation of the IL-23p19.LacZ reporter mouse line and IL-23p19.fl conditional mouse line

JM8A3.N1 embryonic stem (ES) cells [139] heterozygous for the Il23a$^{tm1a(EUCOMM)Hmgu}$ allele were purchased from the European Mouse Mutant Archive, Helmholtz Zentrum München. In these ES cells, the dominant agouti coat color gene is restored by targeted repair of the C57BL/6 nonagouti mutation [139]. ES cell culture and injection in C57BL/6 blastocysts were performed by Dr. Soo Jin Min-Weißenhorn at the Transgenic Core Facility of the Max Planck Institutes of Biochemistry and Neurobiology in Martinsried. Highly chimeric males (agouti/black) were obtained and mated with C57BL/6N female mice, which led to successful germline transmission. Presence of the p19.LacZ reporter allele was verified by genotyping using a gene-specific forward (5' arm) and a cassette-specific reverse primer (LAR3) and presence of the downstream loxP site was confirmed using specific forward and reverse primers (Table 1). To distinguish heterozygous and homozygous mice, the presence of the *Il23a* wild type (WT) allele was tested using gene-specific forward (5' arm) and reverse (3' arm) primers. PCRs were performed using the DreamTaq PCR Master Mix (Thermo Scientific) under the cycling conditions depicted in Table 2. To generate IL-23p19.fl mice, IL-23p19.LacZ mice were crossed to R26-Flpe mice (section 3.1).

Table 1: *Genotyping primers*

Name	Primer type	T_{melt}	Sequence (5'–3')
5' arm	Gene-specific forward	69.9°C	GAACAAGATGCTGGATTGCAGAGC
3' arm	Gene-specific reverse	66.9°C	TTGAAGATGTCAGAGTCAAGCAGG
LAR3	LacZ-specific reverse	63.6°C	CAACGGGTTCTTCTGTTAGTCC
Il23a-FOR	loxP-specific forward	63.3°C	TGAACTAGGGATCTGGAAGATAGG
Il23a-REV	loxP-specific reverse	71.9°C	TGAACTGATGGCGAGCTCAGACC

T_{melt}, melting temperature

Table 2: *Genotyping PCR cycling conditions*

Step	Temperature	Time	Cycles
Initial Denaturation	95°C	3 min	
Denaturation	95°C	30 sec	35 x
Annealing	62°C	30 sec	
Extension	72°C	1 min	
Final extension	72°C	10 min	

3.3 sgRNA design

sgRNAs were designed using the Broad Institute GPP sgRNA Designer (https://portals.broadinstitute.org/gpp/public/analysis-tools/sgrna-design). Three sgRNAs per target gene were designed and validated in parallel. sgRNA sequences are listed in Table 3. For cloning into the BbsI sites of the pMSCV backbone, a CACC overhang was added at the 5' end of the forward sequence and an AAAC overhang was added at the 5' end of the reverse sequence.

Table 3: *SgRNA sequences*

sgRNA name	Sequence (5'–3')
sgIL-6-1	GTATACCACTTCACAAGTCGG
sgIL-6-2	GCCTACTTCACAAGTCCGGAG
sgIL-6-3	GATGGTACTCCAGAAGACCAG
sgTNFα-1	GTAGACAAGGTACAACCCAT
sgTNFα-2	GAAGAAATCTTACCTACGACG
sgTNFα-3	GCTACTGAACTTCGGGGTGAT
sgNT (CTRL)	GCTGCATGGGGCGCGAATCA

3.4 Cloning procedures

3.4.1 Overexpression of cytokines

To be able to overexpress cytokines, pMSCV-based vectors were generated in which the cytokine cDNA sequence followed by an IRES2 and an eGFP reporter sequence was inserted into the multiple cloning site (MCS). The pMSCV-IRES2-eGFP vector was generously provided by Dr. Gurumoorthy Krishnamoorthy. Cytokine constructs were generated by Katarina Pinjusic and Anneli Peters in the lab. All cytokine sequences except *Il23a* were obtained via PCR-amplification from total cDNA isolated from primary mouse cells (B cells stimulated with LPS and anti-CD40 for IL-6; Th1 cells for IFNγ and Th17 cells for IL-10, GM-CSF and IL-21). The specific PCR-primers were designed based on mRNA-reference sequences in the NCBI data base (Table 4). The sequence for *Il23a* was obtained via PCR-amplification from the cDNA clone IRAVp968H0632D (Source Bioscience). All primers contained restriction sites for insertion into the MCS of the pMSCV-IRES2-eGFP vector. Digested cytokine sequences (PCR-products) were ligated into the vector with T4 Ligase. Cytokine-reporter constructs were transformed into competent DH5α bacteria and correct cloning was confirmed via Sanger sequencing.

Table 4: *Cytokine primers*

Primer name	T_{melt}	Sequence (5'–3')	Reference sequence
IL6 FWD (EcoRI)	65.3°C	CGGTAGAATTCAAACCGCTATGAAGTTC	NM_031168.2
IL6 REV (BamHI)	66.6°C	ACTAGGATCCTAGGCATAACGCACTAGG	
IFNg FWD (EcoRI)	70.7°C	CGGTAGAATTCGTTAACCTCGATCTACCAC	NM_008337.4
IFNg REV (BamHI)	75.9°C	ACTAGGATCCATCCGAGTCAGCAGCGACT	
GM-CSF FWD (EcoRI)	69.5°C	CGGTAGAATTCAGGAGGATGTGGCTGCAG	NM_009969
GM-CSF REV (BamHI)	66.6°C	ACTAGGATCCAAGCTGGATTCAGAGCTG	
IL10 FWD (EcoRI)	68.1°C	CGGTAGAATTCATCATGCCTGGCTCAGCA	NM_010548.2
IL10 REV (BamHI)	65.1°C	ACTAGGATCCAATACACACTGCAGGTGT	
IL23a FWD (EcoRI)	74.1°C	CGGTCGAATTCAAGCAGGGAACAAGATGC	IRAVp968H0632D
IL23a REV (SacII)	74.7°C	AATACCGCGGCTGGGCATCCTTAAGCTG	

T_{melt}, melting temperature. Restriction sites are labeled in grey.

3.4.2 CRISPR KO plasmids

To clone the sgRNA sequence, the MSCV-pklv2-gRNA-puroGFP plasmid (kindly provided by Prof. Martin Kerschensteiner) was cut with BbsI-HF (NEB) for 30 min at 37 °C. Dephosphorylation of the 5' ends was performed by addition of Quick CIP (NEB) at 1 µl/µg DNA for the last 10 min of incubation following by heat-inactivation at 80 °C for 2 min. The linearized plasmid was gel-purified using the QIAquick Gel Extraction Kit (Qiagen) and the concentration was adjusted to 50 ng/µl.

Each pair of oligonucleotides was phosphorylated with T4 PNK (NEB) in T4 ligation buffer (NEB) for 30 min at 37 °C and then annealed by heating to 95 °C for 5 min and cooling to 25 °C at 5 °C/min. Annealed oligos were diluted 1:200 and ligated into the gel-purified vectors using Quick Ligase (NEB) at room temperature (RT) for 10 minutes. Cloned plasmids were transformed into Stellar™ Competent Cells (Takara) or JM109 Competent Cells (Promega) following the manufacturer's transformation protocols, amplified in LB medium containing 100 µg/ml ampicillin (Ampicillin Sodium Salt BioChemica, AppliChem) and isolated using the HiSpeed Plasmid Midi Kit (Qiagen) or the NucleoBond Xtra Midi EF Kit (Machery-Nagel).

3.5 Cultivation of feeder cells

40LB cells (BALB/c3T3 fibroblasts expressing CD40L and BAFF) were created and kindly provided by Prof. Daisuke Kitamura [140]. To generate feeder cells, which produce IL-21 themselves, a pMSCV-IL-21-IRES2-CD8a vector was cloned and introduced into 40LB cells via retroviral transduction. Transduced cells were sorted based on CD8a expression and cloned in a limiting dilution assay. Clones were screened for secretion of IL-21 by ELISA and for their capacity to expand primary B cells. This cell line was generated by Katharina Pinjusic and Anneli Peters in the lab and called 40LB-CD8-21 cells. Both feeder cell lines were routinely cultured in 40LB medium (DMEM; Sigma) containing 10 % heat-inactivated FBS (Sigma/Biochrom), 1 % penicillin-streptomycin, 2 mM L-glutamine, 100 µM non-essential amino acids, 1 mM sodium pyruvate and 5.72 µM β-mercaptoethanol (all Sigma) at 37 °C and 10 % CO_2. The cultures were kept subconfluent: cells were detached every 2–3 days with Trypsin-EDTA (Sigma) for 3–5 min at RT. The reaction was stopped by addition of three volumes of 40LB medium and the cells were pelleted by centrifugation at 300 g for 5 min. Subsequently, the cells were resuspended in 40LB medium and diluted at ratios of 1:6, 1:8 or 1:10 for further cultivation.

3.6 Retrovirus production

Phoenix-eco cells [141] were routinely cultured in TCM medium (DMEM containing 10 % heat-inactivated FBS, 1 % penicillin-streptomycin, 2 mM L-glutamine, 360 mg/l asparagine (Sigma), 1 % non-essential amino acids, 1 mM sodium pyruvate and 57.2 µM β-mercaptoethanol). The cultures were kept subconfluent by splitting them every 2–3 days as described for 40LB cells above. For production of retroviral supernatant, Phoenix cells were plated at 1.5–2 x 10^6 cells per 10 cm dish in TCM medium and allowed to attach for 18–24 hours. For transfection, chloroquine diphosphate (Sigma) was added to the cells to a final concentration of 25 µM. Per 10 cm dish 12 µg of pMSCV plasmid DNA and 3.5 µg of pCL-Eco packaging plasmid (generously provided by Dr. Gurumoorthy Krishnamoorthy) were prepared in 438 µl sterile H_2O and 62 µl 2M $CaCl_2$ (Riedel de Haën) was added. Then 500 µl 2x BES (50 mM N,N-bis(2hydroxyethyl)-2-aminoethanesulfonic acid + 280 mM NaCl (both Sigma) + 1.5 mM

Na_2HPO_4 (Roth) in H_2O) was added dropwise while vortexing. The mixture was incubated for 20 min at 37 °C and added dropwise to the cells. After incubating the cells overnight, the medium was replaced with 8 ml fresh and pre-warmed TCM. After another 24 h, the virus-containing supernatant was collected with a 10 ml syringe, filtered through a 0.45 µm filter and stored at 4 °C. 4 ml of fresh and warm TCM was added to each 10 cm dish and the cells were incubated for another 24 hours. Then the supernatant was collected and filtered through a 0.45 µm filter again. Supernatants from both days were pooled and concentrated by centrifugation through Amicon® Ultra 15 mL Centrifugal Filters (100 K; Merck) at 1000 g. The concentrated supernatant was snap frozen and stored at −80 °C.

3.7 Isolation of cells from bone marrow (BM)

BM cells were isolated from femurs and tibiae. Surrounding muscle tissue was removed with soft paper wipes. Intact bones were disinfected in 80 % ethanol and washed with phosphate-buffered saline (PBS). Then, the bones were opened on both sides and the bone marrow was flushed with ~10 ml sterile PBS using a 26 gauge needle. Cell clusters were dissolved by repetitive pipetting. Then, the cells were centrifuged at 300 g for 5 min and used for FACS analysis.

3.8 Isolation of cells from spleen and lymph nodes

Lymph nodes were homogenized and passed through a 70 µm cell strainer. The cells were then centrifuged at 300 g for 5 min and resuspended in iGB medium (RPMI 1640 (Sigma) containing 10 % heat-inactivated FBS, 1 % penicillin-streptomycin, 10 mM HEPES (Sigma), 2 mM L-glutamine, 1 % non-essential amino acids, 1 mM sodium pyruvate and 50 µM β-mercaptoethanol).

Spleens were homogenized and centrifuged. Then, red blood cell lysis was performed by resuspending the cells in ACK buffer (150 mM NH_4Cl, 10 mM $NaHCO_3$ (both Merck), 0.1 mM EDTA (Sigma)) for 1–2 minutes at RT. Lysis was stopped by addition of 8 ml complete iGB medium and the cell suspension was filtered through a 70 µm filter. After centrifugation, the cells were resuspended in iGB medium.

3.9 Stimulation of primary B cells for intracellular cytokine staining

Mouse B cells were isolated from total splenocytes by positive selection using a biotinylated anti-B220 antibody (clone RA3-6B2, BD Pharmingen) and MojoSort™ Streptavidin Nanobeads (BioLegend) according to the manufacturer's instructions. Alternatively, B cells were isolated using the EasySep™ Mouse B Cell Isolation Kit (Stem Cell Technologies) according to the manufacturer's instructions. If applicable, different B cell subsets were sorted by FACS (chapter 3.17). Purified B cells or sorted follicular B cells were cultured at 2 x 10^6 cells/ml in iGB medium containing 10 µg/ml LPS (Sigma) with or without 2.5 µg/ml anti-CD40 (BioLegend) for 12 or 24 hours. Sorted MZ B cells were stimulated at a concentration of 1 x 10^6 cells/ml. For the last 4 hours of stimulation, 50 ng/ml PMA, 1 µg/ml ionomycin and 5 µg/ml brefeldin A (all Sigma) were added to the cultures. Then, the cells were collected, washed and stained for flow cytometry analysis.

3.10 iGB cell culture

iGB culture conditions as described by Nojima et al. [140] were slightly adjusted. One day prior to the start of the culture, 40LB cells were seeded at 3.1 x 10^3 cells/cm^2 and allowed to attach overnight. Then, 2.6 x 10^4/cm^2 purified B cells were cultured on 40LB cells in the presence of 1 ng/ml recombinant mouse (rm)IL-4 (BioLegend) for 3 days (d4 iGB cells). Then, iGB cells were collected by incubation with pre-warmed PBS (Sigma/Gibco) containing 0.5 % BSA (Roth) and 2 mM EDTA. d4 iGB cells were washed, counted and either used for analysis or adoptive transfer or seeded on fresh feeder cells for another round of culture. In the second phase of the culture, the cells were cultured at 1.7 x 10^3/cm^2 on 40LB cells in the presence of 10 ng/ml rmIL-21 (BioLegend) or directly seeded on 40LB-CD8-21 cells without additional cytokines for another 3 days (d7 iGB cells/iPBs).

3.11 Retroviral transduction of iGB cells

For overexpression or CRISPR-Cas9-mediated knock-down of a specific cytokine, iGB cells were retrovirally transduced 48 h after start of the culture by addition of 2 ng/ml rmIL-4, 4 µg/ml polybrene (Sigma) and 1:50-diluted retroviral supernatant to the culture. The next morning, iGB cells were collected, washed, and seeded on fresh feeder cells. For analysis or transfer on day 5, the cells were seeded on fresh 40LB cells with 1 ng/ml IL-4 and incubated overnight. For analysis or transfer on day 7, second phase culture conditions were as described above. For CRISPR-Cas-mediated knock-down, transduced cells were selected by addition of 1.25 µg/ml puromycin (Invivogen) during the second phase of the culture.

3.12 Differentiation of different T cell subsets *in vitro*

Naïve $CD4^+$ T cells were isolated from spleen and LN cells using the Naïve CD4+ T Cell Isolation Kit, mouse (Miltenyi) according to the manufacturer's instructions. The remaining non-naïve $CD4^+$ T cell fraction was collected and irradiated at 35 Gy and used as APCs. Naïve $CD4^+$ T cells were cultured at a concentration of 1.5–2 x 10^6 cells/ml in iGB or T cell medium (RPMI 1640 containing 10 % heat-inactivated FBS, 1 % penicillin-streptomycin, 10 mM HEPES, 2 mM L-glutamine, 1 % non-essential amino acids, 1 mM sodium pyruvate and 50 µM β-Mercaptoethanol) in the presence of 7.5–10 x 10^6/ml irradiated APCs and stimulated with anti-CD3 antibody (clone 145-2C11, BioXCell) at 2.5 µg/ml. Alternatively, the naïve $CD4^+$ T cells were cultured on a plate coated with anti-CD3 and anti-CD28 (clone PV-1, BioXCell) antibodies at 2 µg/ml in PBS for 1 hour at 37 °C. For Tregs, anti-CD3 was coated at 0.5 µg/ml only. Different T cell subsets were generated by addition of different combinations of cytokines. Th1 cells were generated by addition of rmIL-12 (10 ng/ml; BioLegend) and anti-IL-4 (10 µg/ml; clone 11B11, BioXCell). Th17 cells were obtained by addition of rmIL-6 (30 ng/ml; BioLegend), rmIL-1β (20 ng/ml; BioLegend), rmTGFβ (3 ng/ml; BioLegend), anti-IL-4 (10 µg/ml) and anti-IFNγ (10 µg/ml; clone XMG1.2, BioXCell). For Treg differentiation, the cells were cultured in the presence of rmTGFβ (3 ng/ml), anti-IL-4 (10 µg/ml) and anti-IFNγ (10 µg/ml).

After 48 hours, the cells were removed from the coated plate (if applicable) and split 1:3 with fresh medium. For Th1 cells and Tregs, IL-2 was added at a concentration of 10 ng/ml rmIL-2 (BioLegend). Th17 cells were split with medium containing 10 ng/ml rmIL-23 (Miltenyi Biotec). On day 4 of the culture, successful differentiation was tested by intracellular cytokine staining and subsequent flow cytometry.

3.13 *In vitro* B:T cell co-culture

Follicular or MZ B cells from Th mice were sorted by FACS as described in section 3.17. $CD4^+$ T cells were isolated from the spleens of 2D2 mice by negative selection using the EasySep™ Mouse CD4+ T Cell Isolation Kit (StemCell Technologies). $CD4^+$ T cells were labeled with CellTrace™ Violet (Invitrogen) according to the manufacturer's instructions. Briefly, up to 1 x 10^7 cells were resuspended in 1 ml PBS and incubated with 5 µM CellTrace™ Violet for 20 min at RT protected from light. Then, 5 ml iGB medium were added to stop the staining reaction and the cells were incubated for 5 min at RT. After subsequent centrifugation, the cells were resuspended in iGB medium and the cell number was determined. Th B cell subsets and 2D2 $CD4^+$ T cells were co-cultured in a 1:1 ratio at a concentration of 2 x 10^6 total cells/ml for 4 days. Then, $CD4^+$ cell proliferation was assessed by flow cytometry.

3.14 EAE induction

EAE was induced by different protocols described below. Animals were then monitored daily for clinical signs of EAE according to the following scoring criteria: 0, no disease; 0.5, decreased tail tonus; 1, limp tail; 1.5 limp tail and ataxia; 2, hind limb weakness; 2.5, partial hind limb paralysis; 3, complete hind limb paralysis; 3.5, complete hind limb and partial front limb paralysis; 4, complete front and hind limb paralysis; 5, moribund. Mice reaching a score of 2 were provided with gel pads and food pellets on the bottom of the cage.

3.14.1 Active immunization

Mice were injected subcutaneously (s.c.) with 100 µg $MOG_{35–55}$ peptide (BioTrend) emulsified in CFA (complete Freund's adjuvant containing 5 mg/ml *Mycobacterium tuberculosis* H37 RA (Difco)). Additionally, mice received 150–200 ng pertussis toxin (PTX, List labs) intraperitoneally (i.p.) on days 0 and 2 after immunization.

3.14.2 Adoptive transfer of in vitro differentiated Th17 cells

Naïve MOG-specific $CD4^+$ T cells were isolated from spleen and LNs of transgenic 2D2 mice and differentiated into Th17 cells as described in chapter 2.11. After confirming successful differentiation on day 4 of the culture, the cells were further cultured until a resting stage was observed on day 7. Then, the cells were collected and restimulated by culturing at a concentration of 2 x 10^6 cell/ml on a plate coated with anti-CD3 and anti-CD28 antibodies at a concentration of 2 µg/ml. After 48 hours, the cells were collected and washed 3 times with PBS. Then, 4 x 10^6 IL-17-producing cells were injected i.v. or i.p. into C57BL/6 recipient mice.

3.14.3 Co-transfer of iGB cells and MOG-specific 2D2 T cells

iGB cells were collected at indicated time points and washed by centrifugation at 300 g for 10 min. For loading iGB cells with MOG protein, the cells were resuspended at 1 x 10^7 cells/ml in iGB medium and cultured for 3 hours in the presence of mMOG (housemade in HEK-EBNA cells according to the protocol described in Perera et al., JI 2013 [142]) at a concentration of 10 µg/ml. Then, the cells were collected, washed and filtered through a 70 µm filter, washed two more times and resuspended in pre-warmed PBS. Then 1.5–2.5 x 10^7 iGB cells/mouse were injected i.p. into Rag1-KO recipients. MOG-specific $CD4^+$ T cells were isolated from transgenic 2D2 mice. For this, LN and spleen cells were collected, and single cell suspensions were prepared. $CD4^+$ T cells were isolated either by negative selection using the EasySep™ Mouse CD4+ T Cell Isolation Kit (StemCell Technologies) or the MojoSort™ Mouse CD4 T Cell Isolation Kit (BioLegend) or by positive selection using CD4 (L3T4) MicroBeads (Miltenyi) according to the manufacturer's instructions. After isolation, $CD4^+$ 2D2 T cells were resuspended in PBS and 4–5 x 10^6 cells/mouse were injected i.p. or i.v. into Rag1-KO recipients.

3.15 $MOG_{35–55}$ recall

Mice were immunized as described in chapter 3.14.1. Spleens were collected 6 days after immunization and 5 x 10^6 cells/ml were cultured with 10 µg/ml $MOG_{35–55}$ peptide or 10 µg/ml $MOG_{35–55}$ and 10 ng/ml rmIL-23 for 4–6 days. Then, the cells were collected and cytokine production was measured by intracellular flow cytometry.

3.16 Isolation of mononuclear cells from the CNS

Mice were sacrificed at indicated time points and perfused with PBS through the left cardiac ventricle. Brains were removed from the skull using scissors and forceps and spinal cords were flushed out of the vertebral column with PBS using a 21 gauge needle. To further collect the meninges, the vertebrae were opened with scissors and the meninges were collected with fine forceps. Brain and spinal cord were cut into small pieces and digested with Collagenase D (Roche) at a concentration of 3.75 mg/ml and DNase I (Roche) at a concentration of 1 mg/ml for 30 min at 37 °C. Then, the tissues were mashed, passed through a 70 µm cell strainer and centrifuged at 300 g for 10 min. The cell pellet was resuspended in 5 ml of a 70 % Percoll solution (Cytiva) and slowly overlayed with 5 ml of a 37 % Percoll solution. 70 % Percoll was prepared by mixing 30 ml Percoll with 18 ml Percoll Mix Solution (consisting of 90 ml 10x PBS and 264 ml H_2O) and 30 % Percoll was diluted from the 70 % Percoll solution by mixing with 1x PBS. Samples were centrifuged at 650 g for 30 min without breaks. Mononuclear cells were collected from the interface between the 37 % and 70 % layers and washed twice in iGB medium. Then, the cell number was determined and the cells were directly stained for flow cytometry or stimulated for intracellular cytokine staining.

3.17 Flow cytometry and cell sorting

For intracellular cytokine staining, isolated or cultured cells were restimulated for 4 h with 50 ng/ml phorbol 12-myristate 13-acetate (PMA) and 500 ng/ml ionomycin in the presence of 0.7 µl/ml BD GolgiStop™ (containing monensin). PMA is a phorbol diester, which has a similar structure as the signaling molecule diacylglycerol and thereby mimics endogenous TCR signaling by activating protein kinase C (PKC) [143, 144]. Together with

the ionophore ionomycin, which binds calcium ions (Ca^{2+}) and thereby increases intracellular Ca^{2+} levels [145], PMA-induced PKC stimulation leads to T cell activation and cytokine production. Monensin is an ionophoric ether that blocks the protein transport by the Golgi apparatus [146, 147] and thereby prevents the secretion of cytokines, which enhances their detectability by antibody staining and flow cytometry.

For fluorescence-activated cell sorting (FACS), the cells were washed with PBS. Viability staining was performed by incubating the cells with Zombie Violet™ or Zombie UV™ fixable viability dye (BioLegend) diluted 1:500 in PBS for 20 min at RT. Subsequently, the cells were washed with FACS Buffer (PBS containing 2 % FBS and 0.05 % sodium azide) and incubated with TruStain FcX™ (1:50; BioLegend) for 15 min at 4 °C to avoid unspecific binding of FACS antibodies to Fc receptors. Surface staining was performed with fluorescently labeled antibodies (Table 5) diluted in FACS buffer for 20 min at 4 °C. When staining with biotinylated antibodies, surface staining was followed by a washing step and a second incubation with APC-Cy7-conjugated streptavidin (BioLegend). Then, the cells were washed twice with FACS buffer and resuspended for analysis. For intracellular staining, the cells were fixed with 0.4 % paraformaldehyde (PFA) or using the Foxp3/Transcription Factor Fixation/Permeabilization Concentrate and Diluent (eBioscience) for 20 min at RT. Intracellular staining was performed by incubating the cells with indicated antibodies in PBS containing 2 % FBS and 0.1 % saponin (Sigma) or in 1x Permeabilization Buffer (eBioscience) for 30 min at 4 °C. Then, the cells were washed with permeabilization buffer and FACS buffer and resuspended in FACS buffer. All samples were measured on a BD FACSVerse™or a BD LSRFortessa™ flow cytometer and analyzed with FlowJo® software (TreeStar).

For cell sorting, surface staining of up to 6 x 10^7 cells/ml was performed in iGB medium for 30 min at 4 °C. After two washes, the cells were filtered through a 35 µm cell strainer and sorted using a BD FACSAria™ in the Core Facility Flow Cytometry at the Biomedical Center.

Table 5: *Antibodies used for flow cytometry*

Specificity	Clone	Host	Conjugate	Company	Dilution
Surface markers					
anti-human/mouse GL7	GL7	Rat IgM, κ	Biotin, AF 647	eBioscience, BD Pharmingen	1:200
anti-mouse CD11c	N418	Armenian Hamster IgG	BV 605	BioLegend	1:200
anti-mouse CD138	REA104	Recombinant human IgG1	APC	Miltenyi	1:50
anti-mouse CD138	281-2	Rat IgG2a, κ	PE	BD Pharmingen	1:200
anti-mouse CD19	6D5	Rat IgG2a, κ	BV 605	BioLegend	1:200
anti-mouse CD19	1D3	Rat IgG2a, κ	APC, PerCP-Cy5.5	BioLegend	1:200
anti-mouse CD1d	1B1	Rat IgG2b, κ	PerCP-Cy5.5	BioLegend	1:200
anti-mouse CD335	29A1.4	Rat IgG2a, κ	PerCP-Cy5.5	eBioscience	1:200
anti-mouse CD38	90	Rat IgG2a, κ	eFluor® 450	eBioscience	1:200
anti-mouse CD4	RM4-5	Rat IgG2a, κ	BV 605, PerCP-Cy5.5	BioLegend	1:200
anti-mouse CD4	GK1.5	Rat IgG2b, κ	PE	BD Pharmingen	1:200
anti-mouse CD45	30-F11	Rat IgG2b, κ	eFluor® 450	eBioscience	1:200
anti-mouse CD45.1	A20	Mouse IgG2a, κ	APC	BioLegend	1:200
anti-mouse CD5	53-7.3	Rat IgG2a, κ	AF 647	BioLegend	1:200
anti-mouse CD8a	53-6.7	Rat IgG2a, κ	APC-Cy7	BioLegend	1:200
anti-mouse CD95 (Fas)	Jo2	Armenian Hamster IgG2, λ2	PE-Cy7	BD Pharmingen	1:200
anti-mouse IgD	11-26c.2a	Rat IgG2a, κ	FITC	BD Pharmingen	1:200
anti-mouse IgG1	A85-1	Rat IgG1, κ	PE, APC	BD Pharmingen	1:200
anti-mouse IgM	II/41	Rat IgG2a, κ	PE-Cy7	eBioscience	1:200
anti-mouse Ly6C	HK1.4	Rat IgG2c, κ	PE-Cy7	BioLegend	1:200
anti-mouse Ly6G	1A8	Rat IgG2a, κ	APC	BioLegend	1:200
anti-mouse TCR Vα3.2 [b, c]	RR3-16	Rat IgG2b, κ	FITC	BioLegend	1:100
anti-mouse/human B220	RA3-6B2	Rat IgG2a, κ	PerCP-Cy5.5	BioLegend	1:200
anti-mouse/human B220	RA3-6B2	Rat IgG2a, κ	PE	BioLegend	1:200
anti-mouse/human CD11b	M1/70	Rat IgG2b, κ	AF 700, PE-Cy7	BioLegend	1:200

(continued)

Specificity	Clone	Host	Conjugate	Company	Dilution
Intracellular markers					
anti-mouse FoxP3	FJK-16s	Rat IgG2a, κ	APC	eBioscience	1:100
anti-mouse GM-CSF	MP1-22E9	Rat IgG2a, κ	PE	BioLegend	1:100
anti-mouse IFNγ	XMG1.2	Rat IgG1, κ	PE-Cy7	BioLegend	1:100
anti-mouse IL-10	JES5-16E3	Rat IgG2b, κ	PE	BioLegend	1:100
anti-mouse IL-10	REA1008	Recombinant human IgG1	PE	Miltenyi	1:50
anti-mouse IL-6	REA1034	Recombinant human IgG1	APC, PE	Miltenyi	1:50
anti-mouse TNFα	REA636	Recombinant human IgG1	APC	Miltenyi	1:50
anti-mouse/rat IL-17A	eBio17B7	Rat IgG2a, κ	APC	eBioscience	1:100

AF, Alexa Fluor®; APC, Allophycocyanin; BV, Brilliant Violet™; Cy, Cyanine; FITC, Fluorescein isothiocyanate; PE, Phycoerythrin; PerCP, Peridinin chlorophyll protein.

3.18 FACS-Gal assay

β-galactosidase (LacZ) expression was determined using the FACS-Gal assay as previously described [148]. Briefly, cells were resuspended in HBSS+ (Hanks' Balanced Salt Solution; Gibco) containing 2 % heat-inactivated FBS, 10 mM HEPES and 1 % penicillin-streptomycin) and prewarmed for 10 min at 37 °C in a water bath. Then the cells were mixed with equal volumes of prewarmed H_2O containing 2 mM Fluorescein di(β-D-galactopyranoside) (FDG) and incubated for exactly 1 min at 37 °C in the water bath. The reaction was stopped by adding 10 volumes of ice-cold HBSS+. Prior to FACS staining (section 3.17), the cells were kept on ice for 1.5 h to allow for accumulation of fluorescein in $LacZ^+$ cells.

3.19 Enzyme-linked immunosorbent assay (ELISA)

Cytokines and antibodies in cell culture supernatants or serum were measured by ELISA. 96 well high affinity, protein-binding plates (Nunc Maxisorp) were coated with the respective purified antibody at 4 °C overnight. Antibody concentrations and appropriate coating buffers are specified in Table 6. For the detection of MOG-specific antibodies, the plate was coated with rMOG (housemade) at 10 µg/ml in PBS. The next day, the plate was washed three times with wash buffer (PBS containing 0.05 % Tween-20 (Roth)) and blocked with ELISA blocking buffer (PBS containing 10 % FBS) for 1 hour at RT.

Following another three washes, cytokine standards (Table 6), culture supernatants and serum samples were diluted in blocking buffer and incubated for 4 hours at RT or overnight at 4 °C. After subsequent washing, biotin-labeled detection antibodies (Table 6) were diluted to 1 µg/ml in blocking buffer and incubated for 1 hour at RT and washed again. Then, avidin-horseradish peroxidase (HRP; eBioscience) was diluted 1:1000 in blocking buffer and incubated for 30 min at RT. Following five extensive washes, the color reaction was developed by addition of TMB Substrate (BioLegend). The reaction was stopped with TMB Stop Solution (BioLegend) or 1 M sulfuric acid and the optic density (OD) was measured at 450 nm. All results were reported as mean values from samples tested in duplicates and cytokine concentrations were interpolated from the sigmoidal standard curve.

Table 6: *Antibodies used for ELISA*

Specificity	Clone	Host	Company	Concentration	Coating Buffer
Capture antibodies					
anti-mouse IL-6	MP5-20F3	Rat IgG1, κ	eBioscience	2 µg/ml	Carbonate
anti-mouse IL-10	JES5-2A5	Rat IgG1, κ	BioLegend	5 µg/ml	Phosphate
anti-mouse IFNγ	XMG1.2	Rat IgG1, κ	BioXCell	2 µg/ml	Carbonate
anti-mouse GM-CSF	MP1-22E9	Rat IgG2a, κ	BioLegend	2 µg/ml	Carbonate
anti-mouse IgG1	A85-3	Rat IgG1, κ	BD Pharmingen	1 µg/ml	PBS
anti-mouse IL-23 (p19)	MMp19B2	Mouse IgG2b, κ	BioLegend	3 µg/ml	Carbonate
Detection antibodies					
anti-mouse IL-6	MP5-32C11	Rat IgG2a, κ	BioLegend	1 µg/ml	–
anti-mouse IL-10	JES5-16E3	Rat IgG2b, κ	BioLegend	1 µg/ml	–
anti-mouse IFNγ	RA-6A2	Rat IgG1, κ	BioLegend	1 µg/ml	–
anti-mouse GM-CSF	MP1-31G6	Rat IgG1, κ	BioLegend	1 µg/ml	–
anti-mouse IgG1	A85-1	Rat IgG1, κ	BD Pharmingen	1 µg/ml	–
anti-mouse IgM	R6-60.2	Rat IgG2a, κ	BD Pharmingen	1 µg/ml	–
anti-mouse IL-23 p19	Polyclonal	Goat IgG	R&D	0.5 µg/ml	–

Table 7: *Cytokine standards used for ELISA*

Protein	Company	Standard range
Recombinant mouse IL-6	BioLegend	4.9 - 5000 pg/ml
Recombinant mouse IL-10	BioLegend	9.8 - 10000 pg/ml
Recombinant mouse IFNγ	BioLegend	4.9 - 5000 pg/ml
Recombinant mouse GM-CSF	BioLegend	3.9 - 4000 pg/ml
Recombinant mouse IL-23	Miltenyi	7.8 - 8000 pg/ml

3.20 Immunohistochemistry (IHC) of cryosections

For IHC, spleens were fixed in PBS containing 4 % PFA for 2 hours at 4 °C and then dehydrated in PBS containing 30 % sucrose at 4 °C overnight. Spleens were then embedded in O.C.T. compound (VWR Chemicals) and frozen at −80 °C. Spleens were cut longitudinally into 10 µm sections using a Leica CM1950 cryostat. Sections were directly placed on adhesion slides (Superfrost® Plus, Carl Roth) and frozen at −80 °C.

For staining with fluorescently labeled antibodies, the sections were thawed and fixed in acetone for 10 min and residual O.C.T. compound was removed by washing the sections twice with PBS. Sections were then blocked with TruStain FcX™ (1:50 in PBS containing 1 % BSA) for 1 h at RT in a humidified chamber. Subsequently, sections were incubated with anti-mouse MadCAM-1 (clone MECA-367, BioLegend) and biotinylated anti-mouse CD1d (clone 1B1, BioLegend) primary antibodies diluted in PBS containing 1 % BSA for 1 h in a humidified chamber. Then, the sections were washed three times with PBS containing 0.1 % Tween-20 for 10 min and incubated with an Alexa Fluor® 633-conjugated anti-rat IgG secondary antibody and Alexa Fluor® 488-conjugated streptavidin (both Life technologies) for 1 h at RT in a humidified chamber in the dark. After washing the sections with PBS containing 0.1 % Tween-20 three times for 10 min, the slides were mounted with VECTASHIELD® Antifade Mounting Medium containing DAPI (Vector Laboratories) and analyzed in the Core Facility Bioimaging of the Biomedical Center with a Leica SP8X WLL microscope.

3.21 RNA isolation and RT-PCR

RNA was isolated from polarized T cells after 4 days of *in vitro* culture using TRI Reagent® (Sigma) using the manufacturer's instructions. 500 ng RNA were reverse transcribed in a 20 µl reaction using the iScript™ gDNA Clear cDNA Synthesis Kit (Bio-Rad) according to the manufacturer's instructions. 1 µl cDNA were used in a RT-PCR reaction using *Il23a* gene-specific 5' arm and 3' arm primers and cycling conditions described above (section 3.2).

3.22 Western Blot

For western blotting, polarized T cells were lysed in RIPA buffer (150 mM sodium chloride, 50 mM Tris, 1 % NP-40, 0.5 % sodium deoxycholate, 0.1 % sodium dodecyl sulfate) containing protease inhibitor (Roche) for 60 min. After centrifugation, the protein-containing supernatants were collected and protein concentration was determined using the Pierce™ BCA Protein Assay Kit (Thermo Scientific) according to manufacturer's instructions. 16 µg total protein was separated under reducing conditions on a NuPAGE 4–12 % Bis-Tris gel (Invitrogen) and then transferred to a nitrocellulose membrane (iBlot™, Invitrogen) The membrane was blocked in 5 % milk for 1 h at RT and stained with a HRP-conjugated β-actin antibody (Santa Cruz) in PBS containing 0.05 % Tween-20 (PBST) and 5 % BSA for 2 h at RT. Then, the membrane was washed 3 times for 5 min and incubated with a biotinylated anti-mouse IL-23p19 antibody (R&D) at 4 °C overnight while shaking. After 3 washes with PBST, the membrane was incubated with HRP-Avidin (eBioscience) in 5 % milk for 1 h at RT. Subsequently, the membrane was washed again 3 times with PBST and immunoreactive bands were detected using the Amersham ECL Prime Western Blot Substrate (GE Healthcare).

3.23 Statistical analysis

Statistical analyses were performed using Graphpad Prism version 7. Appropriate statistical tests were selected as indicated in the figure legends. Differences between two groups were determined using two-tailed student's *t*-test (including Welch's correction for unequal variances, if necessary) when Gaussian distribution was assumed or non-parametric Mann-Whitney test for non-normally distributed data. The statistical differences between more than two groups were calculated using one-way ANOVA with Tukey's test for multiple comparisons.

4. Results

4.1 Characterization of B cell subsets and cytokines in MOG-specific B cells

4.1.1 Th B cells show an altered B cell subset distribution

Th mice that carry heavy chain knock-in B cells which secrete MOG-specific antibodies show no signs of spontaneous EAE [68]. However, when crossed with 2D2 mice, about 60 % of animals spontaneously develop severe EAE with a progressive disease course indicating that antigen-specific B and T cells cooperate to induce autoimmunity [69, 70]. However, the exact mechanism by which Th B cells contribute to disease development in this model, is not clear. Since MOG-specific antibody levels were similar between sick and healthy mice, whereas CD80 expression was enhanced in sick mice, it is likely that B cells contribute to spontaneous disease development through their APC function rather than antibody production [69, 70]. Furthermore, Th B cells could contribute to disease pathogenesis by secretion of cytokines, thereby promoting differentiation into specific pathogenic T cell subsets, such as Th1 or Th17 cells.

To test whether there are already fundamental differences in the B cell phenotype or activation status in Th mice, their B cells were analyzed by flow cytometry. In the bone marrow, stages of B cell development can be segregated by the differential expression of IgD and IgM (Figure 4A). Interestingly, Th mice showed higher proportions of IgD^+ IgM^+ early mature B cells as compared to WT mice (Figure 4B).

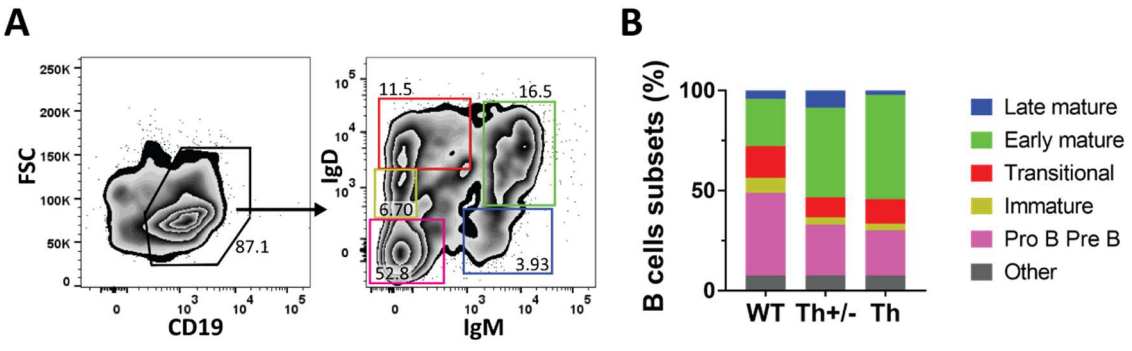

Figure 4: Th mice show an altered B cell subset distribution in the BM. *BM cells were isolated from WT, heterozygous Th+/- or homozygous Th mice and analyzed by flow cytometry. (**A**) Gating strategy. Cells were pre-gated on $B220^+$ $CD138^-$ cells in live singlets (not shown). Within the $CD19^+$ population, different B cell maturation stages can be identified by the differential expression of IgD and IgM. (**B**) B cell subset distribution in WT, heterozygous Th+/- and homozygous Th mice. Data is shown as mean values of different B cell subsets from 3–4 mice per group.*

After B cell maturation, B cells leave the bone marrow and enter the periphery. In the spleen, different B cell subsets can be distinguished: follicular B cells are primarily found in the follicles of the spleen (and also in follicles of lymph nodes). Upon activation, which requires the help of T cells, these B cells differentiate into plasma cells or memory B cells. In contrast, MZ B cells are found outside the follicle, in the marginal zone of the spleen and are thought to be activated primarily through TLR ligation independently of T cells [10]. Analysis of B cell subsets revealed an increase of IgM^{high} $CD1d^{+}$ MZ B cells in the spleens of Th mice (Figure 5A, B). While WT mice usually had less than 10 % MZ B cells, this proportion was increased to approximately 20 % in both heterozygous and homozygous Th mice (Figure 5C). This increase was not only seen relatively but also by increased absolute numbers of MZ B cells, whereas the number of follicular (Fol) B cells was not expanded (Figure 5D, E). These differences in the B cell subset distribution could further be visualized by IHC. In WT mice, $CD1d^{+}$ MZ B cells formed a thin ring around the follicle, separated by mucosal addressin cell adhesion molecule 1 $(MAdCAM\text{-}1)^{+}$ endothelial cells, which line the marginal sinus, a blood-filled vascular channel that regulates entry of cells into the follicle (Figure 5F). In Th mice, this MZ B cell ring was not only thicker, but some MZ B cells were located inside the marginal sinus indicating that they may be in closer proximity to the follicle and the T cell zone of the spleen (Figure 5G). Since there were no differences between heterozygous and homozygous mice, cells from heterozygous and homozygous mice were used interchangeably in the following experiments and just referred to as Th.

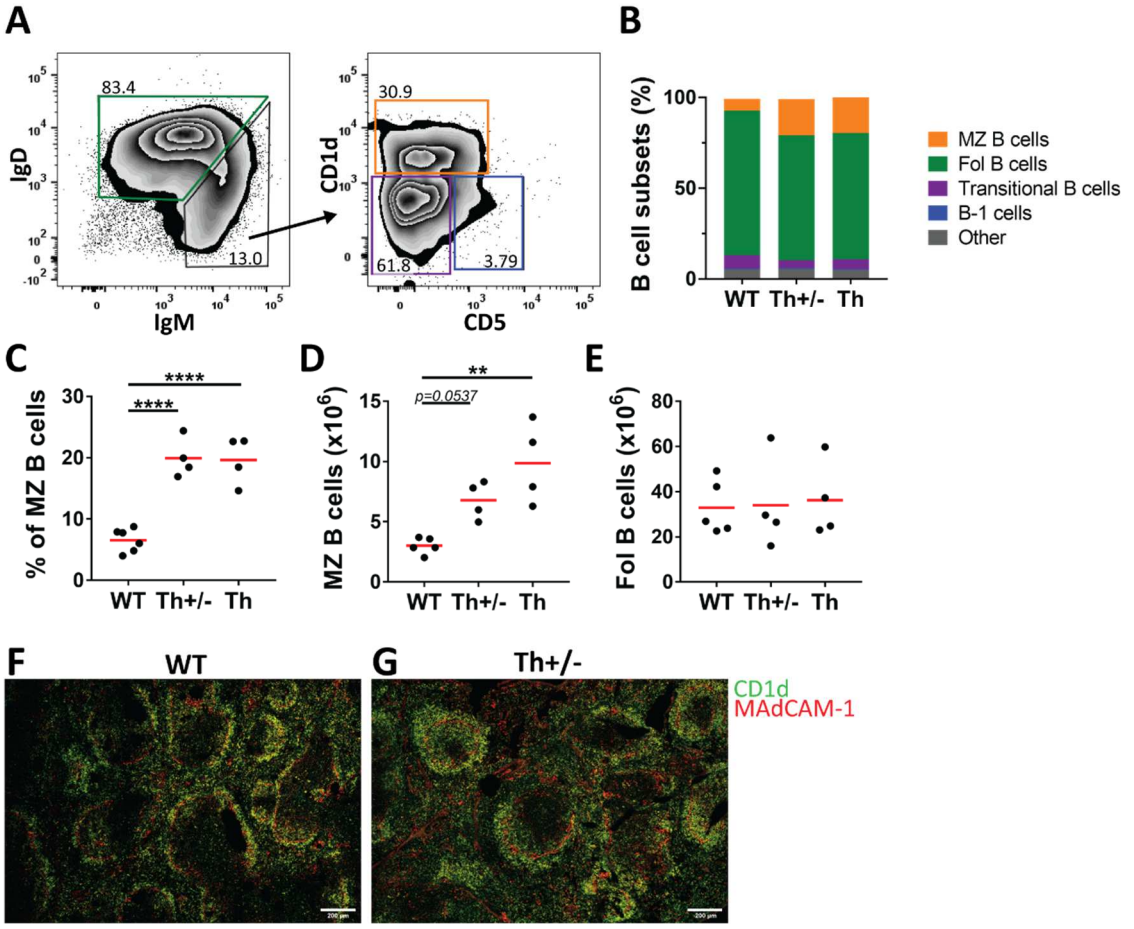

Figure 5: Th mice show increased numbers of MZ B cells in the spleen. *Splenocytes of WT, heterozygous Th+/- and homozygous Th mice were isolated and analyzed by flow cytometry. (**A**) Identification and (**B**) quantification of IgD^{high} follicular (Fol) B cells, IgM^{high} CD1d^{+} MZ B cells, IgM^{high} CD1d^{-} transitional B cells and IgM^{high} CD5^{+} B-1 cells. Data is shown as mean values of different B cell subsets in B220^{+} CD19^{+} B cells of 4–6 mice per group. (**C**) Frequency and (**D**) absolute numbers of MZ B cells or (**E**) Fol B cells in WT, Th+/- or Th mice. Horizontal lines indicate means. Dots represent individual mice. **p < 0.01, ****p < 0.0001, one-way ANOVA with Tukey post-test. (**F, G**) Splenic cryosections from WT or Th+/- mice were stained for MAdCAM-1^{+} marginal sinus-lining cells (red) and CD1d^{+} MZ B cells (green). Scale bars = 200 µm.*

To test whether these differences had an impact on their activation status, B cells from WT and Th mice were stained for the activation and germinal center marker GL7. Upon activation, B cells downregulate CD38 and acquire GL7 expression. However, no difference could be observed in the frequency of CD38^{-} GL7^{+} B cells neither in the spleen nor in the LNs of Th mice (Figure 6). Taken together, the distribution of B cell subsets in Th mice is different from WT mice but this does not lead to increased B cell activation.

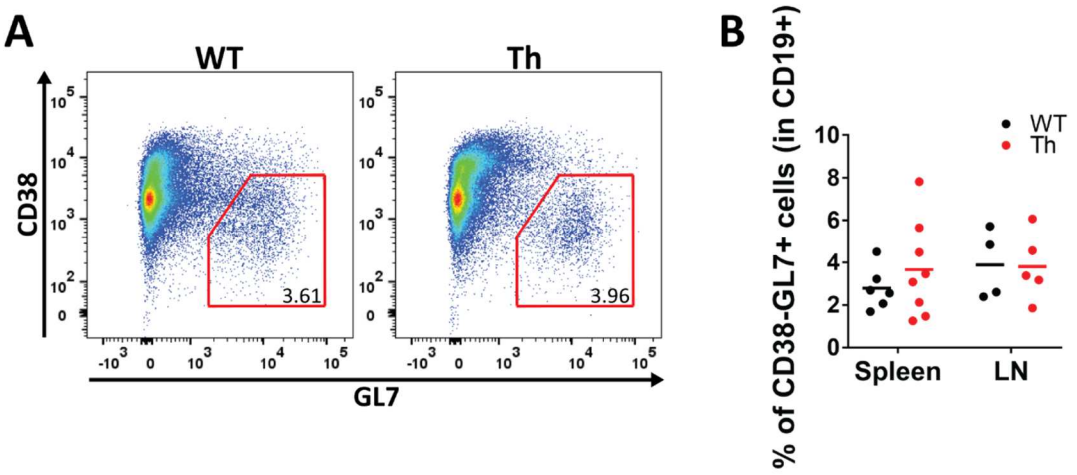

Figure 6: Activation status of WT and Th B cells. *Splenocytes from WT or Th mice were isolated and stained for CD38 and the GC marker GL7. (**A**) Representative FACS plots and (**B**) quantification of $CD38^-$ $GL7^+$ activated/GC B cells in spleen and LNs of WT and Th mice. Horizontal lines indicate means. Dots represent individual mice.*

4.1.2 Both Th follicular and MZ B cells can interact with 2D2 $CD4^+$ T cells

Since MZ B cells were shown to not only respond to T cell-independent antigens but also to interact with $CD4^+$ T cells [13, 14], the ability of Th B cell subsets to activate $CD4^+$ T cells was tested in an *in vitro* co-culture system. Therefore, follicular and MZ B cells were FACS sorted and co-cultured together with MOG-specific 2D2 $CD4^+$ T cells in the presence of MOG protein and $CD4^+$ T cell proliferation was measured by CellTrace™ Violet dye dilution. While 2D2 $CD4^+$ T cells were not able to respond to MOG protein antigen alone, proliferation was efficiently induced in the presence of Th B cells (Figure 7). Interestingly, both follicular and MZ B cells induced $CD4^+$ T cell proliferation equally well (Figure 7) indicating that both Th follicular and MZ B cells can contribute to T cell activation.

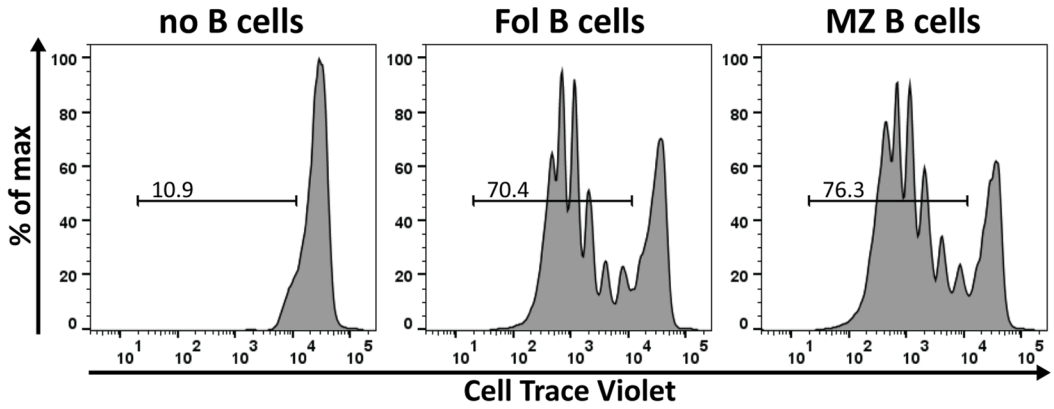

Figure 7: Both Th follicular and MZ B cells are able to activate 2D2 CD4⁺ T cells. *Fol B cells and MZ B cells were sorted based on their expression of IgD, IgM and CD1d (see Figure 5) and co-cultured with Cell Trace Violet (CTV)-labeled CD4⁺ T cells isolated from 2D2 mice at a 1:1 ratio in the presence of 10 µg/ml mMOG protein. CD4⁺ T cell proliferation was measured by CTV dilution after 4 days of co-culture. FACS plots show CTV dilution within the CD4⁺ cell population and are representative of three independent experiments.*

4.1.3 Th B cells show a more pro-inflammatory and less anti-inflammatory cytokine profile

MZ B cells are known to produce more cytokines, especially more IL-6 but also more IL-10 than follicular B cells [149]. To test whether the observed changes in the B cell subset distribution in Th mice affect their cytokine production, isolated B cells from Th or WT mice were stimulated with anti-CD40 + LPS (IL-6 and TNFα) or LPS alone (IL-10). The combination of LPS, which binds and activates TLR4, and agonistic anti-CD40, which mimics help usually obtained from activated T cells, provides both innate and adaptive stimuli and was shown to be the best condition for visualizing IL-6-producing B cells. In contrast, IL-10 was induced more efficiently by LPS stimulation alone [149]. After stimulation, B cell cytokine expression was analyzed by flow cytometry. Th B cells produced significantly more IL-6 and TNFα than WT B cells (Figure 8A, B, D, E). In contrast, IL-10 levels were reduced in Th B cells (Figure 8C, F), indicating that MOG-specific Th B cells have a more pro-inflammatory and less anti-inflammatory cytokine profile.

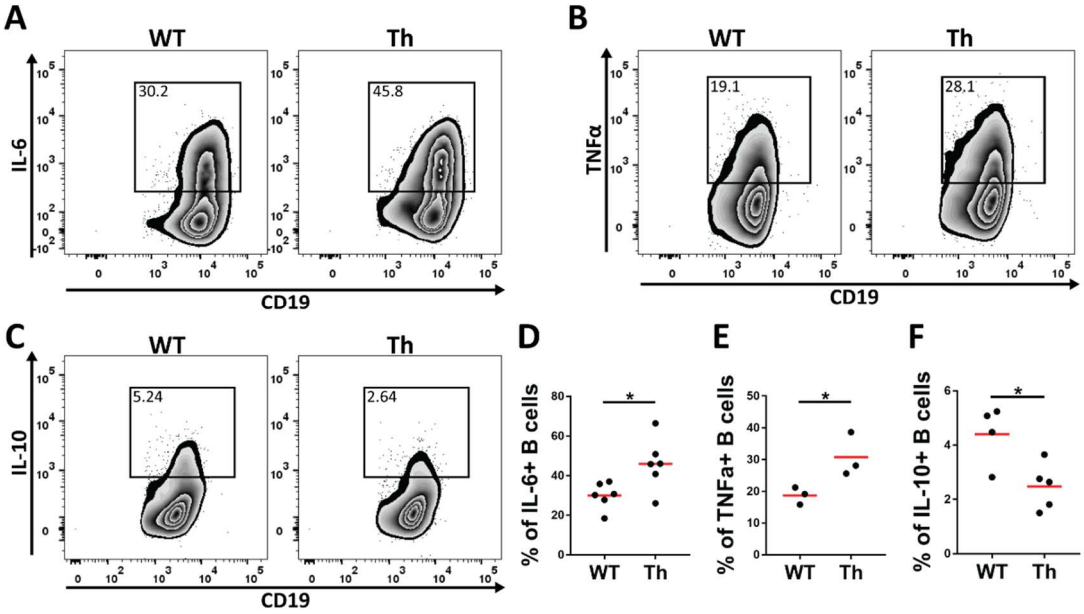

Figure 8: Th B cells show a more pro-inflammatory cytokine profile. *B cells were isolated from the spleens of WT or Th mice and stimulated with anti-CD40 and LPS for 24 hours (IL-6, TNFα) or LPS alone for 12 hours (IL-10). Prior to FACS staining, the cells were stimulated with PMA, ionomycin and brefeldin A for 4 hours. (**A–C**) Representative FACS plots and (**D–F**) quantification of IL-6, TNFα and IL-10 positive cells in CD19⁺ B cells. Horizontal lines indicate means. Dots represent individual mice. *p < 0.05, unpaired t-test.*

Since MZ B cells are known to produce more IL-6 than follicular B cells [149], we aimed to determine whether the differences in the cytokine profile could be explained by the increased numbers of MZ B cells in Th mice. Therefore, follicular and MZ B cells were sorted based on their expression of IgD, IgM and CD1d (Figure 5) and stimulated separately. As expected, IL-6 was mainly produced by MZ B cells, since 60–80 % of MZ B cells produced IL-6, whereas less than 30 % of Fol B cells produced IL-6 in both WT and Th mice (Figure 9A, C). However, the frequency of IL-6^{+} B cells was enhanced in both Fol B cells and MZ B cells from Th mice as compared to WT Fol B cells and MZ B cells respectively (Figure 9A, C). In contrast, TNFα was produced in similar amounts by Fol B cells and MZ B cells but the frequency of TNFα-producers was increased in Th mice both in the Fol B cell and in the MZ B cell compartment (Figure 9B, D). This indicates that both Fol B cells and MZ B cells contribute to the pro-inflammatory cytokine profile of Th B cells.

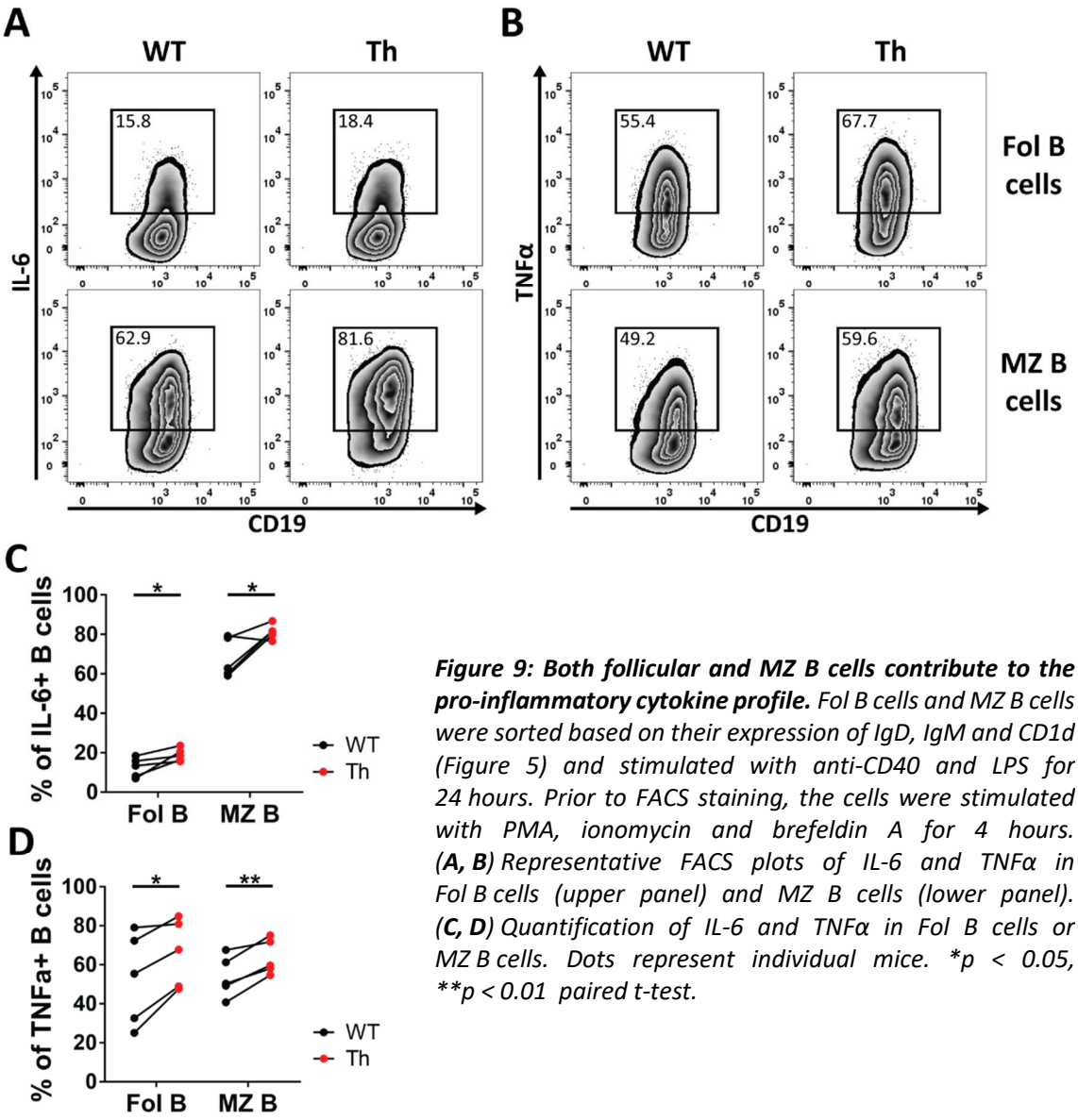

Figure 9: Both follicular and MZ B cells contribute to the pro-inflammatory cytokine profile. *Fol B cells and MZ B cells were sorted based on their expression of IgD, IgM and CD1d (Figure 5) and stimulated with anti-CD40 and LPS for 24 hours. Prior to FACS staining, the cells were stimulated with PMA, ionomycin and brefeldin A for 4 hours. (**A, B**) Representative FACS plots of IL-6 and TNFα in Fol B cells (upper panel) and MZ B cells (lower panel). (**C, D**) Quantification of IL-6 and TNFα in Fol B cells or MZ B cells. Dots represent individual mice. *p < 0.05, **p < 0.01 paired t-test.*

4.1.4 The presence of MOG-specific T cells does not enhance the pro-inflammatory profile of Th B cells

When Th mice are crossed with 2D2 mice, the prescence of both antigen-specific B and T cells leads to spontaneous EAE in about 60 % of animals with a very early onset at the age of 4–5 weeks [69, 70]. To test whether the changes in the B cell subset distribution or the more pro-inflammatory B cell cytokine profile could be futher enhanced in the presence of MOG-specific T cells, Th mice were crossed with 2D2 mice. In our animal facility, however, the spontaneous EAE incidence in 2D2 x Th mice (subsequently called OSE mice) was significantly lower than previously published. Only 17 % of OSE mice developed spontaneous disease and the age at disease onset varied between 5 and 12 weeks. (Table 8). B cell subsets and cytokines were analyzed in sick and healthy OSE mice. Sick mice were analyzed after 3–7 days of disease and healthy mice were analyzed after at least 20 weeks of age, in which no clinical signs of disease could be observed. Neither in healthy nor in sick OSE mice there was any difference in the frequency of MZ B cells or B cell cytokine production compared to age-matched Th littermates (Figure 10). Of note, MZ B cell numbers and IL-6 levels were lower in sick OSE mice and respective Th littermate controls since these mice were analyzed at younger age than healthy OSE mice and controls (Figure 10E, F). This indicates that MZ formation has not yet been completed at the time of disease onset and analysis. Taken together, the presence of MOG-specific T cells does not enhance MZ B cell frequency and pro-inflammatory B cell cytokine profile in Th B cells independent of spontaneous disease.

Table 8: *EAE incidence in OSE mice*

Mouse	Incidence	Age at onset (weeks)
OSE	4/24 (17 %)	8 ± 4.3

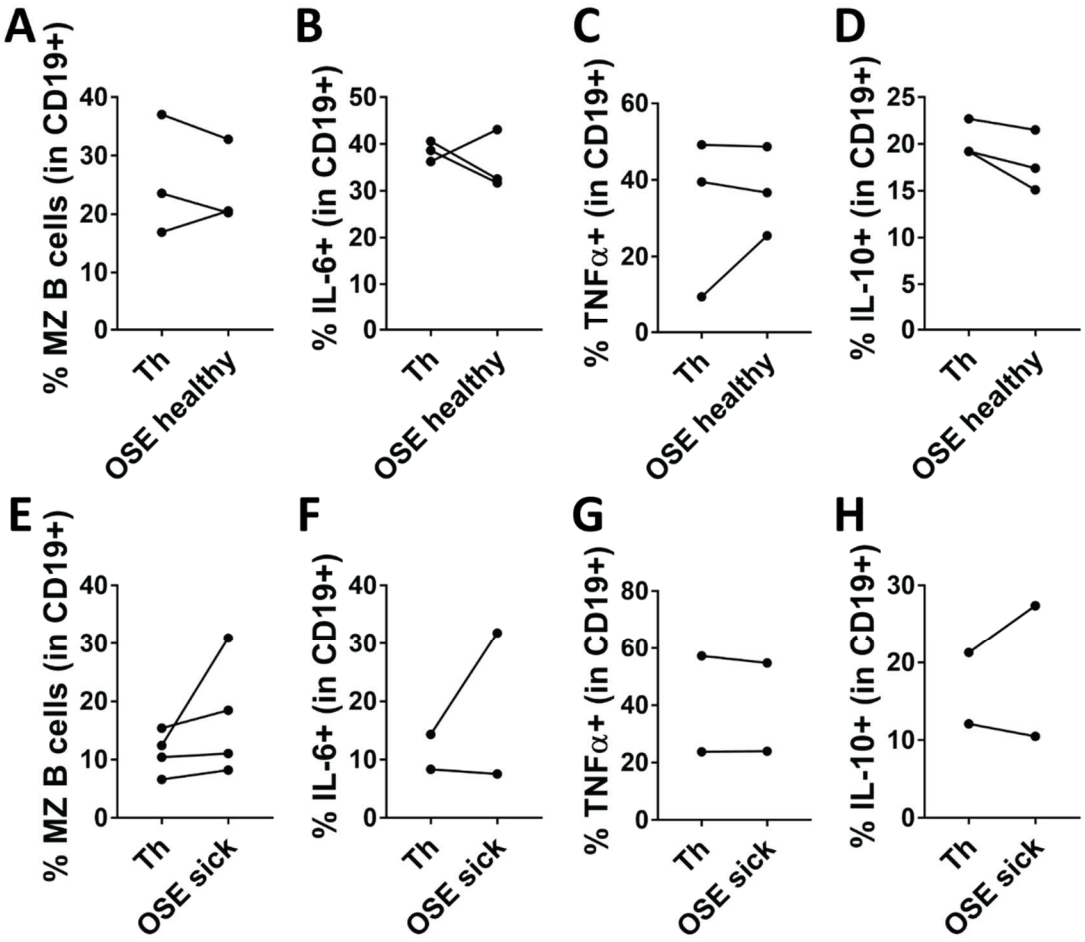

Figure 10: The presence of MOG-specific T cells does not enhance the pro-inflammatory profile of Th B cells. *B cells were isolated from the spleens of Th or OSE mice after 3–7 days of disease or after at least 20 weeks of age (healthy) and analyzed by flow cytometry. (**A**) Frequency of MZ B cells in the spleens of healthy or (**E**) sick OSE mice. For cytokine analysis, the cells were stimulated with anti-CD40 and LPS (IL-6, TNFα) or LPS alone (IL-10) for 24 hours. Prior to FACS staining, the cells were stimulated with PMA, ionomycin and brefeldin A for 4 hours. (**B–D**) Quantification of IL-6, TNFα and IL-10 positive cells in CD19⁺ B cells in Th and healthy or (**F–H**) sick OSE mice. Dots represent individual mice.*

4.2 The role of pro-inflammatory cytokines produced by antigen-specific B cells in EAE

4.2.1 Adoptively transferred Th iGB cells can cooperate with 2D2 T cells to induce EAE

To investigate the mechanisms by which antigen-specific B cells could interact with antigen-specific T cells to induce EAE and to evaluate the role of pro-inflammatory B cell cytokines in this process, a B cell adoptive transfer EAE model was developed. B cells were activated and expanded using the induced germinal center B cell (iGB) culture system published by Nojima et al. [140]. In this system, primary B cells are cultured on fibroblastic feeder cells expressing CD40L and BAFF leading to extensive B cell proliferation and expansion [140]. While CD40L mimics an activation signal usually provided by T_{FH} cells during the GC reaction, BAFF is usually expressed by T cells but also monocytes and DCs and promotes survival of the activated B cells [150]. After 3 days, B cells acquire a germinal center phenotype characterized by the upregulation of the GC markers Fas and GL7. Addition of IL-4, another signal usually provided by T_{FH} cells in the GC, further leads to isotype switching from IgM to IgG1 [140].

To test whether these highly activated iGB cells could induce EAE in an adoptive transfer system, WT or Th B cells were cultured in the iGB culture system for 3 days. To provide antigen and allow for a potential APC function of the iGB cells, the cells were incubated with MOG protein for 3 hours and transferred together with unmanipulated MOG-specific $CD4^+$ T cells isolated from 2D2 mice into Rag1-KO mice that lack endogenous B and T cells (Figure 11A). Importantly, only mice that received Th iGB cells developed disease whereas WT iGB recipients stayed completely healthy throughout the observation period of 30 days (Figure 11B) indicating that B cell antigen-specificity is required to activate 2D2 T cells. Transferred iGB cells could be partly recovered from both Th and WT iGB recipients and were found in the spleen and several LNs but did not migrate to the CNS in sick Th iGB recipients (Figure 11C). Consistent with these data, high titers of MOG-specific IgG1 antibodies could be detected in the serum of Th iGB recipients but not in the serum of WT iGB recipients (Figure 11D).

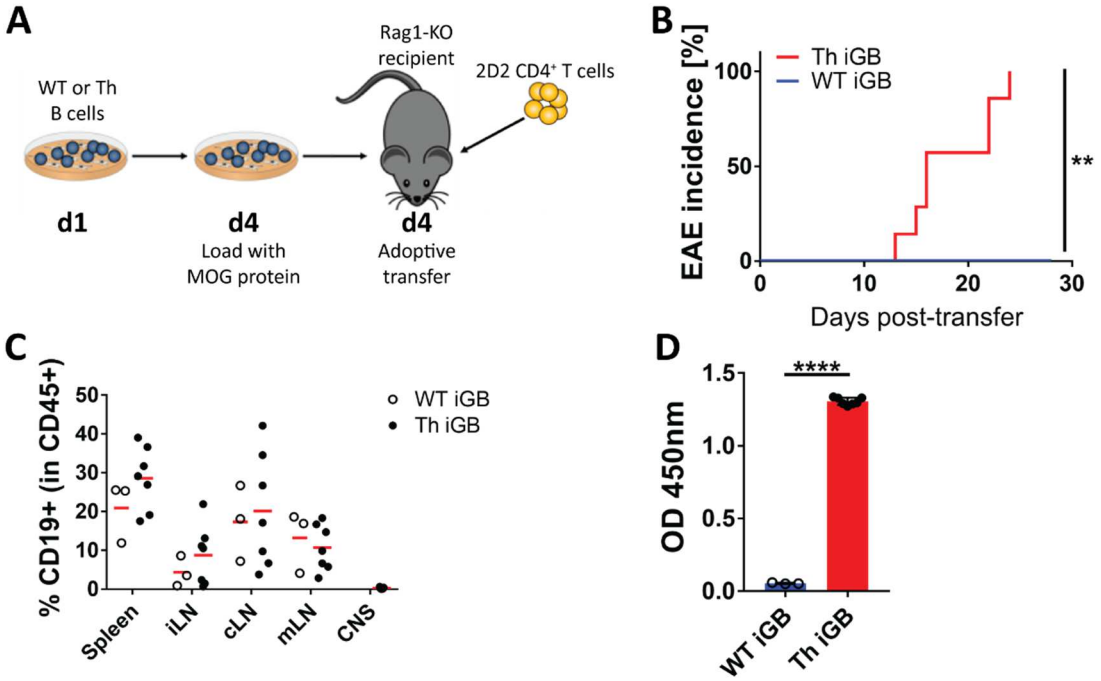

Figure 11: Th iGB cells can cooperate with 2D2 T cells to induce EAE. *(**A**) Experimental outline. WT or Th B cells were activated and expanded in the iGB culture system for 3 days. Then, the cells were loaded with MOG protein for 3 hours and 1.5 x 10^7 iGB cells were adoptively transferred together with 5 x 10^6 unmanipulated 2D2 CD4$^+$ T cells into Rag1-KO recipients. (**B**) EAE incidence in Rag1-KO mice that received either WT or Th iGB cells together with 2D2 CD4$^+$ T cells during the observation period of 30 days. Clinical data is shown for 3 mice (WT) or 7 mice per group (Th) pooled from 2 independent experiments. **p < 0.01 Mantel-Cox Log-rank test. (**C**) Frequency of CD19$^+$ B cells in different organs from recipient mice analyzed at the peak of disease (Th iGB) or at the end of the observation period (WT iGB). Horizontal lines indicate means. Dots represent individual mice. iLN, inguinal lymph node; cLN, cervical lymph node; mLN, mesenteric lymph node. (**D**) MOG-specific IgG1 antibodies in serum samples (1:1000 diluted) from iGB recipients were measured by ELISA. Results are shown as optical density (OD). Bars indicate means. Dots represent individual mice. ****p < 0.0001 unpaired t-test.*

Further phenotypic analysis showed that the transferred iGB cells downregulated Fas and GL7 expression *in vivo.* While more than 80 % of iGB cells expressed Fas and GL7 before transfer, the frequency of Fas$^+$GL7$^+$ B cells was reduced to less than 20 % in most organs (Figure 12A, C). Interestingly, loss of the GC phenotype was more pronounced in Th iGB cells especially in spleen and inguinal (i)LNs (Figure 12C). In contrast, the frequency of IgG1$^+$ cells remained stable or even increased after adoptive transfer (Figure 12B, D). Importantly, the frequency of IgG1$^+$ B cells in spleen and mesenteric (m)LNs, was significantly higher in Th iGB recipients than in WT iGB recipients and a similar trend could be observed in cervical (c)LNs (Figure 12D). This could indicate that the antigen-specific B cells continued to differentiate specifically in spleen and mLN in

response to interaction with antigen-specific CD4$^+$ T cells. Together, these data indicate that Th iGB cells can cooperate with 2D2 CD4$^+$ T cells to induce EAE and that this interaction takes place in the periphery, with a potential focus on spleen and mLNs.

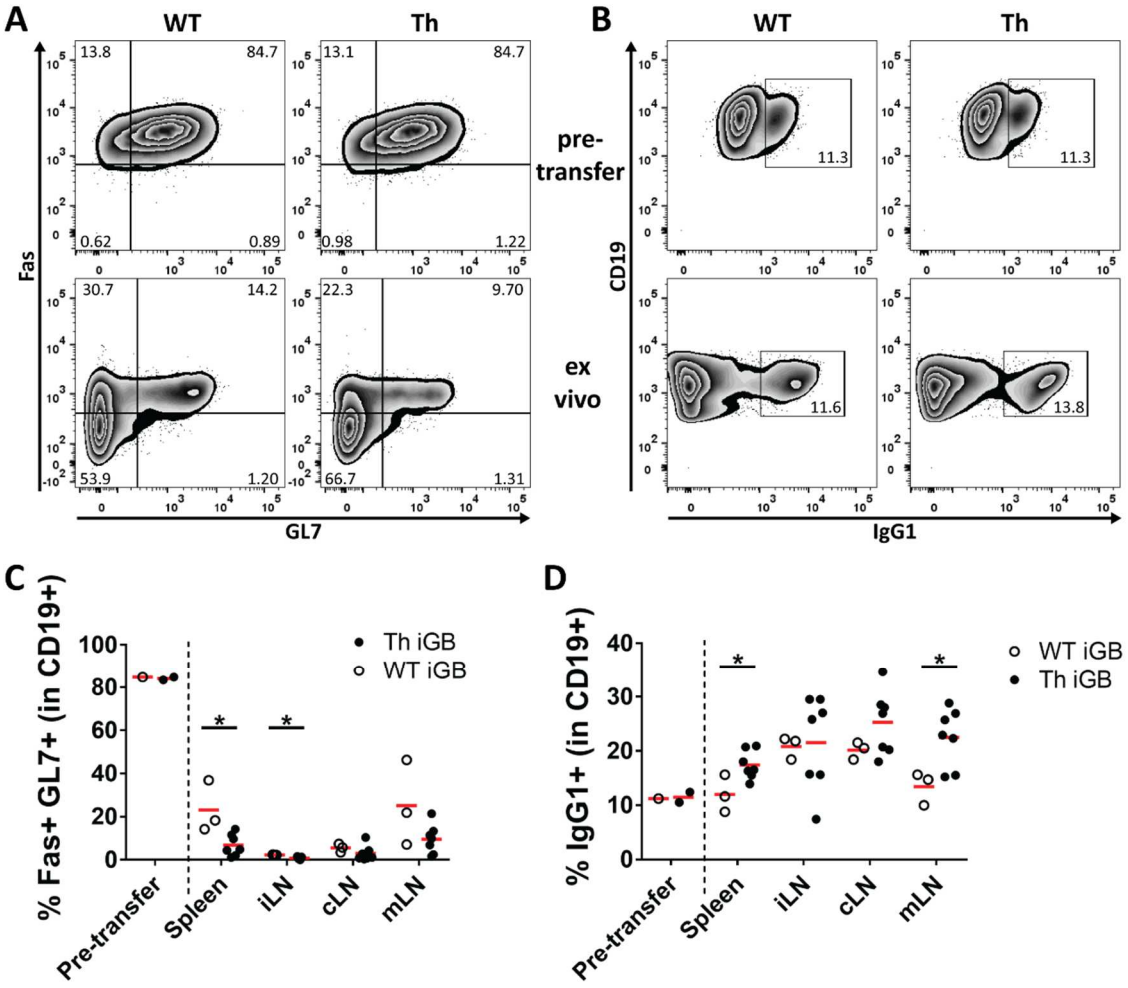

Figure 12: B cell phenotype before and after adoptive transfer. *iGB recipients were analyzed at the peak of disease (Th iGB) or at the end of the observation period (WT iGB) and the B cell phenotype was compared to iGB cells before transfer. Representative flow cytometry plots of (**A**) Fas and GL7 and (**B**) IgG1 expression before and after transfer in the spleen. (**C**) Quantification of Fas$^+$ GL7$^+$ or (**D**) IgG1$^+$ B cells before and after adoptive transfer in different organs. Horizontal lines indicate means. Dots represent individual mice. *p < 0.05 unpaired t-test. iLN, inguinal lymph node; cLN, cervical lymph node; mLN, mesenteric lymph node.*

When analyzing the T cell phenotype, we observed that 2D2 CD4$^+$ T cells in the spleen and in the CNS of Th iGB recipients produced mainly IFNγ with a small population of IFNγ$^+$ IL-17A$^+$ cells (Figure 13A). Furthermore, a small population of IFNγ$^+$ IL-10$^+$ CD4$^+$ T cells could be detected in both spleen and CNS (Figure 13B) indicating that after activation, 2D2 CD4$^+$ T cells primarily differentiate into Th1 cells in this experimental system.

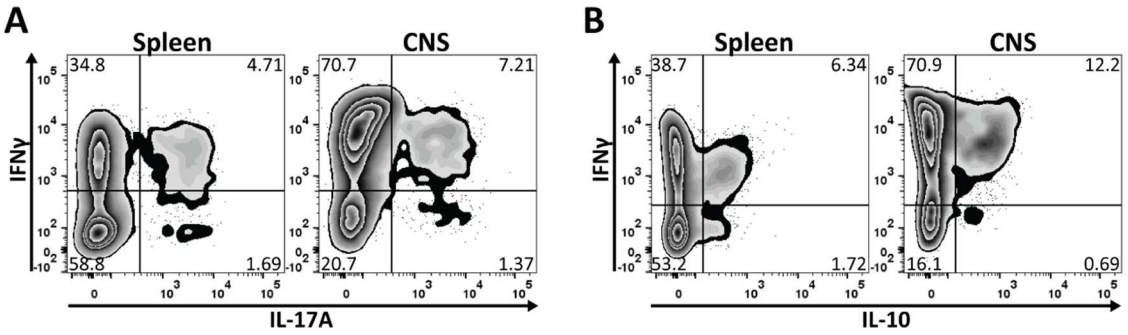

Figure 13: 2D2 CD4$^+$ T cells differentiate into Th1 cells after adoptive transfer. *Th iGB recipients were analyzed at the peak of disease and T cell cytokines in spleen and CNS were measured by intracellular flow cytometry. (**A**) Frequency of IFNγ and IL-17A or (**B**) IFNγ and IL-10 expression in CD4$^+$ T cells in spleen and CNS. Flow cytometry plots are representative for n = 7 mice pooled from 2 independent experiments.*

4.2.2 Both switched and unswitched Th iGB cells can induce EAE

Since Th iGB cells produced very high levels of MOG-specific IgG1 antibodies *in vivo* after adoptive transfer (Figure 11D), the question arose whether MOG-specific IgG1 antibodies mediated pathogenicity of Th iGB cells but not WT iGB cells in this adoptive transfer system. To test this, Th iGB cells were cultured in the absence of IL-4, which is the cytokine that induces isotype switching to IgG1 [22]. Expansion rates of the B cells in iGB culture were similar in the absence or presence of IL-4 (not shown), however, iGB cells cultured without IL-4 showed lower levels of Fas and especially GL7, indicative of a less advanced GC phenotype (Figure 14A). As expected, these cells did not switch their isotype, whereas 10–20 % of $IgG1^+$ B cells could be observed when the cells were cultured in the presence of IL-4 (Figure 14A). When switched versus unswitched Th iGB cells were co-transferred with 2D2 $CD4^+$ T cells into Rag1-KO recipients, both populations could induce EAE with only slightly, but not significantly different incidence and time point of onset (Figure 14B). MOG-specific IgG1 levels were still detectable in the serum of mice receiving unswitched Th iGB cells but were significantly reduced as compared to mice receiving switched Th iGB cells (Figure 14C). In contrast, MOG-specific IgM levels in the serum were similar between the two groups (Figure 14C). Interestingly, mice that developed EAE upon transfer of unswitched Th iGB cells showed higher MOG-specific IgG1 titers than mice from the same group that remained healthy (Figure 14D). This effect was not observed in sick versus healthy mice receiving switched Th iGB cells. Also, no disease-status-dependent differences were observed for MOG-specific IgM titers in any of the two groups (Figure 14D). Consistent with this data, FACS analysis showed slightly higher frequencies of $IgG1^+$ B cells recovered from the spleens of sick mice that received unswitched Th iGB cells as compared to healthy mice receiving the same cells (Figure 14E). This could indicate that when B:T cell interaction takes place and leads to development of EAE, the B cells further develop and start isotype switching, potentially by receiving stimuli from the activated T cells. Furthermore, these data show that the secretion of high levels of MOG-specific IgG1 antibodies is not required to induce EAE and imply that APC function and possibly cytokine production are essential for B cell pathogenicity in this experimental model.

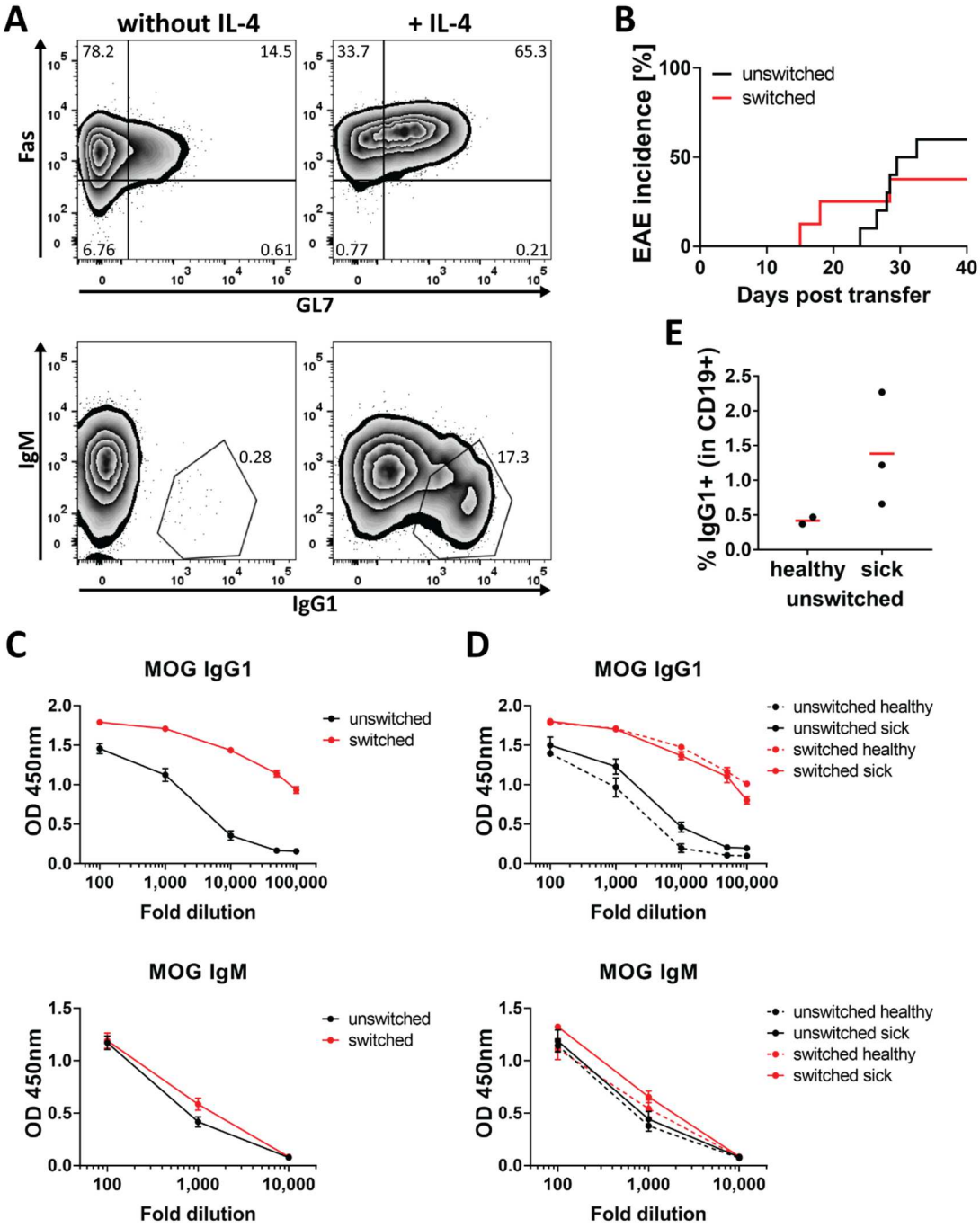

Figure 14: Both switched and unswitched Th iGB cells can induce EAE. *Th B cells were cultured in the iGB culture system for 3 days in the absence or presence of IL-4. Then, the cells were loaded with MOG protein for 3 hours and 1.5 x 10^7 iGB cells were adoptively transferred together with 5 x 10^6 unmanipulated 2D2 CD4⁺ T cells into Rag1-KO recipients. (**A**) iGB phenotype before adoptive transfer in cells cultured in the absence (left panel) or presence (right panel) of IL-4. (**B**) EAE incidence in Rag1-KO mice that received either unswitched (without IL-4) or switched (+ IL-4) Th iGB cells together with 2D2 CD4⁺ T cells during the observation period of 40 days. Clinical data is shown for 10 mice (unswitched) or 8 mice per group (switched) pooled from 2 independent experiments. (**C**) MOG-specific IgG1 and IgM levels in the serum of mice receiving unswitched (black) or switched (red) Th iGB cells. (**D**) Serum antibody levels from (**C**) shown separately for mice that developed EAE (solid lines) and mice that remained healthy (dashed lines). Dots indicate means ± SEM for 10 mice (unswitched) or 8 mice per group (switched) pooled from 2 independent experiments. (**E**) Frequency of IgG1⁺ B cells in the spleen of healthy or sick mice that received unswitched Th iGB cells. Horizontal lines indicate means. Dots represent individual mice.*

4.2.3 Establishment of cytokine overexpression in primary B cells using retroviral transduction

To test whether expression of different cytokines by Th iGB cells would shape the T cell response and thereby influence EAE development or severity, a protocol to retrovirally overexpress different cytokines in iGB cells was developed. For this, B cells were cultured in the iGB culture system for 48 hours and then transduced using murine stem cell virus (MSCV) retrovirus (Figure 15A). MSCV constructs expressed the cytokine of interest together with eGFP from an internal ribosome entry sequence (IRES) allowing to monitor transduction efficacy (Figure 15B) via FACS. Transduction efficacy, as determined by GFP expression on d5 of the culture, ranged between 20 % and 70 % in both WT and Th iGB cells (Figure 15C). Overexpressed cytokines were actively secreted by the transduced iGB cells as very high concentrations of the respective cytokines could be measured in the culture supernatants (Figure 15D). Interestingly, IL-10 was the only cytokine that could be measured in substantial levels in iGB cells transduced with an empty vector indicating that iGB cells naturally express IL-10 under iGB culture conditions.

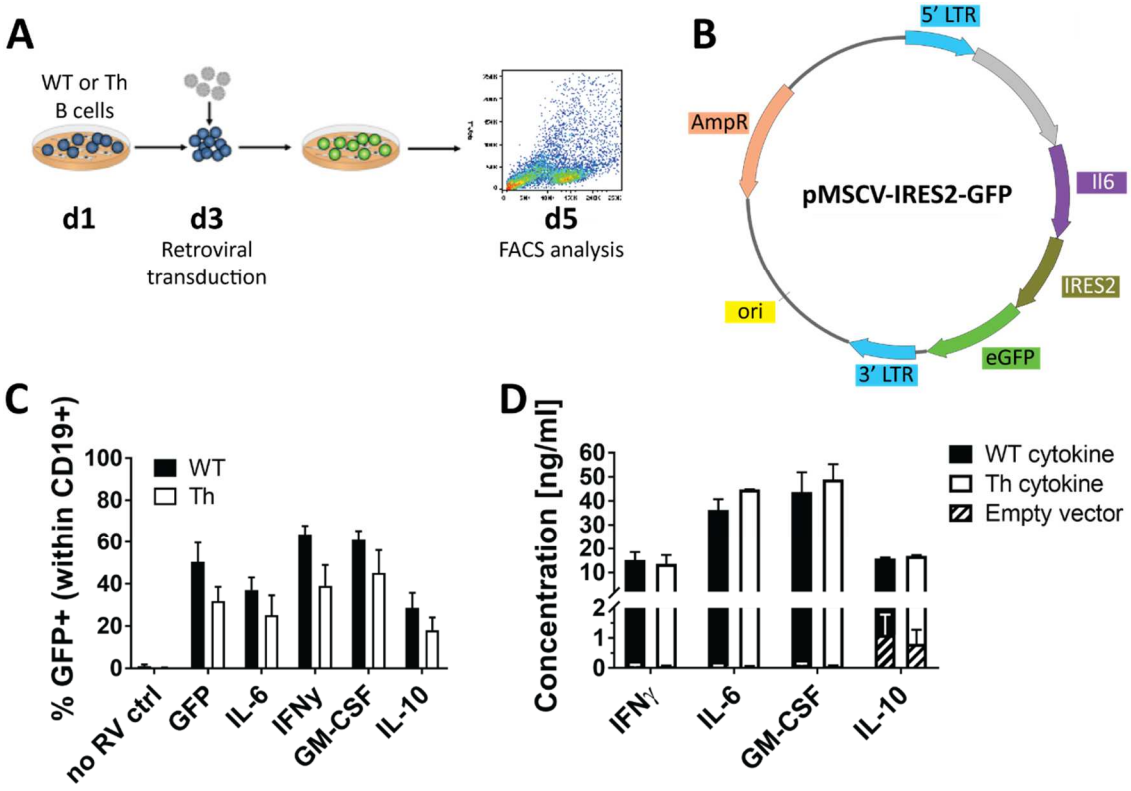

Figure 15: Retroviral overexpression of different cytokines in iGB cells. *(**A**) Experimental outline. WT or Th B cells were cultured in the iGB culture system. After 48 hours, the cells were retrovirally transduced in the presence of IL-4 and IL-21 and then cultured on fresh feeder cells in the presence of IL-21. Two days after retroviral transduction, iGB cells were analyzed by FACS. (**B**) pMSCV-IRES2-GFP construct containing the* Il6 *gene, which is expressed together with an enhanced green fluorescent protein (eGFP) from an internal ribosome entry sequence (IRES). AmpR, Ampicillin resistance; LTR, long terminal repeat; ori, origin of replication. (**C**) Frequency of GFP⁺ cells on d5 of iGB culture in WT (open bars) or Th iGB cells (filled bars). (**D**) Cytokine concentration in the culture supernatants was measured by ELISA. Striped bars represent cytokine levels in cultures transduced with an empty eGFP vector. Data is shown as mean + SEM from 2–5 replicates.*

4.2.4 IL-6 production by antigen-specific B cells can enhance their ability to induce EAE

The initial *in vivo* Th iGB transfer experiments suggested that 2D2 $CD4^+$ T cells primarily differentiated into Th1 cells (section 4.2.1). However, since Th17 cells are highly encephalitogenic and one of the key cytokines for Th17 differentiation is IL-6 [84-86], we wondered, whether IL-6 expression by iGB cells during antigen presentation could skew the T cell phenotype towards a Th17 profile and thereby influence the development of EAE. To test this hypothesis *in vivo* in our iGB adoptive transfer model, IL-6 was retrovirally overexpressed in iGB cells (iGB_6) and WT or Th iGB_6 cells or Th iGB cells transduced with an empty vector (iGB_{GFP}) were co-injected together with 2D2 $CD4^+$ T cells into Rag1-KO recipient mice. GFP levels remained stable after adoptive transfer indicating that both transduced and non-transduced iGB cells survived equally well in Rag1-KO recipient mice (Figure 16A). Furthermore, IL-6 could be measured in the serum of both Th iGB_6 and WT iGB_6 recipients whereas only very low levels of IL-6 were detectable in the serum of Th iGB_{GFP} recipients (Figure 16B).

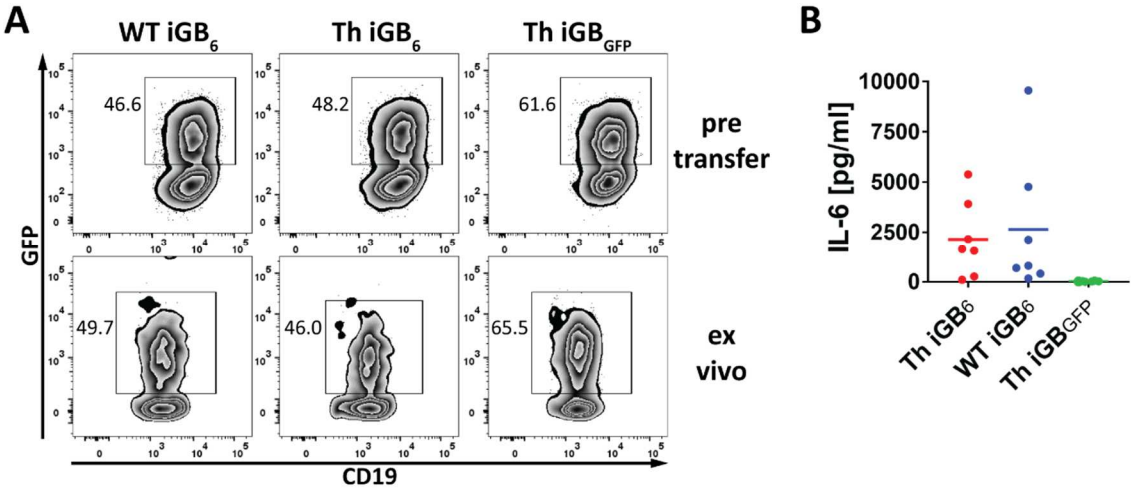

Figure 16: IL-6 overexpression in iGB cells is stable and functional after adoptive transfer. *WT and Th iCB cells were retrovirally transduced with pMSCV-IL-6-IRES2-GFP (iGB_6) or an empty pMSCV-IRES2-GFP vector (iGB_{GFP}). (**A**) Frequency of GFP^+ iGB cells pre-transfer and ex vivo in the spleen of iGB recipients. Flow cytometry plots are representative for 7 mice/group pooled from 2 independent experiments. (**B**) IL-6 levels measured in the serum of recipient mice by ELISA. Horizontal lines indicate means. Dots represent individual mice.*

Importantly, Th iGB_6 recipients developed EAE approximately one week earlier than mice that received Th iGB_{GFP} cells not overexpressing IL-6 (Figure 17A). Interestingly, WT iGB_6 cells were also able to induce EAE with similar time of onset and incidence to Th iGB_{GFP} cells (Figure 17A). EAE severity after disease onset was similar in all groups (not shown). Surprisingly, IL-6 overexpression in transferred iGB cells did not lead to a Th17 response in CNS infiltrating 2D2 $CD4^+$ T cells since these cells still produced mainly IFNγ and the frequencies of $IFN\gamma^+$ $IL\text{-}17A^+$ and $IL\text{-}17A^+$ $CD4^+$ T cells were similar between all experimental groups (Figure 17B).

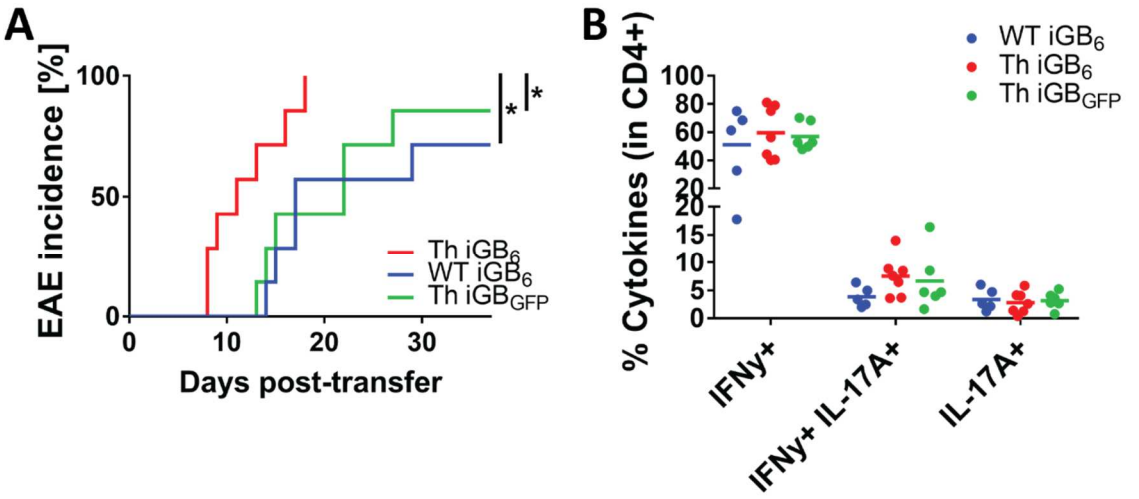

Figure 17: IL-6 production by iGB cells can enhance their ability to induce EAE without inducing a Th17 response. *IL-6-overexpressing WT or Th iGB cells or Th control iGB cells were co-injected together with 2D2 CD4⁺ T cells into Rag1-KO recipients. (**A**) EAE incidence during an observation period of over 37 days. Clinical data is shown for 7 mice per group pooled from 2 independent experiments. *p < 0.05, Mantel-Cox Log-rank test with adjusted p-values for multiple comparisons using the Holm-Sidak method. (**B**) Frequency of IFNγ⁺, IFNγ⁺ IL-17A⁺ and IL-17A⁺ CD4⁺ T cells in the CNS of iGB recipients analyzed at the peak of disease. Horizontal lines indicate means. Dots represent individual mice.*

4.2.5 Enhanced systemic IL-6 levels lead to expansion of myeloid cells in the periphery

Since there were no differences in the CD4⁺ T cell cytokine profile in the CNS, the question remained how IL-6 overexpression by iGB cells enhances their disease-inducing capacity. Closer examination revealed that both WT iGB_6 and Th iGB_6 had enlarged spleens compared to Th iGB_{GFP} recipients (Figure 18A). Accordingly, the number of splenocytes in WT iGB_6 recipients was significantly higher than in Th iGB_{GFP} recipients and the same trend could be observed in Th iGB_6 recipients, although this was not significant (Figure 18B). Interestingly, spleen cell numbers directly correlated with IL-6 levels in the serum of all mice irrespective of the experimental group (Figure 18C). Furthermore, there was a weak but not significant negative correlation between IL-6 levels in the serum and day of disease onset in both WT iGB_6 and Th iGB_6 recipients (Figure 18D). Taken together, enhanced systemic IL-6 levels promote EAE development and lead to splenomegaly in iGB_6 recipients irrespective of the antigen-specificity of the B cells.

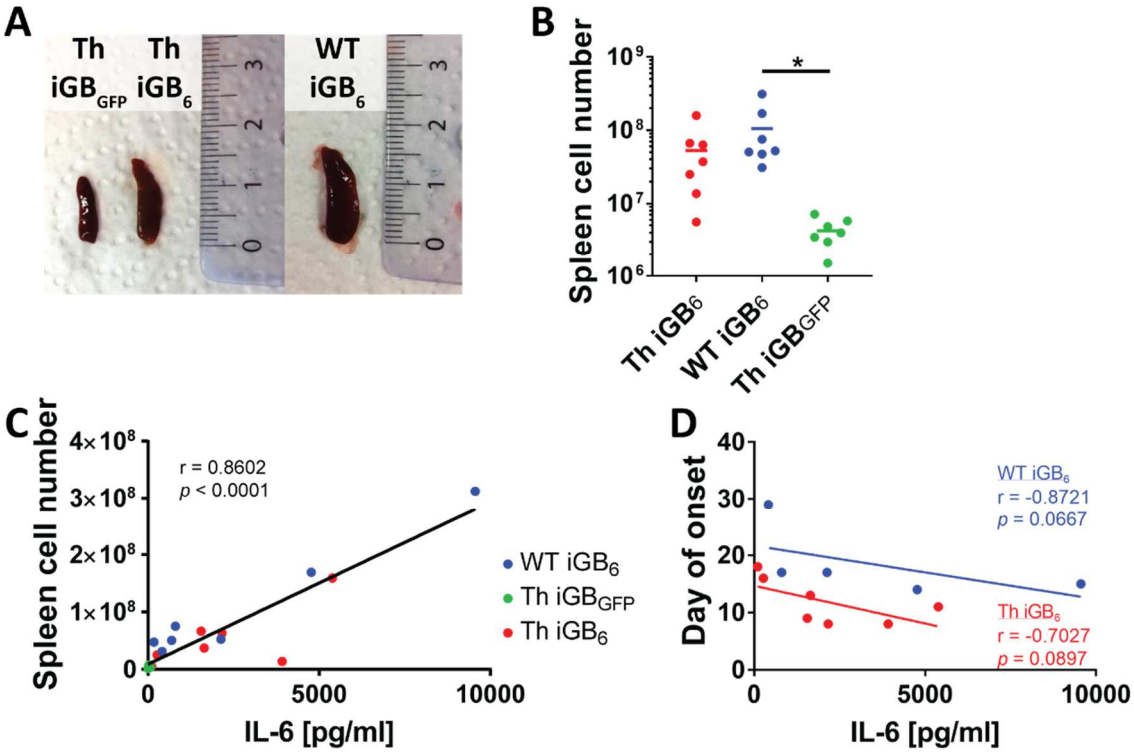

Figure 18: Enhanced systemic IL-6 levels lead to splenomegaly and promote EAE induction. *iGB recipients were sacrificed at the peak of disease or after 37 days without clinical symptoms. (**A**) Representative images of the spleens of Th iGB$_{GFP}$, Th iGB$_6$ and WT iGB$_6$ recipients. (**B**) Quantification of the total number of spleen cells. Horizontal lines indicate means. Dots represent individual mice. *p < 0.05, one-way ANOVA with Tukey post-test. (**C**) Spearman correlation of IL-6 levels in the serum and cell number in the spleen of iGB recipients irrespective of the experimental group. (**D**) Spearman correlation of IL-6 levels in the serum and day of onset in WT iGB$_6$ (blue) and Th iGB$_6$ (red) recipients.*

When analyzing the cellular composition in the enlarged spleens of iGB$_6$ recipients, the CD11b$^+$ myeloid compartment was found to be extremely expanded. Around 80 % of splenocytes were CD11b$^+$ in both Th iGB$_6$ and WT iGB$_6$ recipients, while the spleens of Th iGB$_{GFP}$ recipients consisted of less than 50 % CD11b$^+$ cells (Figure 19A, B). Different subsets of CD11b$^+$ myeloid cells could be distinguished by flow cytometry via additional surface markers, including CD11b$^+$ CD11c$^+$ DCs, CD11b$^-$ CD11c$^+$ DCs, CD11b$^+$ Ly6G$^+$ neutrophils, CD11b$^+$ Ly6C$^+$ inflammatory monocytes or CD11b$^+$ Ly6C^{int} eosinophils (Figure 19C). Careful analysis revealed that highly expanded cells were mainly composed of neutrophils and Ly6C$^+$ inflammatory monocytes (Figure 19D). Taken together, IL-6 overexpression by iGB cells induces a massive expansion of myeloid cells in the periphery, which leads to earlier disease onset, probably by creating a highly pro-inflammatory environment finally leading to T cell activation even in the absence of

MOG-specific iGB cells. Nevertheless, Th iGB_6 cells were superior to both WT iGB_6 cells and Th iGB_{GFP} cells to induce EAE indicating that both antigen-specificity and IL-6 expression add up to enhanced B cell pathogenicity in this system.

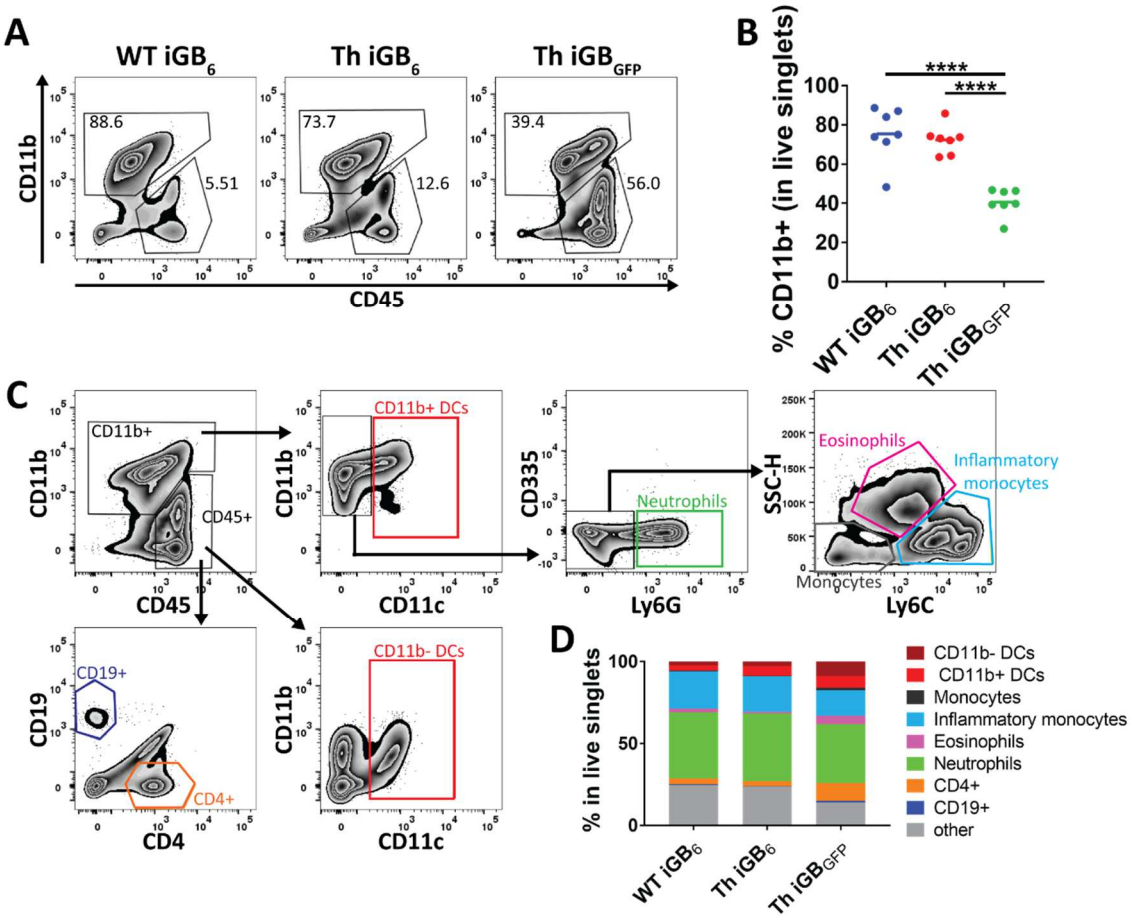

Figure 19: Enhanced systemic IL-6 levels lead to expansion of myeloid cells in the spleens of iGB$_6$ recipients. *(**A**) Representative flow cytometry plots and (**B**) quantification of CD11b$^+$ myeloid cells in the spleens of iGB recipients. Horizontal lines indicate means. Dots represent individual mice. ****p < 0.0001, one-way ANOVA with Tukey post-test. (**C**) Gating strategy to distinguish different myeloid cells and lymphocytes in the spleens of iGB recipients. (**D**) Distribution of different cell populations in the spleens of iGB recipients. Data is shown as mean from 4 mice/group.*

4.2.6 High levels of B cell-derived IL-23p19 can promote EAE development without affecting the CD4⁺ T cell response in the CNS

In addition to IL-6 and TGFβ, the cytokine IL-23 is important for terminal differentiation and stabilization of Th17 cells [83]. Therefore, IL-23 was the next cytokine to test in our adoptive co-transfer system. IL-23 is composed of two subunits, p19 and p40, the latter is shared with IL-12 (Figure 3). Since p19 has been suggested to be the unique and pathogenic subunit of IL-23, a single transduction was performed in our system to overexpress p19 alone in iGB cells. To test the role of B cell-derived p19 in the development of EAE, p19 was overexpressed in Th iGB cells and Th iGB_{p19} cells were co-transferred with 2D2 $CD4^+$ T cells into Rag1-KO mice. EAE development was then compared to mice that received control Th iGB_{GFP} cells together with 2D2 $CD4^+$ T cells. In one experiment, in which 45 % of Th iGB cells were successfully transduced and overexpressed p19, recipients of Th iGB_{p19} cells developed disease about one week earlier than recipients of Th iGB_{GFP} cells (Figure 20A, B). This was associated with high levels of secreted p19 in the serum of Th iGB_{p19} recipient mice (Figure 20C). In contrast, in two other experiments, in which transduction rates of less than 40 % were reached (20 % and 39 %), the Th iGB_{p19} cells were not able to induce earlier disease and both onset and EAE incidence were similar to mice receiving Th iGB_{GFP} cells (Figure 20D, E). In these experiments, p19 could not be detected at all or only in very low amounts in the serum of iGB_{p19} recipients (Figure 20F). These data indicate that high expression levels of p19 are required to produce a clinical effect on the development of EAE.

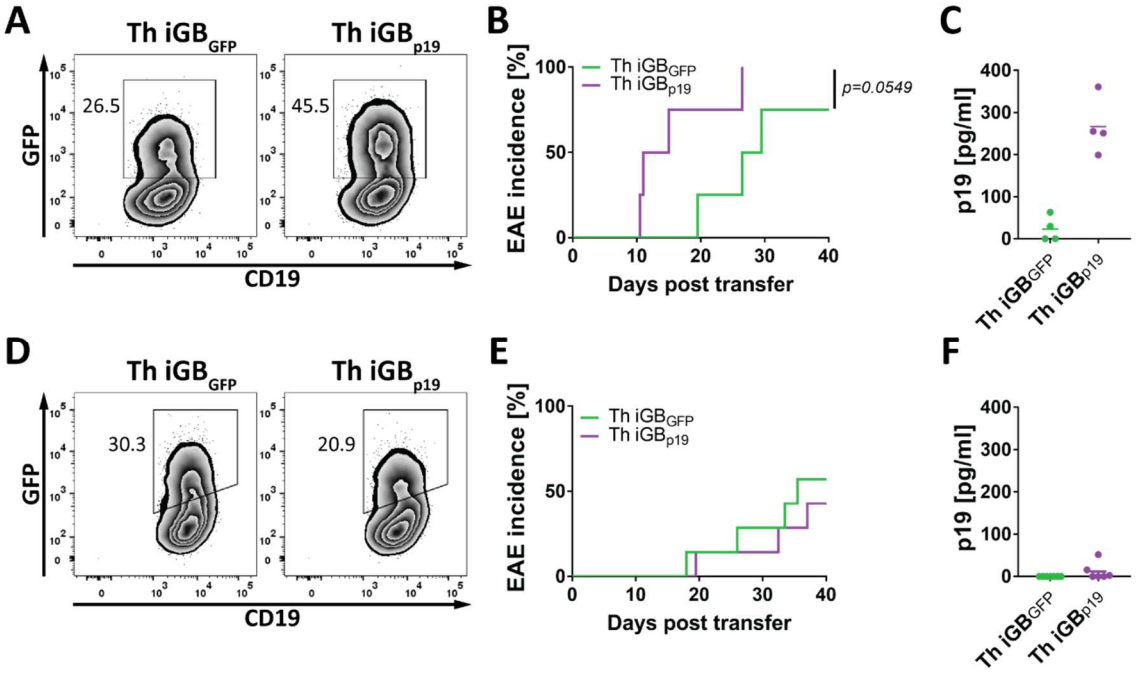

Figure 20: IL-23p19 overexpression by Th iGB cells can promote EAE development when secreted in high levels. *IL-23p19 was overexpressed in Th iGB cells and Th iGB$_{p19}$ or control Th iGB$_{GFP}$ cells were co-transferred together with 2D2 CD4$^+$ T cells into Rag1-KO mice. (**A**) Transduction rates, (**B**) EAE incidence and (**C**) serum p19 levels from an experiment with a transduction rate of more than 40 %. (**D**) Transduction rate, (**E**) EAE incidence and (**F**) serum p19 levels from two pooled experiments with transduction rates of less than 40 %. Clinical data is shown from 4 mice/group in (**B**) and 7 mice/group pooled from two independent experiments in (**E**). p=0.0549 Mantel-Cox Log-rank test. (**C**), (**F**) Horizontal lines indicate means. Dots represent individual mice.*

To test, why high levels of p19 could accelerate EAE development, mice from the experiment that showed a clinical difference (Figure 20A–C) were analyzed at the peak of the disease. Although IL-23 is involved in the differentiation of Th17 cells, IL-17A levels in CNS-infiltrating $CD4^+$ T cells were not enhanced in mice receiving Th iGB_{p19} cells (Figure 21A). $CD4^+$ T cells in the CNS produced mainly IFNγ in both experimental groups and a smaller proportion was IFNγ GM-CSF double-positive, however, also this $IFN\gamma^+$ $GM\text{-}CSF^+$ population was not increased in Th iGB_{p19} recipients (Figure 21B). In addition, and contrary to the overexpression of IL-6, neither splenomegaly nor changes in the myeloid compartment were observed (not shown). Taken together, high levels of p19 can promote EAE development without affecting the $CD4^+$ T cell effector cytokine profile or activating the myeloid compartment but rather through a so far unknown mechanism.

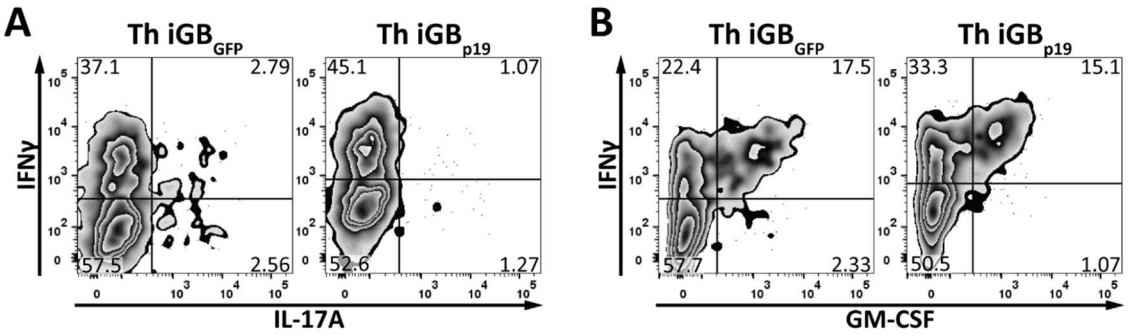

Figure 21: p19 overexpression by iGB cells does not alter the T cell cytokine response. *Representative flow cytometry plots showing the expression of (**A**) IFNγ and IL-17A or (**B**) IFNγ and GM-CSF by $CD4^+$ T cells in the CNS of Th iGB_{GFP} and Th iGB_{p19} recipients at the peak of EAE in an experiment that showed a clinical difference between the two groups. Cells were pre-gated on live $CD45^+$ $CD4^+$ cells and gates were set based on isotype controls stained on the same respective day of analysis.*

4.2.7 CRISPR-Cas9-mediated cytokine knock-down in primary mouse B cells

Th B cells express more pro-inflammatory cytokines such as IL-6 and TNFα than WT B cells (4.1.3) and IL-6 overexpression in iGB cells leads to earlier disease onset in our adoptive co-transfer model (section 4.2.4). However, it is not yet clear whether the production of IL-6 and TNFα is required for the pathogenicity of Th iGB cells. To answer this question, a protocol for the CRISPR-Cas9-mediated knock-down of these cytokines in Th iGB cells was developed. To do this, Th mice were crossed to R26-Cas9 mice, which express the Cas9 protein constitutively under control of the R26 promoter. Three sgRNAs were designed to target the *Il6* and *Tnf* genes respectively and cloned into a MSCV vector, which expresses the respective sgRNA under control of the U6 promoter and allows for GFP reporter expression and puromycin selection (Figure 22B). R26-Cas9 x Th B cells were transduced after 48 h in iGB culture and subsequently selected by culturing in the presence of puromycin and IL-21 and analyzed at different time points after transduction (Figure 22A). Puromycin selection led to the outgrowth of a very pure culture of transduced iGB cells, as more than 80 % of cells were GFP^+ on day 6 and more than 90 % on day 7 (Figure 22C). TNFα knock-down efficiency was determined by FACS on day 7 and revealed successful knock-down of TNFα with all three designed sgRNAs but was most efficient (98 %) with sg1 (Figure 22D). Since IL-6 staining does not work reliably in iGB cells, IL-6 knock-down efficiency was determined by measuring the secreted IL-6 levels in the culture supernatant. To measure only the IL-6 levels produced in the last 24 hours prior to analysis, the full culture medium was replaced 24 h before supernatant collection (Figure 22E). To account for potentially different cell numbers in each well, the IL-6 levels were normalized to 100,000 iGB cells (Figure 22F). Both absolute and normalized data showed significantly reduced IL-6 levels in cells transduced with all three sgRNAs as compared to a non-targeting (NT) control (Figure 22E, F). This shows that CRISPR-Cas9 can be used to successfully knock-down cytokines in Th iGB cells and can be used to test the requirement of Th iGB cell cytokine production for the induction of EAE in our adoptive co-transfer model in the future.

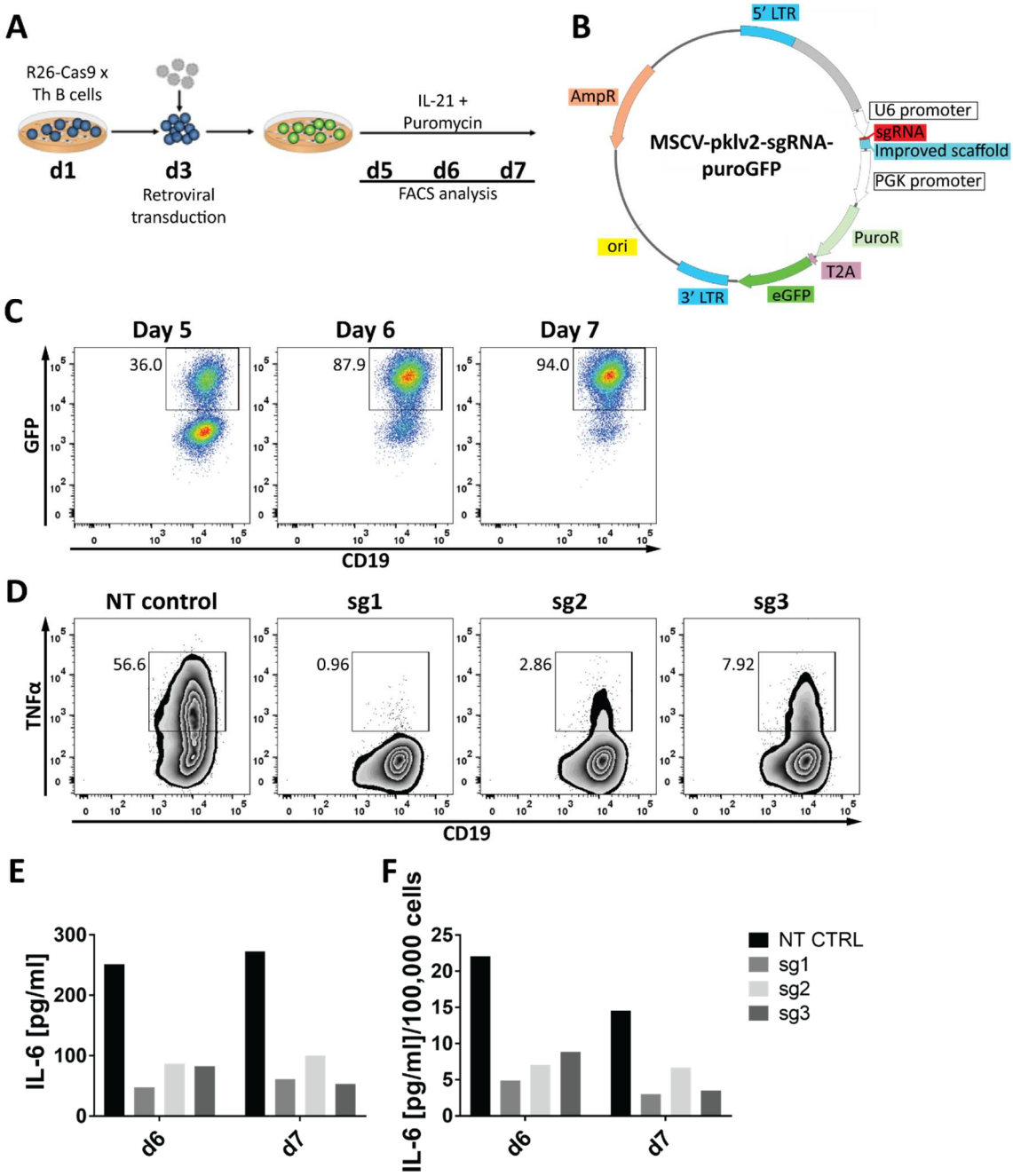

Figure 22: CRISPR-Cas9-mediated knock-down of cytokines in iGB cells. *(**A**) Experimental outline. R26-Cas9 x Th B cells were cultured in the iGB culture system and transduced after 48 hours. After transduction, the cells were cultured on fresh feeder cells in the presence of IL-21 and puromycin and analyzed at different time points. (**B**) Schematic of the MSCV-pklv2-sgRNA-puroGFP construct. The sgRNA is expressed under the control of an U6 promoter and the expression of a puromycin resistance gene (PuroR) and eGFP allows for selection of successfully transduced cells. AmpR, ampicillin resistance; LTR, long terminal repeat; ori, origin of replication; PGK, phosphoglycerate kinase. (**C**) Representative flow cytometry plots showing the frequency of GFP⁺ cells on day 5, 6 or 7 of iGB culture. (**D**) TNFα production by transduced iGB cells was tested by FACS on day 7 of iGB culture. Flow cytometry plots are representative of 3 independent experiments. (**E**) The culture medium was replaced 24 h prior to supernatant collection and IL-6 levels were measured by ELISA. (**F**) IL-6 levels were normalized to the number of cells in each well. Data in (**E**) and (**F**) is representative for 3 independent experiments. NT CTRL, non-targeting control.*

4.3 The role of B cell-derived anti-inflammatory cytokines in the regulation of Th17-mediated EAE

4.3.1 Th iPBs enhance Th17-mediated EAE irrespective of the production of anti-inflammatory cytokines

MOG-specific Th B cells are able to cooperate with MOG-specific $CD4^+$ T cells to induce disease both in a spontaneous EAE mouse model [69] as well as in our co-transfer experiments. The production of pro-inflammatory cytokines such as IL-6 and IL-23p19 further enhances their pathogenic potential in our iGB transfer EAE model. However, B cells are known to also produce anti-inflammatory cytokines and it was shown that IL-10 and IL-35-expressing B cells and plasma cells are able to ameliorate EAE [114, 115]. In those studies, B cell-mediated suppression required CD40 signaling indicating a cognate interaction with $CD4^+$ T cells, and the regulatory effect was mediated in the periphery [114, 115]. It remains unclear, however, whether B cells are able to regulate pathogenic effector cell responses directly in the CNS. A good model to study the role of B cells in the CNS during EAE is the Th17 adoptive transfer model [92]. In this model, a pure MOG-specific Th17 cell population induces severe EAE and leads to the formation of eLFs in the CNS, which, among other immune cells, contain high numbers of B cells and plasma cells [101]. Therefore, a protocol was developed combining Th17-mediated EAE with the injection of IL-10-overexpressing iGB cells. Since anti-inflammatory properties have been primarily ascribed to plasma cells [115, 151], the iGB culture conditions were adjusted to generate induced plasmablasts (iPBs)/plasma cells (iPCs) rather than GC B cells used for previous experiments. Thus, after retroviral transduction, the cells were cultured on feeder cells expressing IL-21 for 4 days (Figure 23). IL-10-overexpressing iPBs/iPCs were injected 7 days after the Th17 transfer. This time point was chosen to maximize the chances that the injected iPBs would not interfer with the injected Th17 cells in the periphery, but rather be recruited directly to the CNS.

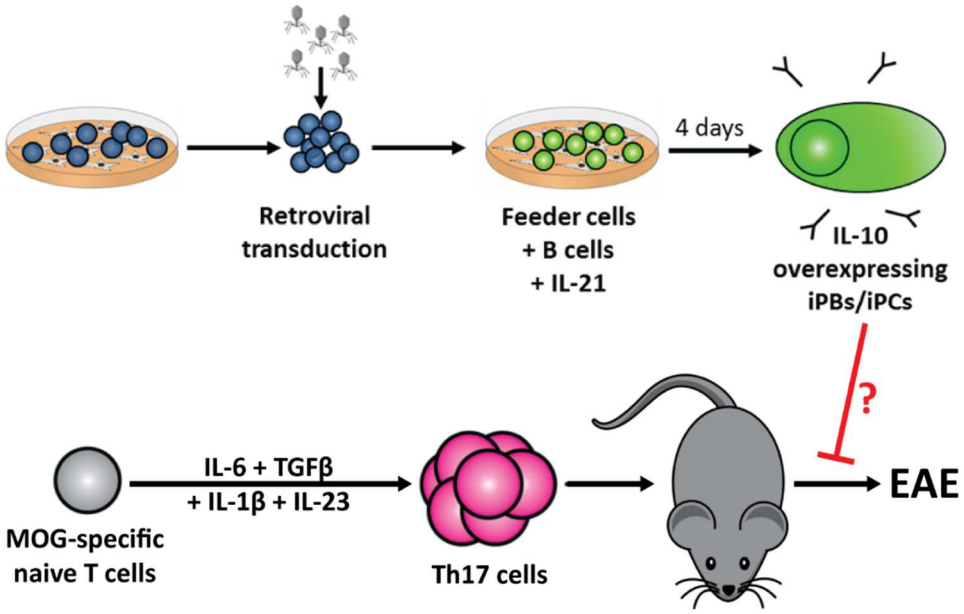

Figure 23: Experimental outline of Th17 transfer EAE combined with injection of IL-10-overexpressing plasmablasts/plasma cells. *MOG-specific naïve T cells were isolated from 2D2 mice and differentiated into Th17 cells in the presence of IL-6, TGFβ, IL-1β and IL-23. After 8 days, differentiated Th17 cells were restimulated in the presence of anit-CD3 and anti-CD28 for 48 hours and then transferred into C57BL/6 WT recipients. B cells were expanded using the iGB culture system. After 48 hours, the cells were retrovirally transduced and then cultured on fresh feeder cells expressing high levels of IL-21 for 4 days. IL-10-overexpressing induced plasmablasts (iPBs)/ plasma cells (iPCs) were injected 7 days after the Th17 transfer.*

Since the suppressive capacity of B cells required antigen-specificity in previous reports [114], a first experiment was performed using MOG-specific Th B cells. Before transfer, Th iPBs had switched their isotype completely to IgG1 and 45 % of them were successfully transduced (GFP^+) to overexpress IL-10 (Figure 24A, B). Consistent with this, IL-10 could be measured in the serum of Th iPB_{10} recipients but not at all or only in very low levels in the serum of mice that received Th iPB_{GFP} cells (Figure 24C). Surprisingly, however, both Th iPB_{GFP} and Th iPB_{10} recipients showed an even earlier EAE onset and enhanced incidence as compared to mice that did not receive any B cells (Figure 24D) and there was no difference in disease severity between Th iPB_{GFP} and Th iPB_{10} recipients either (Figure 24E). High levels of MOG-specific IgG1 antibodies could be detected in the serum of Th iGB_{GFP} and Th iGB_{10} recipients whereas mice that received no B cells showed only low levels of MOG-specific IgG1 antibodies in the serum (Figure 24F). Taken together, these data indicate that Th iPBs did not ameliorate but rather enhanced Th17-mediated EAE, potentially due to the high MOG-specific IgG1 titers and irrespective of the production of anti-inflammatory IL-10.

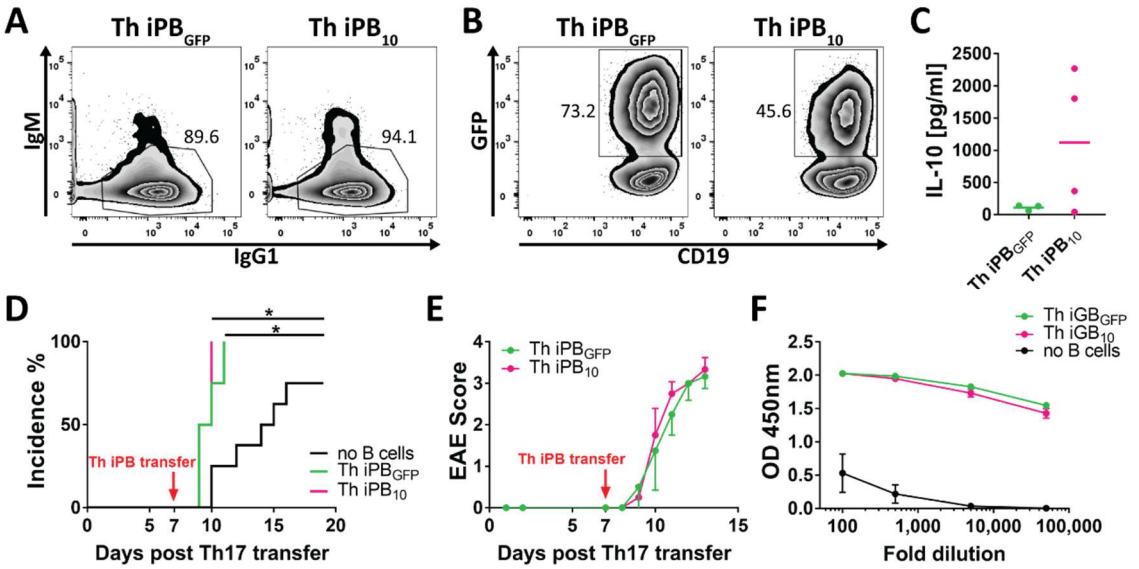

Figure 24: Th iPBs enhance Th17-mediated EAE irrespective of the production of anti-inflammatory IL-10. *Th B cells were retrovirally transduced with pMSCV-IL-10-IRES2-GFP (iPB$_{10}$) or an empty pMSCV-IRES2-GFP vector (iPB$_{GFP}$) and subsequently cultured on IL-21-expressing feeder cells for 4 days. (**A**) The frequency of IgG1$^+$ cells and (**B**) GFP$^+$ cells was determined at the time of iPB transfer into recipients that had been injected with 2D2 Th17 cells 7 days earlier. (**C**) IL-10 levels in the serum of recipient mice at the peak of disease measured by ELISA. Horizontal lines indicate means. Dots represent individual mice. (**D**) EAE incidence and (**E**) clinical scores of Th17 recipients that received either Th iPB$_{GFP}$, Th iPB$_{10}$ cells or no B cells. Clinical data is shown for 4–8 mice per group. *p < 0.05 Mantel-Cox Log-rank test with adjusted p-values for multiple comparisons using the Holm-Sidak method. (**F**) MOG-specific IgG1 levels in the serum of mice receiving Th iGB$_{GFP}$, Th iGB$_{10}$ or no B cells. Dots indicate means ± SEM for 4–5 mice per group.*

4.3.2 WT iPB$_{10}$ cells cannot ameliorate clinical disease but induce a more anti-inflammatory T cell profile in the CNS

Since antigen-specificity of the transferred iPBs enhanced Th17-mediated EAE, the same experiments were performed using WT CD45.1 congenic iPBs, of which 42–49 % overexpressed IL-10. Unlike MOG-specific Th iPBs, injection of WT iPBs did not lead to an earlier disease onset but both incidence and day of onset did not differ between iPB recipients and mice that only received PBS injections (Figure 25A, B). In addition, no clear clinical difference could be observed between mice that received iPB$_{GFP}$ cells and mice that received iPB$_{10}$ cells neither regarding the day of disease onset nor regarding disease severity (Figure 25A–C). However, both iPB$_{GFP}$ and iPB$_{10}$ recipients showed significantly lower frequency of CD19$^+$ B cells in the CNS than mice that only received PBS injections (Figure 25D). iPBs could be detected in the CNS by the expression of the congenic marker CD45.1 and varied between 0.5–30 % of CNS B cells in both iPB$_{GFP}$ and

iPB$_{10}$ recipients, suggesting that, similar to endogenous B cells, the iPBs were actively recruited to the CNS by Th17 cells (Figure 25E, F). Injected iPBs retained their GFP expression and IgG1$^+$ phenotype in the CNS, while most of the endogenous B cells expressed IgM (Figure 25E). In contrast, CD45.1$^+$ iPBs could not be detected in the spleen or other peripheral organs such as LNs or BM (not shown) indicating that the transferred iPBs preferentially migrated to the inflamed CNS after adoptive transfer.

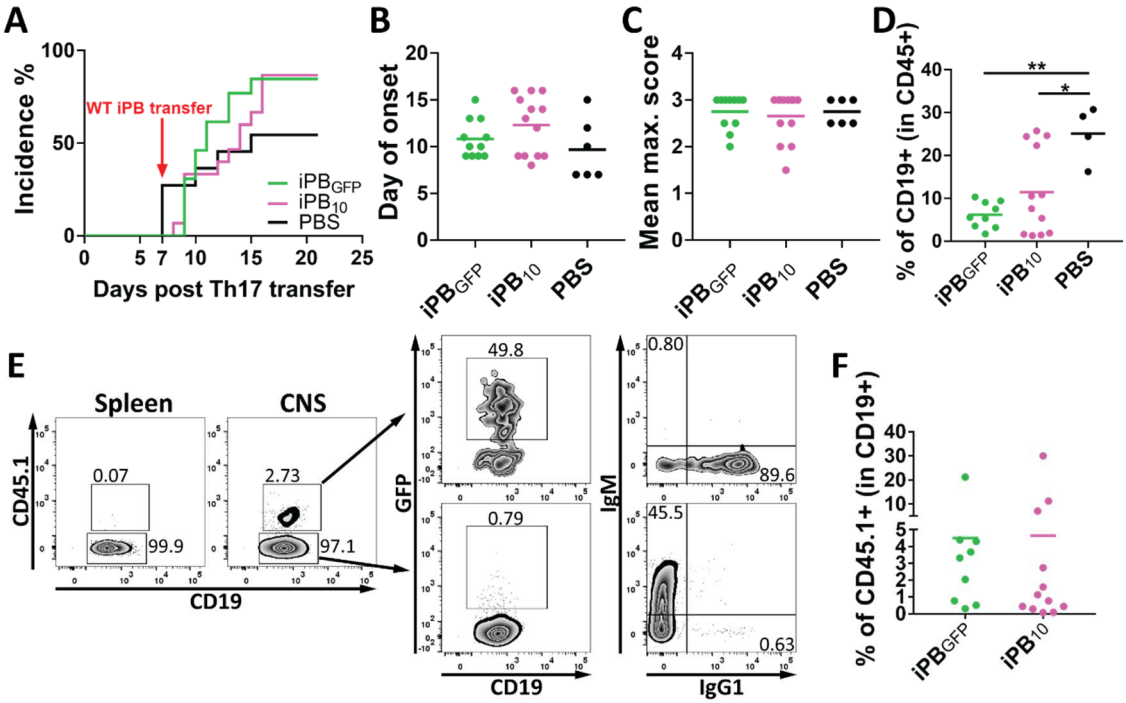

Figure 25: Injection of WT iPBs does not ameliorate clinical disease but prevents B cell accumulation in the CNS. *CD45.1 B cells were retrovirally transduced with pMSCV-IL-10-IRES2-GFP (iPB$_{10}$) or an empty pMSCV-IRES2-GFP vector (iPB$_{GFP}$), subsequently cultured on IL-21-expressing feeder cells for 4 days and injected into WT recipients that had been injected with 2D2 Th17 cells 7 days earlier. (**A**) EAE incidence of Th17 recipients that received either iPB$_{GFP}$ or iPB$_{10}$ cells or were injected with PBS only. Clinical data is shown for 11–15 mice per group. (**B**) Day of onset and (**C**) mean max. score of mice that developed clinical disease. (**D**) Frequency of CD19$^+$ B cells in the CNS of Th17 recipients at the peak of disease. Horizontal lines indicate means. Dots represent individual mice. *p < 0.05, **p < 0.01 one-way ANOVA with Tukey post-test. (**E**) Representative flow cytometry plots showing the frequency of transferred CD45.1$^+$ cells in the spleen and CNS at the peak of disease (pre-gated on live CD45$^+$ CD19$^+$ cells), as well as the phenotype of transferred CD45.1$^+$ cells (upper row) and endogenous CD45.1$^-$ B cells (lower row) in the CNS. (**F**) Quantification of the frequency of CD45.1$^+$ cells in the CNS of iPB$_{GFP}$ and iPB$_{10}$ recipients. Horizontal lines indicate means. Dots represent individual mice.*

In addition to lower endogenous B cell frequencies in the CNS of both iPB_{GFP} and iPB_{10} recipients, mice that received iPB_{10} cells showed lower frequencies of transferred 2D2 Th17 cells, which can be detected by the expression of the transgenic TCR Vα3.2 (Figure 26A, B). Most likely, this was caused by reduced migration or proliferation of transferred Vα3.2$^+$ cells in the CNS rather than enhanced recruitment of Vα3.2$^-$ endogenous T cells since the absolute number of Vα3.2$^+$ cells was decreased in the CNS of iPB_{10} as compared to iPB_{GFP} recipients (Figure 26C). In contrast, the absolute number of Vα3.2$^-$ cells was similar between the two groups (Figure 26D). The cytokine profile of Vα3.2$^+$ cells, however, was not affected in the presence of iPB_{10} cells since transferred Vα3.2$^+$ cells in both groups expressed mainly IL-17A, but also IFNγ and GM-CSF (Figure 26E).

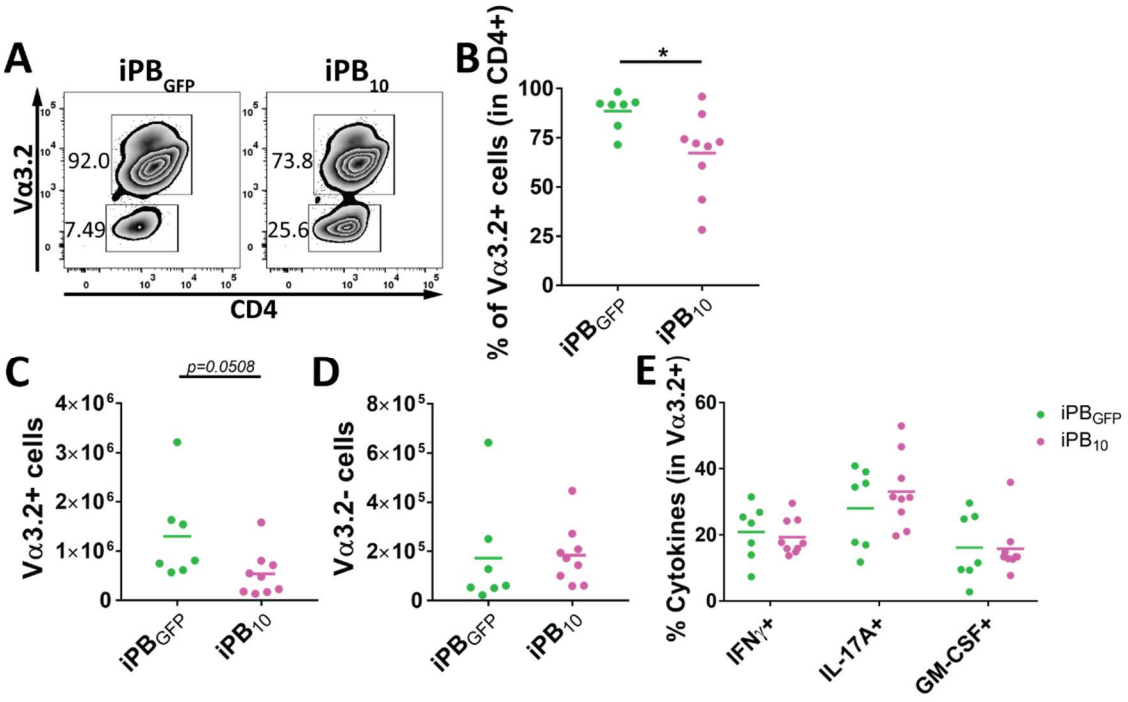

Figure 26: iPB_{10} cells curb the accumulation of transferred Th17 cells in the CNS. *(**A**) Representative flow cytometry plots showing the frequency of Vα3.2$^+$ transferred Th17 cells and Vα3.2$^-$ endogenous T cells (pre-gated on live CD45$^+$ CD4$^+$ cells) in the CNS of iPB_{GFP} and iPB_{10} recipients at the peak of disease. (**B**) Quantification of frequency and (**C**) absolute number of Vα3.2$^+$ T cells and (**D**) Vα3.2$^-$ T cells in the CNS of Th17 + iPB recipients at the peak of disease. (**E**) Frequency of IFNγ$^+$, IL-17A$^+$ and GM-CSF$^+$ cells within the Vα3.2$^+$ T cell population in the CNS. Horizontal lines indicate means. Dots represent individual mice. *p < 0.05, unpaired t-test.*

In contrast to Vα3.2$^+$ cells, the phenotype of endogenous Vα3.2$^-$ T cells was changed in iPB$_{10}$ recipients: although the frequency of FoxP3$^+$ Tregs was not increased significantly within the Vα3.2$^-$ population, the higher frequency of Vα3.2$^-$ cells led to a significantly increased frequency of FoxP3$^+$ Tregs among the total CD4$^+$ T cell population in the CNS of iPB$_{10}$ recipients (Figure 27A, B). Endogenous FoxP3$^+$ T cells produced high levels of IL-10 but in similar levels in both iPB$_{GFP}$ and iPB$_{10}$ recipients (Figure 27C). In contrast, higher frequencies of IFNγ$^+$ and IFNγ$^+$ IL-10$^+$ cells were detected in the FoxP3$^-$ Vα3.2$^-$ population of iPB$_{10}$ recipients as compared to iPB$_{GFP}$ recipients (Figure 27D, E). Taken together, both iPB$_{GFP}$ and iPB$_{10}$ cells prevent the accumulation of endogenous B cells in the CNS of Th17 recipients, but only iPB$_{10}$ cells inhibit the accumulation or proliferation of transferred Vα3.2$^+$ Th17 cells in the CNS. In addition, IL-10 overexpression by iPBs leads to a more anti-inflammatory profile of endogenous Vα3.2$^-$ T cells in the CNS of Th17 cell recipients.

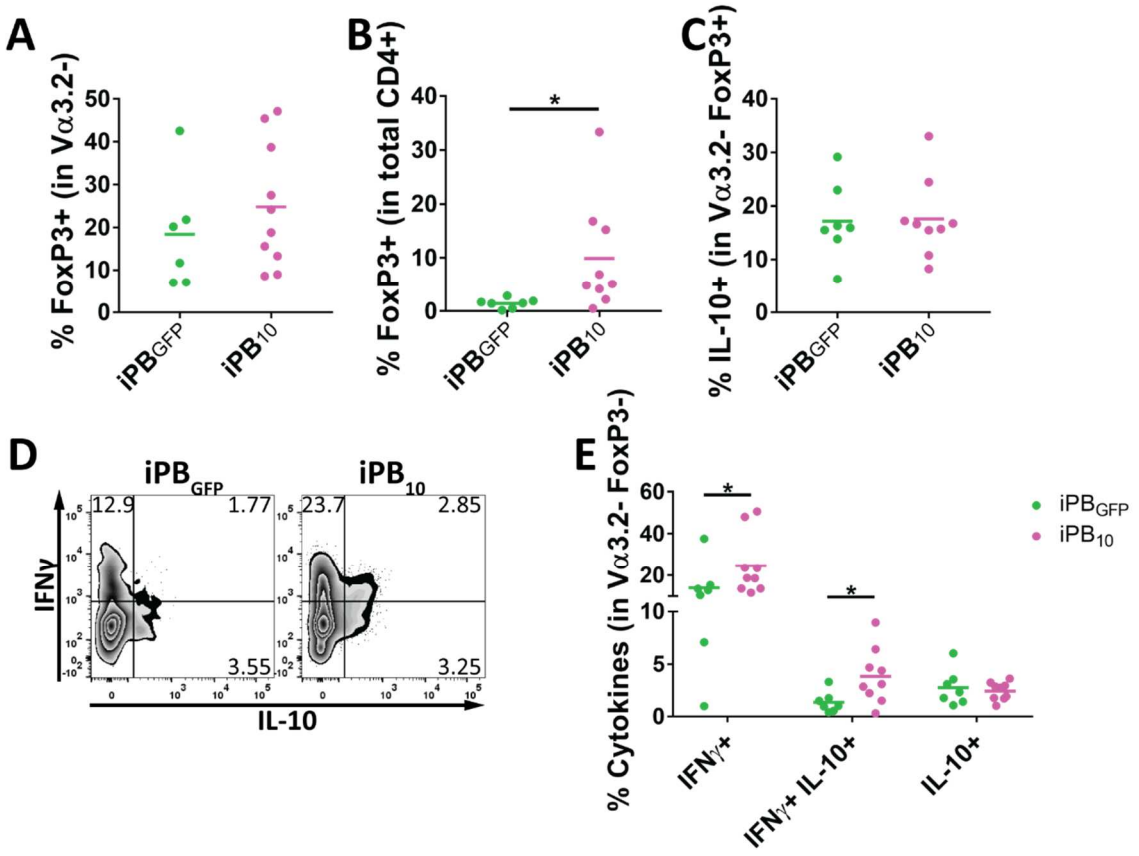

Figure 27: Endogenous T cells in the CNS of iPB$_{10}$ recipients show a more anti-inflammatory profile. *(**A**) Frequency of FoxP3$^+$ T cells in the Vα3.2$^-$ or (**B**) in the total CD4$^+$ T cell population in the CNS of Th17 + iPB recipients at the peak of disease. (**C**) Frequency of IL-10$^+$ cells in the Vα3.2$^-$ FoxP3$^+$ T cell population. Horizontal lines indicate means. Dots represent individual mice. *p < 0.05, Welch's t test. (**D**) Representative flow cytometry plots showing IFNγ and IL-10 production by Vα3.2$^-$ FoxP3$^-$ T cells in the CNS. (**E**) Quantification of IFNγ$^+$, IFNγ$^+$ IL-10$^+$ and IL-10$^+$ cells in the Vα3.2$^-$ FoxP3$^-$ population. Horizontal lines indicate means. Dots represent individual mice. *p < 0.05, Mann-Whitney test.*

4.4 The role of IL-23p19 in CNS autoimmunity

4.4.1 Generation of an IL-23p19 reporter and conditional knock-out mouse

Th17 differentiation, stability and pathogenicity depends on the cytokine IL-23, which consists of the two subunits p19 and p40 (Figure 3). Deficiency of either of the two subunits leads to EAE resistance [80, 82] and, as shown here, p19 overexpression by MOG-specific B cells can enhance their ability to induce EAE (Figure 20). IL-23 can be produced by APCs, however, due to the lack of reliable reagents, tools to thoroughly study cellular sources of the IL-23p19 subunit specifically are limited. Therefore, a novel IL-23p19 reporter mouse line was generated, in which a LacZ-hbactP-neo cassette is inserted at the end of exon 1 of the *Il23a* gene (Figure 28A). Thus, IL-23p19 expression can be detected by LacZ activity in heterozygous reporter mice, whereas homozygosity leads to disruption of *Il23a* gene function. Since the LacZ-hbactP-neo cassette is flanked by Flippase Recognition Target (FRT) sites, a conditional KO allele can be created in the presence of the recombinase flippase (Flp). Here, the critical exons 2–4 are flanked by loxP sites (Figure 28A) and subsequent Cre expression results in a tissue-specific KO.

Presence of the p19.LacZ reporter allele was verified by genotyping using a gene-specific forward (5’ arm) and a cassette-specific reverse primer (LAR3) (Figure 28A, B). After crossing the mice with R26-Flpe mice [138], excision of the LacZ-hbactP-neo cassette and presence of the downstream loxP site using loxP forward and reverse primers was confirmed by PCR analysis (Figure 28A, C).

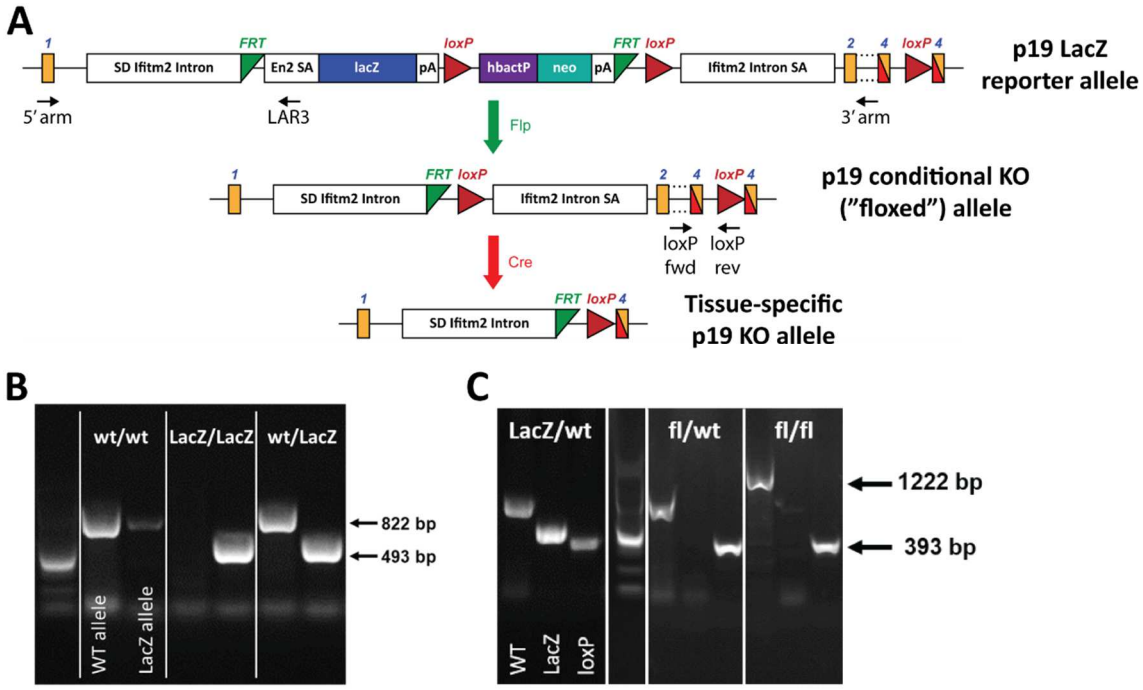

Figure 28: Generation of an IL-23p19 reporter and conditional KO mouse. *(**A**) Schematic of the p19.LacZ reporter locus (upper row). The cassette is inserted at the end of exon 1 and is composed of an artificial intron derived from the Ifitm2 gene containing a FRT site followed by the lacZ gene and a first loxP site. This is followed by neomycin resistance gene (neo) under the control of the human beta-actin promoter (hbactP) and by a second FRT and loxP site. A third loxP site is located downstream of the targeted exons 2–4. After Flp recombination, the LacZ-hbactP-neo cassette is excised resulting in a conditional KO allele, in which the critical exons 2–4 are flanked by loxP sites (middle row). Subsequent Cre recombination creates a tissue-specific p19-KO allele (lower row). Black horizontal arrows indicate the localization of genotyping primers. Maps are not to scale. (**B**) Genotyping of WT, homozygous LacZ/LacZ and heterozygous wt/LacZ mice. Gene-specific forward (5'arm) and reverse (3'arm) primers amplify an 822 bp WT allele, whereas usage of the cassette-specific reverse primer (LAR3) results in a 493 bp LacZ allele. (**C**) Genotyping of heterozygous LacZ/wt, as well as fl/wt and homozygous fl/fl mice after Flp recombination. In heterozygous fl/wt and homozygous fl/fl mice, the LacZ-hbactP-neo cassette has been excised leading to the loss of the LacZ-specific 493 bp product. Presence of the downstream loxP site can be verified using specific primers (loxP fwd, loxP rev) and results in a 393 bp product. In homozygous fl/fl mice, a 1222 bp product is generated using the gene-specific 5'arm and 3'arm primers.*

4.4.2 Activated CD4⁺ T cells express IL-23p19

Using our novel IL-23p19.LacZ reporter mouse line, IL-23p19 expression was examined in different cells and under different stimulation conditions. To do so, LacZ signal was determined by flow cytometry using the FACS-Gal assay. This assay makes use of the fluorogenic substrate Fluorescein di-β-galactopyranoside (FDG), which is cleaved by β-galactosidase to generate galactose and fluorescein that can be detected in the FITC channel of the flow cytometer [152]. WT cells were used as gating controls in all experiments, since they do not express the *lacZ* gene. Surprisingly, the highest LacZ

reporter signal could be observed in *in vitro* activated and differentiated CD4$^+$ T cells with this FACS Gal assay. About 10–20 % of both Th1 and Th17 cells expressed IL-23p19 whereas the highest levels of IL-23p19 (30 %) were found in differentiated iTregs (Figure 29A, B). Consistent with these data, *Il23a* mRNA could be detected in all three T cell subsets from both WT and heterozygous reporter mice (Figure 29C). Furthermore, IL-23p19 protein could be detected in the culture supernatants (Figure 29D) showing that activated and differentiated CD4$^+$ T cells do not only express, but also secrete IL-23p19. Surprisingly, no convincing p19.LacZ signal could be detected in different types of APCs in the FACS-Gal assay, such as LPS-stimulated bone marrow-derived DCs (BMDCs), macrophages or B cells stimulated with anti-CD40 or LPS (not shown).

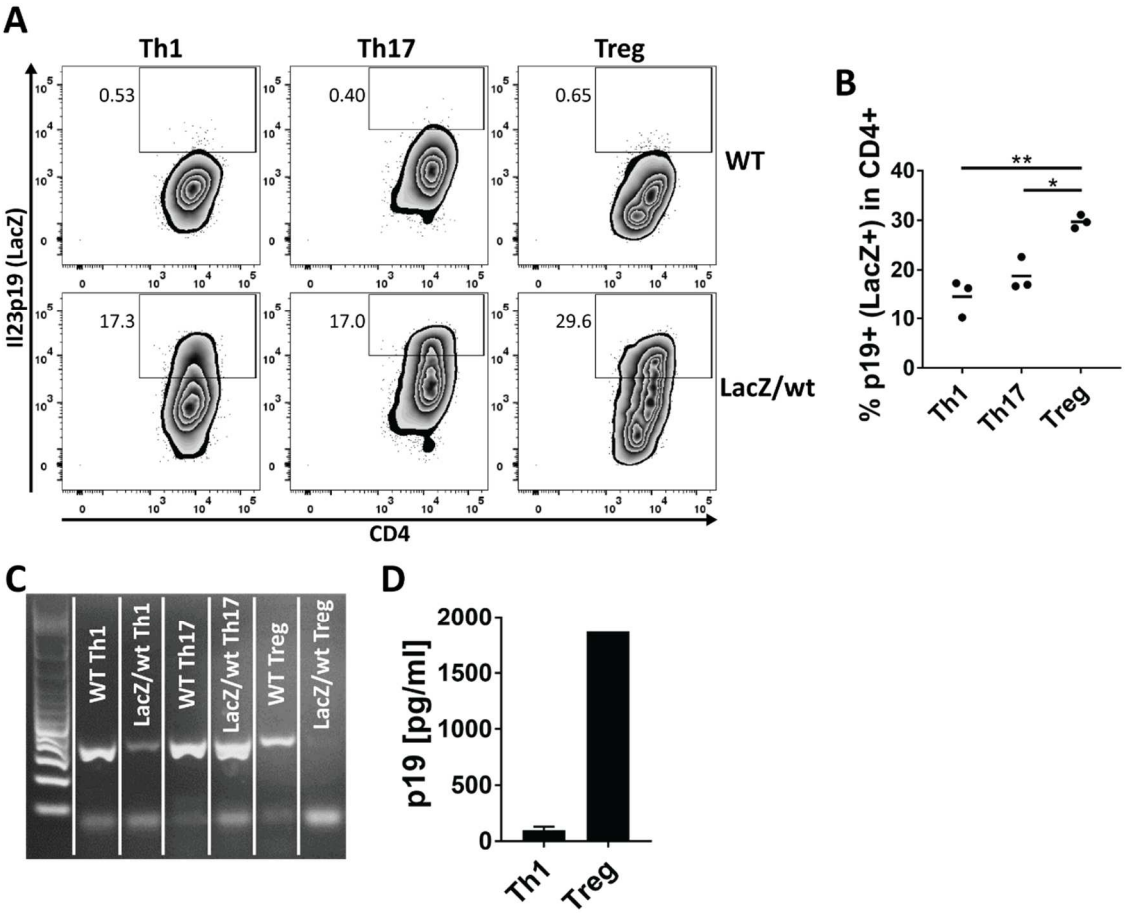

Figure 29: Activated CD4$^+$ T cells express IL-23p19. *Naïve CD4$^+$ T cells were isolated from WT or LacZ/wt mice and cultured in the presence of anti-CD3 and irradiated APCs (Th1, Th17) or anti-CD28 (Treg) and polarizing cytokines for 4 days. After stimulation with PMA/ionomycin and monensin for 4 hours, IL-23p19 expression was measured by LacZ reporter activity using the FACS-Gal assay. (**A**) Representative flow cytometry plots showing the frequency of p19$^+$ (LacZ$^+$) cells within the CD4$^+$ T cell population. (**B**) Quantification of p19$^+$ (LacZ$^+$) cells within the CD4$^+$ T cell population. Horizontal lines indicate means. Dots represent individual mice. *p < 0.05, **p < 0.01, one-way ANOVA with Tukey post-test. (**C**) RNA was isolated from the differentiated T cell populations and p19 mRNA expression was tested by RT-PCR. (**D**) Culture supernatants from LacZ/wt cultures were collected prior to the stimulation with PMA/ionomycin and p19 levels were measured by ELISA. Data is shown as mean + SEM.*

4.4.3 Microglia and macrophages show no IL-23p19.LacZ signal during EAE

Stimulation of different cell types *in vitro* showed strong reporter signals in activated and differentiated $CD4^+$ T cells but not in APCs. Since it was shown previously that during EAE microglia and macrophages express *Il23a* mRNA directly in the CNS [82], EAE was induced in WT and heterozygous LacZ reporter mice. As expected, LacZ reporter mice developed EAE with a similar incidence and time of onset as WT control mice (Table 9). At the peak of disease, only little p19 signal could be detected in PMA/ionomycin-stimulated $CD4^+$ T cells isolated from spleen, iLN or CNS as only around 2–5 % of $CD4^+$ T cells produced p19 in any of the three organs (Figure 30A). In contrast, up to almost 20 % of $CD8^+$ T cells expressed IL-23p19 in the spleen and iLN but not in the CNS (Figure 30B). In contrast to previous reports but consistent with our *in vitro* data, no p19 signal could be detected neither in $CD11b^+$ $CD45^{int}$ microglia nor in $CD11b^+$ $CD45^{high}$ monocytes in the CNS via FACS-Gal (Figure 30C, D). This indicates that either the FACS-Gal assay is not sensitive enough or generates too much background signal in monocytes and microglia to detect low levels of IL-23p19 expression or monocytes and microglia do not express relevant levels of IL-23p19 during EAE.

Table 9: *EAE incidence in WT and p19.LacZ reporter mice*

Mouse	Incidence	Mean day of onset (± SD)
WT	2/2 (100 %)	12.7 ± 1.5
LacZ/wt	4/4 (100 %)	14.3 ± 3.4

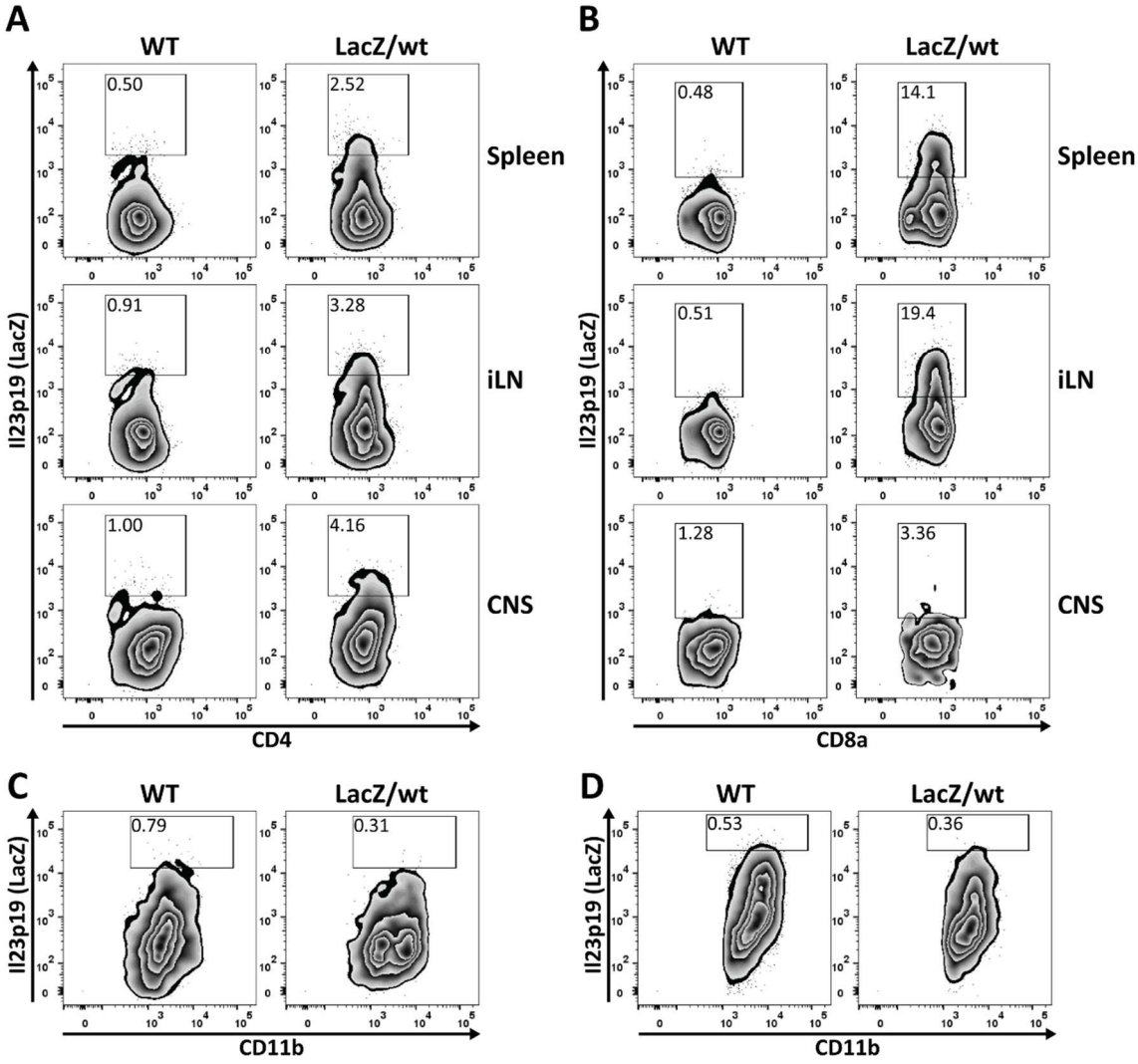

Figure 30: IL-23p19 reporter signal at the peak of EAE. *EAE was induced in WT and heterozygous LacZ/wt reporter mice by immunization with 100 µg $MOG_{35–55}$ emulsified in CFA. Mice were sacrificed at the peak of disease and p19 expression was measured by FACS-Gal assay after stimulating the cells with PMA/ionomycin and monensin for 4 hours. Representative flow cytometry plots showing the frequency of IL-23p19$^+$ (LacZ$^+$) cells in (**A**) CD4$^+$ T cells, (**B**) CD8a$^+$ T cells in spleen, iLN or CNS as well as in (**C**) CD11b$^+$ CD45^{int} microglia or (**D**) CD11b$^+$ CD45^{high} monocytes in the CNS. Gates were set based on WT cells not expressing the lacZ gene which were analyzed on the same day.*

4.4.4 IL-23p19 is not required for the in vitro *differentiation of CD4⁺ T cells*

Since we observed high levels of IL-23p19 expression in T cells but not in APCs both *in vitro* and during EAE, we asked whether T cell-specific p19 expression was also required for differentiation of pathogenic T effector cells during EAE. To test this hypothesis, IL-23p19$^{fl/fl}$ mice were crossed to CD4-Cre mice to obtain T cell-specific p19-KO mice. Successful KO of the *Il23a* gene was confirmed on both mRNA and protein level in *in vitro* differentiated iTregs. *Il23a* mRNA could not be detected by RT-PCR in iTregs derived from CD4-Cre x p19$^{fl/fl}$ mice (Figure 31A) and p19 protein could neither be detected in cell lysates by western blotting nor in the culture supernatants by ELISA (Figure 31B, C).

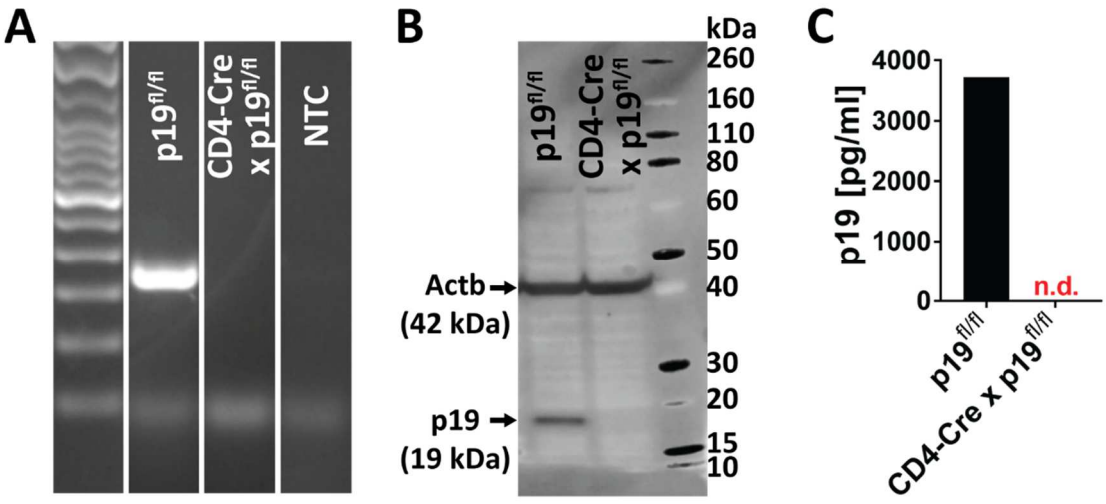

Figure 31: Validation of the p19-KO in* in vitro *differentiated Tregs. *Naïve T cells were isolated from p19$^{fl/fl}$ and CD4-Cre x p19$^{fl/fl}$ mice and cultured in the presence of anti-CD3 and anti-CD28 antibodies and 3 ng/ml rmTGFβ, 10 µg/ml anti-IL-4 and 10 µg/ml anti-IFNγ for 4 days. (**A**) After stimulation with PMA/ionomycin and monensin for 4 hours, the expression p19 mRNA was determined by RT-PCR. (**B**) p19 protein levels in PMA/ionomycin and monensin-stimulated Tregs were tested by western blotting of cell lysates. (**C**) Culture supernatants were collected prior to PMA/ionomycin stimulation and p19 levels were quantified by ELISA. n.d, not detectable. NTC, No Template Control.*

Next, p19-deficient CD4⁺ T cells were tested for their ability to differentiate into different T cell subsets *in vitro*. Therefore, naïve CD4⁺ T cells from p19$^{fl/fl}$ and CD4-Cre x p19$^{fl/fl}$ mice were cultured in the presence of anti-CD3 antibody and irradiated APCs (Th1/Th17) or anti-CD28 antibody (Treg) in the presence of polarizing cytokines. p19-deficient CD4⁺ T cells isolated from CD4-Cre x p19$^{fl/fl}$ mice showed no defect in differentiation into

Th1, Th17 or Tregs *in vitro*, as they expressed similar levels of IFNγ, IL-17A and FoxP3 as CD4⁺ T cells isolated from p19$^{fl/fl}$ control mice (Figure 32). This indicates that p19 is not required for initial T cell activation and differentiation of CD4⁺ T cells.

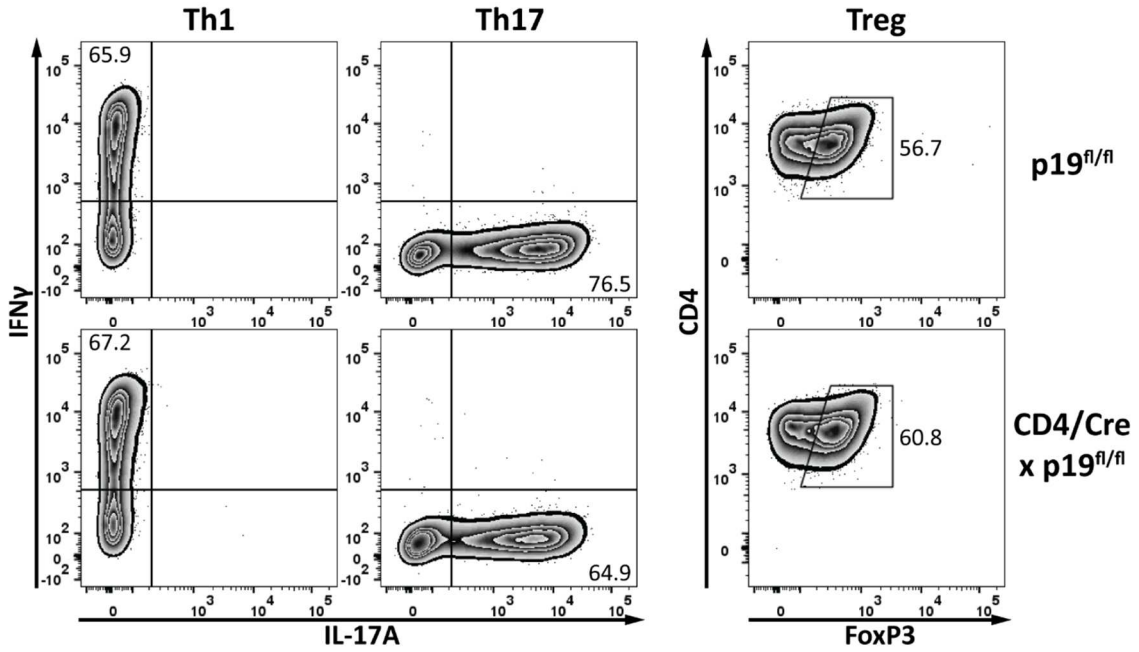

Figure 32: p19 is not required for the differentiation of CD4⁺ T cells. *Naïve T cells were isolated from p19$^{fl/fl}$ and CD4-Cre x p19$^{fl/fl}$ mice and cultured in the presence of anti-CD3 and irradiated APCs (Th1, Th17) or anti-CD28 (Treg) and polarizing cytokines for 4 days. After stimulation with PMA/ionomycin and monensin for 4 hours, the differentiation status was evaluated by flow cytometry.*

4.4.5 T cell-derived IL-23p19 is not required for in vivo *activation of T cells and EAE induction*

In addition to *in vitro* CD4⁺ T cell differentiation, we tested whether T cell-derived p19 was required for EAE induction. Therefore, EAE was induced in p19$^{fl/fl}$ and CD4-Cre x p19$^{fl/fl}$ mice by immunization with $MOG_{35–55}$ peptide in CFA. On day 6 after immunization, prior to disease onset, T cell activation was evaluated by measuring the levels of CD44, CD69 and CD62L on CD4⁺ T cells in the spleen and skin-draining iLNs. However, CD4⁺ T cells from CD4-Cre x p19$^{fl/fl}$ showed similar levels of CD44, CD69 and CD62L as p19$^{fl/fl}$ control cells indicating that initial T cell activation was not affected by p19 deficiency in CD4⁺ T cells (Figure 33A). In addition, CD4⁺ T cell differentiation and cytokine production was measured by culturing *in vivo* primed CD4⁺ T cells from the

spleens of immunized mice in the presence of $MOG_{35–55}$ peptide and with or without IL-23 for 4 days. After 4 days of *in vitro* culture, $CD4^+$ T cells produced high levels of IL-17 and GM-CSF, however, no difference could be observed in the cytokine recall response to $MOG_{35–55}$ peptide (Figure 33B, left graph). When the cells were cultured in the presence of IL-23, a significant increase of $IFN\gamma^+$ cells was observed in CD4-Cre x $p19^{fl/fl}$ cells as compared to $p19^{fl/fl}$ mice (Figure 33B, right graph). However, since less than 2 % of T cells produced IFNγ in both groups, the overall cytokine response was similar between $p19^{fl/fl}$ and CD4-Cre x $p19^{fl/fl}$ cells. Taken together, T cell-specific p19 deficiency does not lead to impaired *in vivo* activation, priming and differentiation of $CD4^+$ T cells after immunization with $MOG_{35–55}$ peptide in CFA.

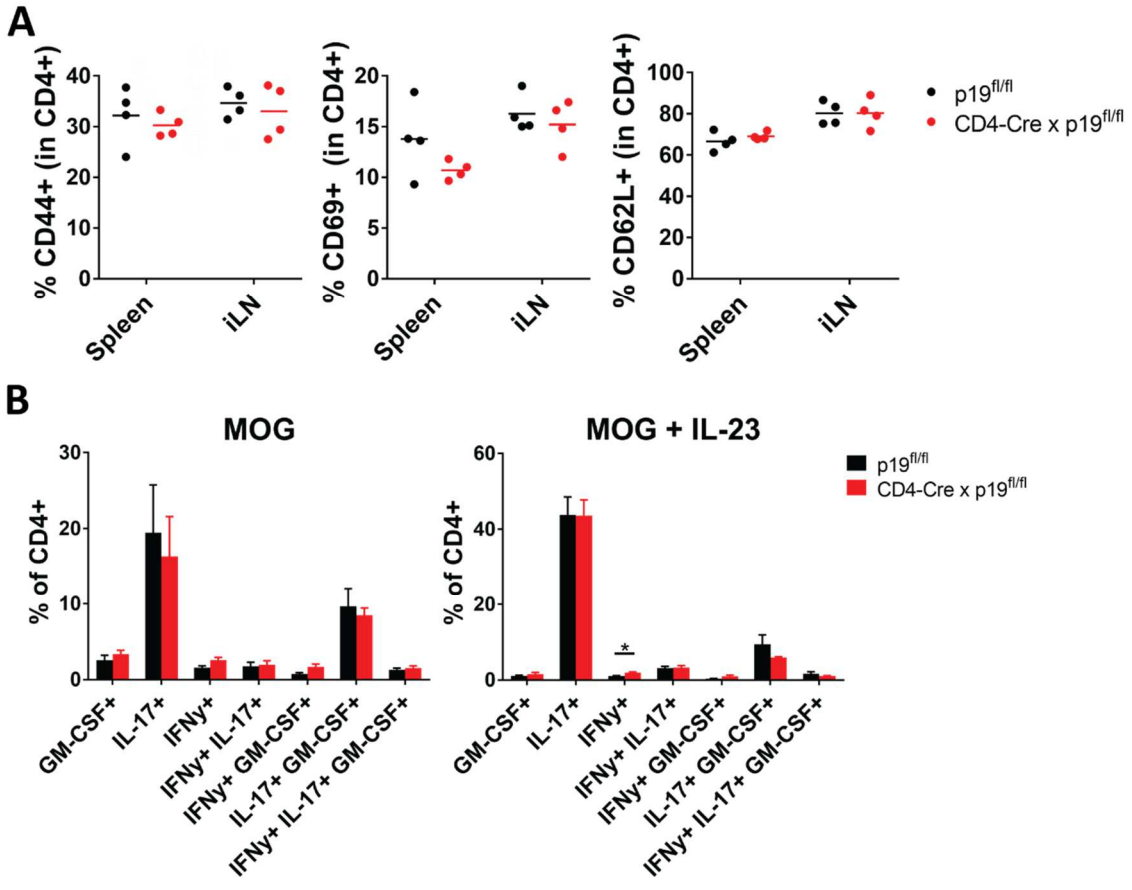

Figure 33: T cell-derived p19 is not required for* in vivo *T cell activation after $MOG_{35–55}$ immunization. *$p19^{fl/fl}$ and CD4-Cre x $p19^{fl/fl}$ mice were immunized with 100 µg $MOG_{35–55}$ emulsified in CFA (**A**) Spleens and inguinal LNs (iLNs) were collected 6 days after immunization and analyzed by flow cytometry. Horizontal lines indicate means. Dots represent individual mice. (**B**) Splenocytes isolated on day 6 after immunization were cultured with 10 µg/ml $MOG_{35–55}$ in the presence (left panel) or absence (right panel) of 10 ng/ml rmIL-23. After 4 days of culture, the cells were stimulated with PMA/ionomycin and monensin for 4 hours and the cytokine response was analyzed by flow cytometry. Data is shown as mean + SEM from 4 mice per group.*

In addition to investigating CD4$^+$ T cell activation prior to disease onset, p19$^{fl/fl}$ and CD4-Cre x p19$^{fl/fl}$ mice immunized with MOG$_{35–55}$ in CFA were monitored for the development of clinical disease. However, no clear clinical differences could be observed in regard to EAE incidence or severity in CD4-Cre x p19$^{fl/fl}$ mice as compared to p19$^{fl/fl}$ mice (Figure 34A, B). Furthermore, when analyzed at the peak of disease, the effector cytokine profile of CD4$^+$ T cells in the CNS of sick CD4-Cre x p19$^{fl/fl}$ mice was similar to p19$^{fl/fl}$ mice and there was no difference in the frequency of FoxP3$^+$ Tregs between p19$^{fl/fl}$ and CD4-Cre x p19$^{fl/fl}$ mice (Figure 34C, D). In summary, T cell-specific p19 is not required for EAE development in this active immunization model and does not affect the CD4$^+$ T cell phenotype in the CNS at the peak of disease.

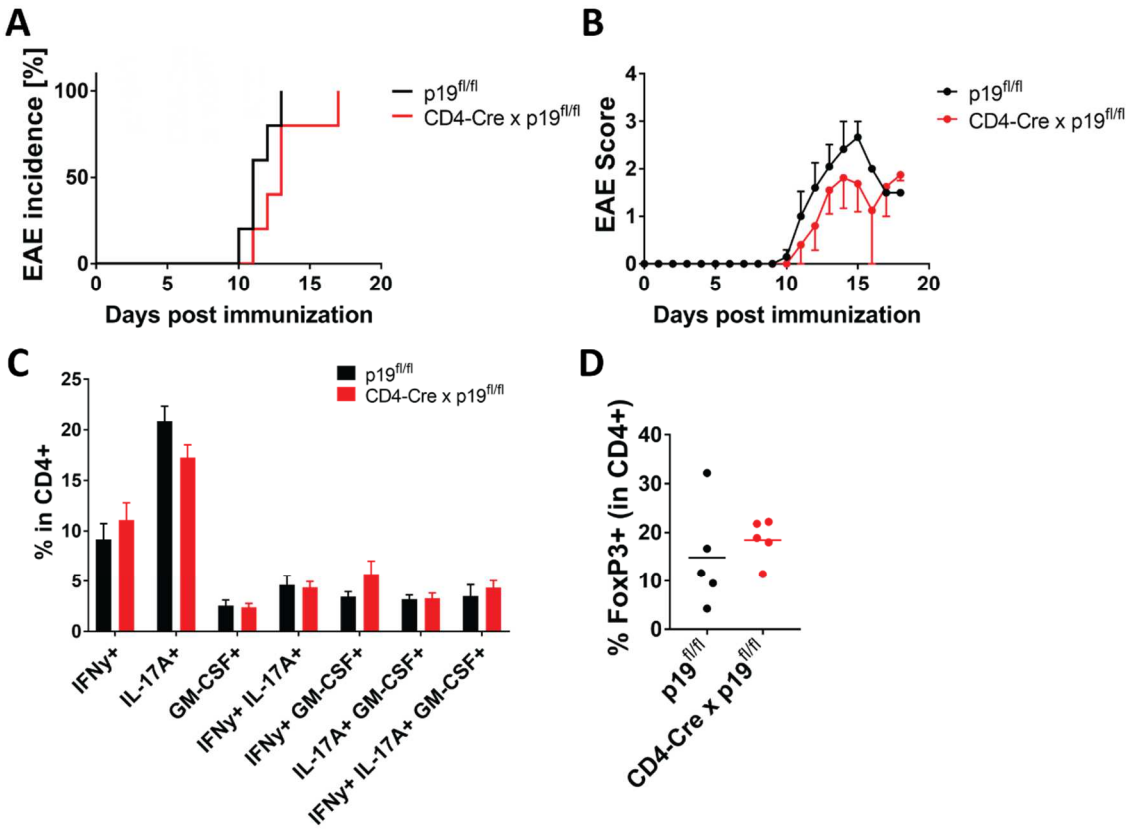

Figure 34: T cell-specific p19 deficiency does not impair EAE development. *p19$^{fl/fl}$ and CD4-Cre x p19$^{fl/fl}$ mice were immunized with 100 µg MOG$_{35–55}$ emulsified in CFA and observed for clinical signs of EAE. (**A**) EAE incidence from 5 mice per group. (**B**) EAE scores are shown as mean + SEM from 5 mice/group. (**C**) Mice were analyzed at the peak of disease and CNS-infiltrating cells were isolated and stimulated with PMA/ionomycin + monensin for 4 hours. Cytokine production by CD4$^+$ T cells was analyzed by flow cytometry. Data is shown as mean + SEM from 5 mice/group. (**D**) Frequency of FoxP3$^+$ cells in the CD4$^+$ population isolated from the CNS at the peak of disease. Horizontal lines indicate means. Dots represent individual mice.*

5. Discussion

5.1 Differences in B cell subset distribution and cytokine profile in Th mice

In the present study, we aimed to investigate the mechanisms by which antigen-specific B cells can interact with T cells of the same specificity to induce EAE. To do so, we used Th mice, which carry knock-in B cells specific for MOG and thereby secrete MOG-specific antibodies [68]. Since Th B cells cooperate with MOG-specific 2D2 $CD4^+$ T cells in double-transgenic mice to induce spontaneous EAE [69, 70], the B cell phenotype, activation status and cytokine profile of Th B cells was investigated. Flow cytometry analysis revealed that MOG-specific Th B cells show increased levels of early mature B cells in the bone marrow and increased levels of MZ B cells in the spleen (Figure 4, Figure 5). Interestingly, an expanded MZ B cell compartment has been described in many B cell transgenic lines such as mice with B cells specific for hen-egg-lysozyme (MD2, MD4 C57BL/6 and SW_{HEL} C57BL/6 [153, 154]), DNA (3H9 Balb/c and 3-32 NZB/W [155, 156]) or phosphorylcholine (M167 C57BL/6 [157]). This indicates that the increased number of MZ B cells in Th mice may be a result of the reduced repertoire diversity in transgenic and heavy chain knock-in mice. This limited repertoire diversity probably leads to an altered selection process of B cells during development and may therefore also explain the higher proportions of IgD^+ IgM^+ early mature B cells in the BM of Th mice (Figure 4). However, an expanded MZ B cell compartment was also described in several autoimmune conditions in mice and humans. For instance, MZ B cells were shown to be reactive against type II collagen and are involved in the initiation of autoimmune processes in collagen-induced arthritis (CIA) [158, 159]. Moreover, an expansion of MZ Bcells was observed in different models of SLE as well as in type 1 diabetes [160-164]. Furthermore, MZ B cells have been demonstrated to be activated in human disease such as Sjörgen's syndrome (SS) and Graves' disease [165, 166]. The autoimmune potential of MZ B cells may be explained by their functional properties: MZ B cells express high levels of MHC-II, CD80 and CD86 making them highly efficient APCs [14, 167]. In fact, presentation of self-antigen to T cells by MZ B cells was demonstrated in animal models of CIA, type 1 diabetes and SLE [158, 163, 168]. Similarly, MZ B cells isolated from Th mice were able to process and present MOG to 2D2 T cells in our *in vitro* co-culture experiments (Figure 7) and bind more MOG per cell than follicular Th B cells (unpublished data from our lab). In addition to increased numbers of

MZ B cells, which can act as APCs, Th B cells also showed a more pro-inflammatory B cell cytokine profile with elevated production of IL-6 and TNFα (Figure 8). Similar to our findings, enhanced IL-6 secretion by MZ B cells was also found in CIA and mouse models of SS [169, 170]. Furthermore, IL-6-expressing MZ B cells were increased during EAE induced by immunization with $MOG_{35–55}$ in CFA [110]. In Th mice, IL-6 and TNFα were not only increased in MZ B cells but also in follicular B cells, indicating that both the expansion of the MZ B cell compartment, as well as the more pro-inflammatory cytokine profile of both follicular and MZ B cells may contribute to their autoimmune potential. When Th mice are crossed to 2D2 mice, which harbor MOG-specific $CD4^+$ T cells, the mice develop spontaneous EAE [69, 70](Table 8). In this double-transgenic model, however, the observed changes in B cell subset distribution and pro-inflammatory cytokine profile were not further enhanced (Figure 10) as no differences could be observed between B cells of Th and OSE mice. Interestingly, MZ B cell numbers and IL-6 levels were even lower in OSE mice that developed disease than in mice that stayed healthy. This may be explained by the early time point of analysis as OSE mice develop spontaneous disease at around 4–5 weeks of age while the MZ takes about 3 weeks to develop [171] indicating that MZ formation could still be incomplete at the time of analysis. Nevertheless, a contribution of the pro-inflammatory cytokines secreted by Th B cells during cognate B:T cell interaction to disease development in OSE mice cannot be excluded. Thus, additional experiments such as the comparison of the B cell compartments in Th, single transgenic 2D2 and double-transgenic OSE mice of different ages are required to understand the different mechanism by which Th B cells contribute to EAE development in the OSE model.

5.2 B cell pro-inflammatory cytokines and their role in initiation of EAE

To investigate the mechanisms by which antigen-specific B cells could interact with antigen-specific T cells to induce EAE *in vivo*, an adoptive transfer model was established. By co-transferring highly activated MOG-specific Th B cells and unmanipulated MOG-specific 2D2 $CD4^+$ T cells, we were able to induce EAE in the first B cell adoptive transfer model that does not require immunization. In this system, B cells are expanded in the iGB culture system generating highly activated GC B cells, which

were shown to differentiate into memory B cells *in vivo* after adoptive transfer, where they express higher levels of MHC-II and CD80 than naïve B cells [140]. To make use of this potential APC function in our system, the expanded iGB cells were loaded with MOG protein prior to adoptive transfer. Using this novel B cell adoptive transfer system, we found that only MOG-specific Th iGB cells could stimulate 2D2 $CD4^+$ T cells to induce EAE, whereas WT iGB cells were not able to do so (Figure 11). Of course, it is likely that only Th B cells are able to bind and process their cognate antigen MOG and present it to 2D2 T cells. However, the pathogenicity of Th B cells in this system could also be mediated by MOG-specific antibodies, which are secreted in high levels by the injected Th iGB cells. Indeed, transfer of MOG-specific antibodies into naïve 2D2 mice has been shown to trigger activation of MOG-specific $CD4^+$ T cells and induce EAE, potentially by opsonization of otherwise undetected CNS antigen [172]. However, 4 % of 2D2 mice develop spontaneous EAE and 35 % develop spontaneous optic neuritis in the absence of MOG-specific antibodies [64] indicating that the blood-brain-barrier may already be leaky in 2D2 mice and may therefore lead to higher levels of MOG in the periphery, which can be opsonized by antibodies in the previously mentioned study. Another study using MOG-specific B and T cell co-transfer into C57BL/6 mice followed by active immunization showed that MOG-specific antibodies enhance antigen presentation by CNS-resident APCs and facilitate T cell reactivation directly in the CNS [173]. However, due to immunization, the T cells may already receive enough activating signals from other cell types and therefore antigen-presentation by B cells may not be required in this model. In contrast to these studies, others have shown that MOG-specific B cells can serve as APCs in EAE: Molnarfi et al. demonstrated that B cell APC function is required for EAE independent of MOG-specific antibodies [106]. Furthermore, B cell antigen presentation is sufficient for EAE induction in mice, in which MHC-II is expressed exclusively by B cells [105]. To determine the pathogenic contribution of antigen presentation vs. antibody production in our adoptive co-transfer model, the pathogenic potential of Th iGB cells that have not switched their isotype to IgG1 was compared to regular, switched Th iGB cells, and both switched and unswitched Th iGB cells were able to induce EAE with similar onset and incidence (Figure 14). Of course, this experiment cannot completely exclude a role of antibodies in this model, since unswitched Th iGB cells still secreted high levels of MOG-specific IgM and low levels of IgG1

antibodies. However, considering that MOG-specific IgG1 serum levels were significantly lower whereas the EAE incidence was even slightly higher in recipients of unswitched Th iGB cells, it is unlikely that MOG-specific IgG1 antibodies are critical for disease development in our co-transfer model. Another possibility to evaluate the role of MOG-specific antibodies in this system would be the use of genetically modified B cells that are not able to secrete antibodies. Here, *Prdm1*-KO B cells, which lack the transcription factor B lymphocyte-induced maturation protein-1 (Blimp-1) and thus cannot terminally differentiate into antibody-secreting plasma cells [174], could be used. These cells are able to switch their isotype but are impaired in antibody secretion and would therefore serve as a good control in our experimental setting; however, as these cells still secrete residual antibodies, they have some limitations as well. Interestingly, we found slightly higher levels of IgG1 antibodies in sick vs. healthy mice receiving unswitched iGB cells (Figure 14), as well as in spleens and mLNs of mice receiving switched Th iGB cells as compared to mice receiving switched WT iGB cells (Figure 12). This also supports the hypothesis that direct B:T cell interactions occur in our model (probably during antigen-presentation) leading to T cell activation and subsequently to continued isotype switching of the B cells in response to T cell-derived stimuli. Here, a co-transfer of Th iGB cells together with WT instead of MOG-specific 2D2 $CD4^+$ T cells could help to confirm whether the cognate B:T cell interaction is required for the continued isotype switching and differentiation of Th iGB cells *in vivo*.

Another mechanism by which Th B cells could promote disease development is the production of pro-inflammatory cytokines in context with APC function. Since investigating the role of B cell cytokines in EAE induction was the main objective of this study, a protocol for retroviral overexpression of different cytokines in B cells using the iGB culture system was established. Mean transduction rates of 40–60 % led to secretion of high cytokine levels by iGB cells both *in vitro* and after adoptive transfer *in vivo* (Figure 15, Figure 16). Since 2D2 $CD4^+$ T cells in the CNS mainly exhibited a Th1 phenotype in the initial adoptive co-transfer experiments, the first candidate cytokine to test in our model was IL-6, which is one of the key cytokines for differentiation into Th17 cells [84-86]. Furthermore, B cell-specific IL-6 deficiency was shown to reduce EAE severity and Th17 responses, and B cell depletion therapy eliminated pathogenic IL-6-producing B cells [106, 110]. Here, IL-6 overexpression by

iGB cells led to an earlier disease onset without inducing a Th17 response (Figure 17). One reason for this could be the experimental system using Rag1-KO recipients, in which a Th1 phenotype may be favored over differentiation and stabilization of Th17 cells. This idea is supported by our own observations showing that even highly activated, *in vitro* generated Th17 cells lose their IL-17A expression and easily convert into IFNγ-producing cells upon transfer into Rag1-KO mice (unpublished). Rather than enhancing IL-17A production, IL-6 overexpression was associated with splenomegaly and an expansion of myeloid cells in the periphery in our model (Figure 18, Figure 19). A similar phenotype was described in IL-6 transgenic mice, in which high systemic IL-6 levels led to an expansion of megakaryocytes in the bone marrow as well as splenomegaly induced by extramedullary hematopoiesis, but also massive expansion of plasma cells [175, 176]. Furthermore, in another transgenic mouse, in which IL-6 is selectively overexpressed by $CD11c^+$ DCs, IL-6 overexpression led to a massive expansion of $Ly\text{-}6G^+$ neutrophils and $Ly\text{-}6C^{high}$ monocytes [177]. The pleiotropic effects of IL-6 overexpression can be explained by the many different functions IL-6 has under physiological conditions: after synthesis at the site of inflammation, IL-6 is released to the blood stream thereby reaching different organs. In the liver, IL-6 induces the production of acute phase proteins such as C-reactive protein, serum amyloid A or fibrinogen [178]. When IL-6 reaches the bone marrow, it promotes expansion and maturation of megakaryocytes thereby leading to the generation of enhanced platelet numbers [179]. Both platelet counts as well as the changes in acute phase proteins are often used for the evaluation of inflammatory severity in many infectious diseases. Furthermore, by inducing the production of vascular endothelial growth factor (VEGF), IL-6 leads to enhanced angiogenesis and increased vascular permeability, which are often seen in rheumatoid arthritis (RA) [180, 181]. As discussed above, IL-6 is crucial for the differentiation of Th17 cells, but it also acts on other lymphocytes e.g. by inducing differentiation of $CD8^+$ T cells or by promoting differentiation of antibody-secreting plasma cells, all of which can contribute to chronic inflammation and autoimmunity [175, 182]. Importantly, IL-6 shifts the differentiation of monocytes from DCs to macrophages [183], which could explain the expansion of myeloid cells in our model. Due to the wide range of biological functions and its pathogenic role in various diseases, targeting IL-6 is a promising treatment strategy for many different immune-mediated diseases. Thus,

tocilizumab, a monoclonal humanized anti-IL-6 receptor antibody was developed that blocks IL-6-mediated signal transduction. Tocilizumab showed great efficacy and is now approved for the treatment of RA as well as for systemic juvenile idiopathic arthritis, giant cell arthritis and Castleman's disease, a benign tumor of B cells [184]. Furthermore, tocilizumab significantly reduced the relapse rate in patients with neuromyelitis optica spectrum disorder in a phase 2 trial [185]. In contrast, the case of a 48-year-old female RA patient was reported who developed MS while on treatment with tocilizumab indicating that newly arising white matter lesions may be a critical complication of anti-IL-6 receptor therapy and may limit the use of tocilizumab for demyelinating diseases [186]. The causal relationship of these two conditions still needs to be investigated; however, this case suggests that IL-6 may have immunosuppressive properties as well. Indeed, IL-6 was shown to induce the proliferation of myeloid-derived suppressor cells and to promote their immunosuppressive capacity [187-189]. In addition, IL-6 has been shown to be neuroprotective by stimulating neurotrophin production in astrocytes thereby supporting neuronal and oligodendroglial survival [190]. As described above, IL-6 also promotes differentiation of plasma cells, which have been shown to produce anti-inflammatory cytokines and can thereby ameliorate EAE [114, 115, 151]. Furthermore, high numbers of IL-6-expressing cells were found in inactive demyelinating lesions of MS patients where they correlated with oligodendrocyte preservation indicating a protective role for IL-6 in the CNS in the context of MS [191]. Most likely, the systemically high IL-6 levels in our co-transfer experiments led to a very pro-inflammatory environment, which, after expansion of the myeloid compartment, especially of neutrophils and $Ly6C^+$ inflammatory monocytes, led to an accelerated T cell activation and finally to EAE induction. This highly inflammatory environment was even enough to induce EAE in mice that received polyclonal WT iGB cells overexpressing IL-6. However, the fact that Th iGB_6 cells were superior to both WT iGB_6 cells and Th iGB_{GFP} cells to induce EAE indicates that both the unspecific pro-inflammatory effect of IL-6 overexpression and the antigen-specificity of the B cells synergize resulting in an earlier disease onset in our system.

Similar to Th iGB_6 transfer experiments, overexpression of IL-23p19 by transferred Th iGB cells led to an earlier EAE onset, however, this effect was only seen when transduction rates exceeded 40 % and p19 was detectable in high levels in the serum of

recipient mice (Figure 20). This could indicate that p19 levels need to pass a certain threshold before influencing T cell activation and thereby contributing to EAE development. Another reason for this inconsistency may lie in the overall condition of the transferred iGB cells. Transduction rates in our iGB culture system crucially depend on the proliferation rate of the B cells since MSCVs are only able to infect exponentially growing cells efficiently. Conversely, a low transduction rate indicates that not enough cells were actively dividing at the time of transduction and reduced proliferation could be a sign of suboptimal activation of the iGB cells. Thus, weakly transduced iGB cells could also be less activated and therefore less able to interact with $CD4^+$ T cells after adoptive transfer *in vivo*. However, since we have not identified the mechanism by which p19 overexpression can lead to earlier disease onset, this remains speculative. In contrast to iGB_6 cell transfer, p19 overexpression did not lead to an expansion of myeloid cells in the spleen indicating that the effects of p19 are mediated by a different mechanism. One possibility is that, in addition to overexpressing p19, iGB cells endogenously express p40 leading to the secretion of heterodimeric IL-23. However, we could not detect p40 expression in iGB cells neither on mRNA level nor as secreted IL-23, and not even in iGB cells transduced with both the p19 and the p40 subunits (not shown). In line with these data, murine B cells fail to secrete IL-12 and p40 in response to bacterial stimuli or upon antigen-specific interaction with T cells [192]. In contrast, it was shown recently that B cells can secrete the novel cytokine IL-39, which consists of p19 and Ebi3, and that B cell-derived IL-39 leads to an expansion of neutrophils in a mouse model of SLE [132, 133]. Indeed, we have found some baseline expression of *ebi3* mRNA in our iGB cells making IL-39 an interesting candidate to investigate in our model in the future. Additionally, p19 could also act on its own without binding to any β-subunit. An individual, intracellular function of IL-23p19 was described in human endothelial cells, where it leads to increased expression of ICAM-1 and VCAM-1, thereby facilitating the attachment and transendothelial migration of leukocytes [134]. Thus, it is possible that p19 overexpression in our model has an intracellular or autocrine effect on the iGB cells themselves e.g. by inducing the expression of other pro-inflammatory molecules. Other subunits of the IL-12 family can be secreted autonomously and act independent of their normal binding partner as well. For example, p28, the α-subunit of IL-27, can antagonize signaling through the receptor subunit gp130 and thereby limit

IL-6-mediated production of IL-17 and IL-10 [193]. In addition, p40 can be secreted both as a monomer and as a homodimer and can have very divergent functions [194-197]. Therefore, it is possible that p19 also has individual functions as a monomer or homodimer and more research is required to investigate these additional, p40-independent functions. To uncover possible mechanisms by which p19 overexpression in Th iGB cells leads to an earlier EAE onset in our co-transfer system, RNA sequencing of Th iGB_{p19} versus Th iGB_{GFP} cells could help to identify differentially expressed genes and pathways associated with p19 overexpression. In addition, the role of p19 in B cell biology and function could be explored using global and B cell-specific p19-KO mice which can be generated from the mice described in section 4.4.1.

MOG-specific Th B cells produced more IL-6 and TNFα than WT B cells and IL-6 overexpression could contribute to the pro-inflammatory potential of both WT and Th B cells. However, whether the expression of IL-6 and TNFα is also necessary for the induction of EAE in our adoptive co-transfer system is not yet clear. To test this, B cells deficient for these cytokines of interest are useful, however, generating and crossing specific KO mice to our Th mice takes quite a long time. A faster and easier approach to knock-down certain molecules is the CRISPR-Cas9 system [198, 199]. We used this method in our established retroviral overexpression system and successfully generated iGB cells with significantly reduced expression of IL-6 and TNFα (Figure 22). In contrast to cytokine overexpression experiments, in which a 40–50 % transduction rate leads to a massively increased cytokine secretion, puromycin selection is necessary for the CRISPR-Cas9 experiments to generate a pure iGB population, in which the respective cytokine is knocked-down efficiently. As the selection process takes 2–3 days, slight adjustments of the culture conditions may be necessary to ensure that the transduced iGB cells still exhibit an APC phenotype and have not yet differentiated into plasma cells. However, after optimization of the transduction and selection protocol, these iGB cells can be used to test the requirement for the expression of different cytokines to induce EAE in our adoptive co-transfer model. A comparison of overexpression and CRISPR-Cas9-mediated knock-down may provide further insights into the relevance of enhanced or reduced cytokine levels for the pathogenicity of MOG-specific B cells.

5.3 The role of IL-10-producing B cells in regulation of Th17-mediated EAE

In addition to producing high levels of pro-inflammatory cytokines such as IL-6 and TNFα, B cells and especially plasma cells are also known to produce anti-inflammatory cytokines including IL-10 and IL-35. Thereby, they are able to ameliorate EAE by mediating a regulatory effect in the periphery [114, 115, 151]. However, in MS, B cells do not only act in the periphery but are recruited efficiently to the CNS. In addition to intrathecal antibodies and plasma cells in the CSF of MS patients, eLFs can be found in a fraction of SPMS patients, which contain clusters of B cells and plasma cells [100, 102]. Although some studies suggested a correlation between the presence of eLFs and disease severity [100, 200-202], it is also possible that eLFs regulate inflammation by harboring anti-inflammatory B and T cells. Overall, the clinical relevance of eLFs in MS patients remains controversial. A good model to study the role of eLFs in EAE is the Th17 adoptive transfer model, in which high numbers of B cells and plasma cells are recruited to the CNS [92, 101]. To test whether IL-10-producing plasma cells are recruited to eLFs and can regulate EAE directly in the CNS, we combined the Th17 adoptive transfer model with injection of IL-10-overexpressing iPBs generated in the iGB culture system (Figure 23).While antigen-specificity was required for the suppressive capacity of B cells in a previous study [114], transfer of MOG-specific Th iPBs into Th17 recipients led to accelerated EAE development in our hands (Figure 24). Considering that others have shown that transfer of MOG-specific antibodies facilitates EAE development in 2D2 mice and that MOG-specific antibodies enhance EAE in C57BL/6 mice induced by active immunization by promoting T cell reactivation in the CNS [172, 173], it is very likely that the observed exacerbation was caused by the high levels of MOG-specific IgG1 antibodies produced by the injected Th iPBs. Consistent with this observation, experiments by our group showed that Th17 transfer into Th recipients resulted in significantly earlier disease onset while this effect was abrogated when Th17 cells were transferred into Th x Mb1-Cre x $Prdm1^{fl/fl}$ mice, in which a B cell-specific Blimp-1-KO leads to defects in antibody secretion (unpublished own observations).

In contrast, injection of IL-10-overexpressing WT iPBs resulted in lower number of transferred Th17 cells, but higher frequencies of anti-inflammatory endogenous $CD4^+$ T cells in the CNS of Th17 recipients without affecting the clinical outcome (Figure 27). This may be due to the fact that despite these differences the number of

highly activated encephalitogenic Th17 cells still outnumbered the anti-inflammatory $CD4^+$ T cells in the CNS. Furthermore, the Th17 adoptive transfer model is generally characterized by severe clinical disease with high scores and no recovery, which makes it difficult to study a possible resolution of inflammation mediated by anti-inflammatory cells. Nevertheless, the fact that the transferred IL-10-overexpressing iPBs were injected just before disease onset and could be recovered from the CNS but not from any peripheral organ of the recipient mice indicates that the injected iPBs preferentially migrate to the CNS and thus have the unique potential to act directly at the site of inflammation. It has been shown previously that the CNS may serve as a niche for anti-inflammatory plasma cells as gut-derived IgA^+ plasma cells migrate to the inflamed CNS and are a relevant source of IL-10 in the CNS during EAE [203]. In addition, it was shown recently that a substantial proportion of B cells in meningeal B cell aggregates in the CNS of sick OSE mice produced either IL-10 or IL-35 suggesting that they fulfill an immunoregulatory function in this spontaneous EAE model [204]. Thus, it would be interesting to determine whether the transferred iPB_{10} cells were localized within the eLFs or elsewhere in the CNS in our model. However, due to the low frequency of endogenous B cells in both iPB_{GFP} and iPB_{10} recipients, identification of big B cell aggregates and eLFs may be difficult. The mechanism by which iPBs inhibit the accumulation of B cells in the CNS is yet unclear. One possible explanation could be that WT iPBs already have anti-inflammatory properties irrespective of the overexpression of IL-10. Indeed, we found substantial levels of baseline IL-10 expression in iPBs cultured in the presence of IL-21 (Figure 15). Similarly, iPBs could produce other anti-inflammatory cytokines such as IL-35 and TGFβ or mediate suppression via surface receptors such as PD-L1 and LAG3, mechanisms by which plasma cells can impair anti-tumor immunity and immunity against *Salmonella typhimurium* [205-207]. Thus, additional experiments using IL-35 or TGFβ-overexpressing iPBs may provide further insights into the role of different anti-inflammatory cytokines in our model. In addition to a possible anti-inflammatory function of iPBs, which prevents migration and/or proliferation of endogenous B cells in the CNS compartment, iPBs could have an advantage over endogenous B cells by enhanced responsiveness to CNS-derived chemokines. For example, CXCL10 levels are increased in the CNS of mice with EAE as well as in the CSF of MS patients [208, 209]. CXCL10 binds to the chemokine receptor

CXCR3, which is upregulated on memory B cells and IgG1$^+$ plasma cell precursors [210]. Interestingly, several studies show that CXCL10 KO or blockade leads to increased EAE severity [211, 212], potentially by inhibiting the migration of regulatory plasma cells. Furthermore, compared with naïve and mature B cells, plasma cells express higher levels of CXCR4 and are thereby more responsive to CXCL12, which is expressed by astrocytes during inflammation [213, 214]. Thus, due to their higher expression of chemokine receptors and their preferential recruitment to the CNS, our iPBs could then deprive other B cells of chemokines and other survival factors, which may limit accumulation of endogenous B cells in the CNS. Analysis of the mice at an earlier time point e.g. at the onset of disease just after iPB transfer may reveal whether iPBs are in fact the first B cells that migrate to the CNS and inhibit recruitment of endogenous B cells but also transferred Th17 cells directly from there.

Taken together, B cells can have very divergent roles in EAE initiation and regulation, as well as in human MS. Mature memory B cells and MZ B cells contribute to the pathogenic functions of B cells by acting as APCs or by the production of pro-inflammatory cytokines such as IL-6 and TNFα. Therefore, B cell depletion therapy with anti-CD20 antibodies such as rituximab or ocrelizumab is beneficial for MS patients by depleting pathogenic B cell subsets that may secrete pro-inflammatory cytokines but sparing anti-inflammatory plasma cells, which do not express CD20 [103, 110]. In contrast, atacicept, a human recombinant fusion protein targeting BAFF and A Proliferation-Inducing Ligand (APRIL) blocks late stage developing B cells and plasma cells while sparing B cell progenitors and memory B cells [215]. Clinical trials using atacicept in MS patients were suspended after substantially increased inflammatory activity was observed, potentially due to the depletion of anti-inflammatory plasma cells but not pro-inflammatory memory B cells. This illustrates the importance of understanding the role of different B cell subsets in MS pathogenesis to be able to develop novel therapies to selectively target pathogenic B cell subsets while sparing beneficial regulatory B cells.

5.4 Identification of IL-23p19-expressing cells during EAE and the role of IL-23p19 in T cell biology

To identify the cellular sources of IL-23p19 during EAE we successfully generated a novel reporter mouse, in which IL-23p19 expression can be measured by LacZ activity using the FACS-Gal assay. Using this reporter mouse, we unexpectedly found high signal in *in vitro* activated and differentiated $CD4^+$ T cells, as well as some signal in $CD4^+$ and $CD8^+$ T cells during EAE (Figure 29, Figure 30). In contrast, we could not detect any signal in DCs, macrophages or microglia neither after stimulation *in vitro* nor during EAE. This was surprising since IL-23 was often proposed to be secreted by APCs thereby shaping T cell responses. However, so far it is difficult to assess the accuracy of our novel reporter mouse as the LacZ reporter construct may have some disadvantages. First, FDG is hydrophilic and therefore requires a hypotonic shock to be introduced into cells, which may lead to uneven substrate loading. Furthermore, fluorescein produced after cleavage of FDG diffuses rapidly out of the cell, which can be minimized but not completely inhibited by keeping the cells on ice during the loading and staining process [216]. This may lead to a loss of signal and therefore reduce the sensitivity of the reporter. In addition, the reporter construct consists of a gene-trap leading to disruption of gene activity (Figure 28). Thus, only heterozygous mice can be used as reporter mice. However, under certain circumstances some cytokines seem to be expressed monoallelic due to stochastic regulation mechanisms, which makes it possible to overlook cytokine-producing cells when they express the cytokine from the allele that does not contain the reporter. Such a mechanism has been shown for several cytokines including IL-10, IL-4 and IL-2, but whether it also applies to IL-23p19 remains to be investigated [217-219]. Especially in the case of macrophages and microglia, the sensitivity of the FACS-Gal assay may be suboptimal due to high autofluorescence or enhanced uptake of the substrate leading to a strong background signal in the FITC channel. Indeed, the mean fluorescence intensity of the ‘negative’ population was much higher in myeloid cells as compared to T cells (Figure 30). In contrast to insufficient sensitivity, LacZ reporter activity could also overreport p19 expression, since LacZ has a very long half-life of approximately 30 hours in mammalian cells and may therefore still show signal even when p19 is not actively expressed anymore [220]. To finally evaluate the sensitivity and specificity of our novel p19.LacZ reporter mouse line, comprehensive

experiments are needed in which p19 mRNA levels from different cell types during EAE are quantitatively measured and compared to the reporter signal.

Il23a mRNA was detected in microglia and monocytes in the CNS during EAE, suggesting that IL-23 is important for the disease effector phase in the CNS [82]. However, results in this study were reported as relative expression and the comparison to other cells such as T cells is missing, which makes it difficult to judge whether p19 levels in microglia and monocytes are high or rather low. Interestingly, *Il23a* mRNA expression was already detected in T cells in early studies [81], but since T cells do not express p40 and thus cannot assemble and secrete functional IL-23, a potential function of p19 in T cells was never investigated. However, as discussed in section 5.2, p19 may have p40-independent functions and T cell-derived p19 may even be crucial for EAE development. Indeed, Thakker et al. showed that T cells isolated from immunized global p19-KO mice caused delayed and less severe EAE when injected into WT recipients as compared to mice that received WT donor cells [221]. Conversely, injection of WT donor cells into p19-KO mice resulted in normal EAE development [221]. The authors concluded that IL-23 plays an important role in the early generation of effector T cells and during the induction phase of EAE but – in contrast to the data from Cua et al. [82] – is not required for the disease effector phase in the CNS. However, these results could as well point to a T cell-intrinsic defect in the absence of IL-23p19, which leads to reduced encephalitogenicity. To test this hypothesis, we generated CD4-Cre x $p19^{fl/fl}$ mice, in which p19 is selectively knocked-out in T cells and successfully confirmed the KO using different techniques including RT-PCR, western blot and ELISA (Figure 31). p19-deficient $CD4^+$ T cells did not show any obvious defect in activation or differentiation, and CD4-Cre x $p19^{fl/fl}$ mice developed EAE similarly to $p19^{fl/fl}$ control mice upon immunization with $MOG_{35–55}$ in CFA (Figure 32, Figure 34). These results are contrary to a very recently published study that described reduced EAE severity in CD4-Cre x $p19^{fl/fl}$ mice associated with reduced GM-CSF production by encephalitogenic $CD4^+$ T cells [222]. This discrepancy may be explained by different scenarios: first, Hasegawa et al. used a different strain of floxed mice, in which the two loxP sites flank all four exons of the p19 gene resulting in a loss of all four exons after Cre recombination [221]. In contrast, in our novel mouse line the critical exons are exons 2–4 leaving exon 1 intact after recombination (Figure 28). Second, different mouse facilities and therefore

different composition of the microbiota may influence the outcome of EAE, since the gut microbiome was shown to be associated with EAE susceptibility [223, 224]. A third, experimental reason may be the amount of $MOG_{35–55}$ peptide and/or PTX used for immunization. By using a suboptimal immunization protocol, it may be possible to uncover subtle differences that we could not observe using our standard immunization protocol. Lastly, the time points of analysis were chosen very differently in our study as compared to Hasegawa et al. In our experiment, the mice were analyzed at the peak of disease to study the T effector cells at their maximal inflammatory activity and at this time point, we could not observe any differences in the cytokine profile of CNS-infiltrating $CD4^+$ T cells. In contrast, Hasegawa et al. analyzed the mice very late during the recovery phase, when CD4-Cre x $p19^{fl/fl}$ mice showed almost no disease activity anymore. Thus, it is possible that the cytokine profile of p19-deficient CNS T effector cells changes only during the recovery phase of EAE, and therefore additional experiments with different $MOG_{35–55}$/PTX dosage and adjusted time points of analysis are needed to draw final conclusions.

Although we could not detect p19 expression in different APCs such as macrophages, BMDCs or microglia with our LacZ reporter mouse, possibly due to the limitations of the reporter as discussed above, APCs are still considered important producers of heterodimeric IL-23. Many studies point towards a role of APC-derived IL-23 in different contexts [81, 225, 226] but most studies have measured relative expression of *Il23a* mRNA thereby making it difficult to judge the biological relevance of IL-23p19 in these cells. In the context of EAE, it is still controversial whether IL-23p19 is important during the priming or rather the effector phase of the disease [82, 221]. Hence, to test the role of IL-23p19 produced by APCs during EAE, different genetic models are needed. For example, CX3CR1-CreERT2 mice express a tamoxifen-inducible Cre recombinase in mononuclear phagocytes such as monocytes and macrophages, but also in microglia [227]. Furthermore, treatment with tamoxifen followed by a wash-out period of 1–2 months will allow for targeting microglia exclusively since they have a much longer lifespan than monocytes and will be uniquely targeted by this protocol [228]. Thus, crossing these mice to our $p19^{fl/fl}$ mice may allow to evaluate the role of IL-23p19 derived from a broad variety but also single subsets of APCs during EAE.

6. Conclusion

The aim of this thesis was to investigate the mechanisms by which antigen-specific B cells can cooperate with MOG-specific $CD4^+$ T cells to induce EAE, specifically focusing on cytokine production of the MOG-specific B cells. First, the phenotype of MOG-specific B cells isolated from Th mice was analyzed. Doing so we found that Th B cells showed an altered B cell subset distribution with a significantly larger MZ B cell compartment. Furthermore, both MZ B cells and follicular B cells from Th mice produced more pro-inflammatory IL-6 and TNFα but less anti-inflammatory IL-10 than polyclonal WT B cells. To translate these findings into an *in vivo* system, an adoptive co-transfer model was developed, in which only MOG-specific Th iGB cells but not WT iGB cells were able to stimulate MOG-specific 2D2 $CD4^+$ T cells to induce EAE. To our knowledge, this is the first B cell adoptive transfer EAE model that does not require immunization, and MOG-specific B cells induced EAE probably by a combination of antigen presentation, cytokine production, and autoantibody production. Whether antigen presentation or rather antibody production is the dominant pathogenic feature in this system could not be definitely resolved; however, we could show that high levels of anti-MOG IgG1 antibodies are not required for the induction of EAE in this system. Overexpression of IL-6 by iGB cells led to a highly inflammatory environment characterized by an expanded myeloid compartment in the periphery. This unspecific pro-inflammatory effect acted synergistically with the BCR-specificity of the B cells to promote EAE development. In contrast, overexpression of IL-23p19 led to an earlier disease onset without affecting the myeloid compartment. This effect was only observed when very high levels of IL-23p19 could be detected in the recipients and the mechanism by which IL-23p19 contributes to accelerated EAE remains unclear.

While the expression of pro-inflammatory cytokines could enhance the pathogenic potential of B cells in our iGB adoptive transfer EAE system, IL-10-overexpressing plasmablasts could induce a more anti-inflammatory $CD4^+$ T cell profile in the CNS of Th17 recipients. Although IL-10-overexpressing plasmablasts could not significantly ameliorate clinical disease in Th17 adoptive transfer EAE, the fact that they specifically migrated to the CNS and modulated the endogenous B and T cell response indicates that they can contribute to regulation of Th17-mediated EAE and studying the mechanisms

by which anti-inflammatory plasmablasts fulfill their regulatory function will help to further explore their therapeutic potential.

In a second part of the study, we aimed to identify cellular sources of IL-23p19 and therefore successfully generated a novel IL-23p19.LacZ reporter mouse with conditional potential. Using this reporter mouse, we discovered that T cells express high levels of IL-23p19 after *in vitro* activation and differentiation, as well as during EAE. To test the role of T cell-derived IL-23p19 in EAE, a conditional CD4-Cre x $p19^{fl/fl}$ mouse was generated, in which IL-23p19 is selectively deleted in T cells. We found that p19-deficient T cells had no obvious defects in activation or differentiation and p19 deficiency in T cells did not influence EAE development upon immunization with MOG/CFA. However, as the effects of p19 in T cells may be masked by strong activation signals, more experiments are needed to conclusively understand the role of IL-23p19 in T cells, but also in myeloid APCs such as monocytes, macrophages or microglia. With our new $p19^{fl/fl}$ line, we have generated a precise tool to comprehensively address these open questions.

Overall, we found that B cells can have very divergent roles in EAE initiation and regulation. This shows that it is crucial to understand the role of different B cell subsets in EAE and MS pathogenesis to be able to develop therapies that selectively deplete pathogenic B cells while preserving the beneficial ones. Furthermore, identifying and understanding the role of IL-23p19-producing cells during EAE may give insights into the potential of IL-23p19 as therapeutic target in MS.

7. References

1. Medzhitov, R. and C. Janeway, Jr., *Innate immunity.* N Engl J Med, 2000. **343**(5): p. 338-44.
2. Kawai, T. and S. Akira, *The role of pattern-recognition receptors in innate immunity: update on Toll-like receptors.* Nature Immunology, 2010. **11**(5): p. 373-384.
3. Vivier, E., et al., *Innate Lymphoid Cells: 10 Years On.* Cell, 2018. **174**(5): p. 1054-1066.
4. Vivier, E., et al., *Innate or adaptive immunity? The example of natural killer cells.* Science (New York, N.Y.), 2011. **331**(6013): p. 44-49.
5. Fearon, D.T. and R.M. Locksley, *The Instructive Role of Innate Immunity in the Acquired Immune Response.* 1996. **272**(5258): p. 50-54.
6. Parkin, J. and B. Cohen, *An overview of the immune system.* The Lancet, 2001. **357**(9270): p. 1777-1789.
7. Smith-Garvin, J.E., G.A. Koretzky, and M.S. Jordan, *T Cell Activation.* 2009. **27**(1): p. 591-619.
8. Harty, J.T., A.R. Tvinnereim, and D.W. White, *CD8+ T cell effector mechanisms in resistance to infection.* Annu Rev Immunol, 2000. **18**: p. 275-308.
9. Lenschow, D.J., T.L.W. and, and J.A. Bluestone, *CD28/B7 SYSTEM OF T CELL COSTIMULATION.* 1996. **14**(1): p. 233-258.
10. Allman, D. and S. Pillai, *Peripheral B cell subsets.* Curr Opin Immunol, 2008. **20**(2): p. 149-57.
11. Fagarasan, S. and T. Honjo, *Intestinal IgA synthesis: regulation of front-line body defences.* Nat Rev Immunol, 2003. **3**(1): p. 63-72.
12. Cerutti, A., M. Cols, and I. Puga, *Marginal zone B cells: virtues of innate-like antibody-producing lymphocytes.* Nat Rev Immunol, 2013. **13**(2): p. 118-32.
13. Song , H. and J. Cerny *Functional Heterogeneity of Marginal Zone B Cells Revealed by Their Ability to Generate Both Early Antibody-forming Cells and Germinal Centers with Hypermutation and Memory in Response to a T-dependent Antigen.* Journal of Experimental Medicine, 2003. **198**(12): p. 1923-1935.
14. Attanavanich, K. and J.F. Kearney, *Marginal Zone, but Not Follicular B Cells, Are Potent Activators of Naive CD4 T Cells.* The Journal of Immunology, 2004. **172**(2): p. 803-811.
15. Genestier, L., et al., *TLR agonists selectively promote terminal plasma cell differentiation of B cell subsets specialized in thymus-independent responses.* Journal of immunology (Baltimore, Md. : 1950), 2007. **178**(12): p. 7779-7786.
16. Garside, P., et al., *Visualization of specific B and T lymphocyte interactions in the lymph node.* 1998. **281**(5373): p. 96-99.
17. Foy, T.M., et al., *gp39-CD40 interactions are essential for germinal center formation and the development of B cell memory.* 1994. **180**(1): p. 157-163.
18. Han, S., et al., *Cellular interaction in germinal centers. Roles of CD40 ligand and B7-2 in established germinal centers.* 1995. **155**(2): p. 556-567.
19. MacLennan, I.C., et al., *Extrafollicular antibody responses.* 2003. **194**(1): p. 8-18.
20. Mandel, T.E., et al., *The follicular dendritic cell: long term antigen retention during immunity.* Immunol Rev, 1980. **53**: p. 29-59.
21. Vinuesa, C.G., et al., *Follicular Helper T Cells.* Annu Rev Immunol, 2016. **34**: p. 335-68.

22. Coffman, R.L., H.F. Savelkoul, and D.A. Lebman, *Cytokine regulation of immunoglobulin isotype switching and expression.* Semin Immunol, 1989. **1**(1): p. 55-63.
23. Reinhardt, R.L., H.E. Liang, and R.M. Locksley, *Cytokine-secreting follicular T cells shape the antibody repertoire.* Nat Immunol, 2009. **10**(4): p. 385-93.
24. Gitlin, A.D., Z. Shulman, and M.C. Nussenzweig, *Clonal selection in the germinal centre by regulated proliferation and hypermutation.* Nature, 2014. **509**(7502): p. 637-40.
25. Berek, C., A. Berger, and M.J.C. Apel, *Maturation of the immune response in germinal centers.* 1991. **67**(6): p. 1121-1129.
26. Hogquist, K.A., T.A. Baldwin, and S.C. Jameson, *Central tolerance: learning self-control in the thymus.* Nature Reviews Immunology, 2005. **5**(10): p. 772-782.
27. Mueller, D.L., *Mechanisms maintaining peripheral tolerance.* Nat Immunol, 2010. **11**(1): p. 21-7.
28. Marrack, P. and J. Kappler, *Control of T cell viability.* Annu Rev Immunol, 2004. **22**: p. 765-87.
29. ElTanbouly, M.A. and R.J. Noelle, *Rethinking peripheral T cell tolerance: checkpoints across a T cell's journey.* Nat Rev Immunol, 2021. **21**(4): p. 257-267.
30. Apostolou , I. and H. von Boehmer *In Vivo Instruction of Suppressor Commitment in Naive T Cells.* Journal of Experimental Medicine, 2004. **199**(10): p. 1401-1408.
31. Chen, W., et al., *Conversion of Peripheral CD4⁺CD25[−] Naive T Cells to CD4⁺CD25⁺ Regulatory T Cells by TGF-β Induction of Transcription Factor Foxp3.* The Journal of Experimental Medicine, 2003. **198**(12): p. 1875-1886.
32. Azukizawa, H., et al., *Steady state migratory RelB+ langerin+ dermal dendritic cells mediate peripheral induction of antigen-specific CD4+ CD25+ Foxp3+ regulatory T cells.* Eur J Immunol, 2011. **41**(5): p. 1420-34.
33. Walunas, T.L., et al., *CTLA-4 can function as a negative regulator of T cell activation.* Immunity, 1994. **1**(5): p. 405-13.
34. Freeman, G.J., et al., *Engagement of the PD-1 immunoinhibitory receptor by a novel B7 family member leads to negative regulation of lymphocyte activation.* J Exp Med, 2000. **192**(7): p. 1027-34.
35. Vieira, P.L., et al., *IL-10-secreting regulatory T cells do not express Foxp3 but have comparable regulatory function to naturally occurring CD4+CD25+ regulatory T cells.* J Immunol, 2004. **172**(10): p. 5986-93.
36. Cottrez, F., et al., *T regulatory cells 1 inhibit a Th2-specific response in vivo.* J Immunol, 2000. **165**(9): p. 4848-53.
37. Groux, H., et al., *A CD4+ T-cell subset inhibits antigen-specific T-cell responses and prevents colitis.* Nature, 1997. **389**(6652): p. 737-42.
38. Groux, H., *Type 1 T-regulatory cells: their role in the control of immune responses.* Transplantation, 2003. **75**(9 Suppl): p. 8s-12s.
39. Nemazee, D., *Mechanisms of central tolerance for B cells.* Nature Reviews Immunology, 2017. **17**(5): p. 281-294.
40. Fulcher, D.A. and A. Basten, *Reduced life span of anergic self-reactive B cells in a double-transgenic model.* Journal of Experimental Medicine, 1994. **179**(1): p. 125-134.

41. Cyster, J.G., S.B. Hartley, and C.C. Goodnow, *Competition for follicular niches excludes self-reactive cells from the recirculating B-cell repertoire.* Nature, 1994. **371**(6496): p. 389-395.
42. Brownlee, W.J., et al., *Diagnosis of multiple sclerosis: progress and challenges.* The Lancet, 2017. **389**(10076): p. 1336-1346.
43. Reich, D.S., et al., *Multiple Sclerosis.* New England Journal of Medicine, 2018. **378**(2): p. 169-180.
44. Metz, I., et al., *Pathologic heterogeneity persists in early active multiple sclerosis lesions.* 2014. **75**(5): p. 728-738.
45. Lassmann, H., W. Brück, and C. Lucchinetti, *Heterogeneity of multiple sclerosis pathogenesis: implications for diagnosis and therapy.* Trends Mol Med, 2001. **7**(3): p. 115-21.
46. Brex, P.A., et al., *A longitudinal study of abnormalities on MRI and disability from multiple sclerosis.* N Engl J Med, 2002. **346**(3): p. 158-64.
47. Kutzelnigg, A., et al., *Cortical demyelination and diffuse white matter injury in multiple sclerosis.* Brain, 2005. **128**(Pt 11): p. 2705-12.
48. Dyment, D.A., G.C. Ebers, and A.D.J.T.L.N. Sadovnick, *Genetics of multiple sclerosis.* 2004. **3**(2): p. 104-110.
49. Sawcer, S., P.N. Goodfellow, and A.J.T.i.G. Compston, *The genetic analysis of multiple sclerosis.* 1997. **13**(6): p. 234-239.
50. Cotsapas, C. and M. Mitrovic, *Genome-wide association studies of multiple sclerosis.* Clin Transl Immunology, 2018. **7**(6): p. e1018.
51. Jörg, S., et al., *Environmental factors in autoimmune diseases and their role in multiple sclerosis.* Cellular and Molecular Life Sciences, 2016. **73**(24): p. 4611-4622.
52. Chen, J., et al., *Multiple sclerosis patients have a distinct gut microbiota compared to healthy controls.* Scientific Reports, 2016. **6**(1): p. 28484.
53. Miyake, S., et al., *Dysbiosis in the Gut Microbiota of Patients with Multiple Sclerosis, with a Striking Depletion of Species Belonging to Clostridia XIVa and IV Clusters.* PLOS ONE, 2015. **10**(9): p. e0137429.
54. Cantarel, B.L., et al., *Gut microbiota in multiple sclerosis: possible influence of immunomodulators.* J Investig Med, 2015. **63**(5): p. 729-34.
55. Rivers, T.M. and F.F. Schwentker, *ENCEPHALOMYELITIS ACCOMPANIED BY MYELIN DESTRUCTION EXPERIMENTALLY PRODUCED IN MONKEYS.* The Journal of experimental medicine, 1935. **61**(5): p. 689-702.
56. Kabat, E.A., A. Wolf, and A.E. Bezer, *THE RAPID PRODUCTION OF ACUTE DISSEMINATED ENCEPHALOMYELITIS IN RHESUS MONKEYS BY INJECTION OF HETEROLOGOUS AND HOMOLOGOUS BRAIN TISSUE WITH ADJUVANTS.* J Exp Med, 1947. **85**(1): p. 117-30.
57. Johns, T.G. and C.C.A. Bernard, *The Structure and Function of Myelin Oligodendrocyte Glycoprotein.* Journal of Neurochemistry, 1999. **72**(1): p. 1-9.
58. Mendel, I., N. Kerlero de Rosbo, and A. Ben-Nun, *A myelin oligodendrocyte glycoprotein peptide induces typical chronic experimental autoimmune encephalomyelitis in H-2b mice: fine specificity and T cell receptor V beta expression of encephalitogenic T cells.* Eur J Immunol, 1995. **25**(7): p. 1951-9.
59. Tuohy, V.K., et al., *Identification of an encephalitogenic determinant of myelin proteolipid protein for SJL mice.* J Immunol, 1989. **142**(5): p. 1523-7.

60. Hemmer, B., J.J. Archelos, and H.-P. Hartung, *New concepts in the immunopathogenesis of multiple sclerosis.* Nature Reviews Neuroscience, 2002. **3**(4): p. 291-301.
61. Paterson , P.Y., *TRANSFER OF ALLERGIC ENCEPHALOMYELITIS IN RATS BY MEANS OF LYMPH NODE CELLS.* Journal of Experimental Medicine, 1960. **111**(1): p. 119-136.
62. Zamvil, S., et al., *T-cell clones specific for myelin basic protein induce chronic relapsing paralysis and demyelination.* Nature, 1985. **317**(6035): p. 355-358.
63. Ben-Nun, A., H. Wekerle, and I.R. Cohen, *The rapid isolation of clonable antigen-specific T lymphocyte lines capable of mediating autoimmune encephalomyelitis.* European Journal of Immunology, 1981. **11**(3): p. 195-199.
64. Bettelli, E., et al., *Myelin oligodendrocyte glycoprotein-specific T cell receptor transgenic mice develop spontaneous autoimmune optic neuritis.* J Exp Med, 2003. **197**(9): p. 1073-81.
65. Hjelmström, P., et al., *Cutting Edge: B Cell-Deficient Mice Develop Experimental Allergic Encephalomyelitis with Demyelination After Myelin Oligodendrocyte Glycoprotein Sensitization.* The Journal of Immunology, 1998. **161**(9): p. 4480-4483.
66. Lyons, J.A., et al., *B cells are critical to induction of experimental allergic encephalomyelitis by protein but not by a short encephalitogenic peptide.* Eur J Immunol, 1999. **29**(11): p. 3432-9.
67. Lyons, J.A., M.J. Ramsbottom, and A.H. Cross, *Critical role of antigen-specific antibody in experimental autoimmune encephalomyelitis induced by recombinant myelin oligodendrocyte glycoprotein.* Eur J Immunol, 2002. **32**(7): p. 1905-13.
68. Litzenburger, T., et al., *B lymphocytes producing demyelinating autoantibodies: development and function in gene-targeted transgenic mice.* J Exp Med, 1998. **188**(1): p. 169-80.
69. Bettelli, E., et al., *Myelin oligodendrocyte glycoprotein-specific T and B cells cooperate to induce a Devic-like disease in mice.* J Clin Invest, 2006. **116**(9): p. 2393-402.
70. Krishnamoorthy, G., et al., *Spontaneous opticospinal encephalomyelitis in a double-transgenic mouse model of autoimmune T cell/B cell cooperation.* J Clin Invest, 2006. **116**(9): p. 2385-92.
71. Pöllinger, B., et al., *Spontaneous relapsing-remitting EAE in the SJL/J mouse: MOG-reactive transgenic T cells recruit endogenous MOG-specific B cells.* The Journal of Experimental Medicine, 2009. **206**(6): p. 1303-1316.
72. Mosmann, T.R., et al., *Two types of murine helper T cell clone. I. Definition according to profiles of lymphokine activities and secreted proteins.* J Immunol, 1986. **136**(7): p. 2348-57.
73. Abbas, A.K., K.M. Murphy, and A. Sher, *Functional diversity of helper T lymphocytes.* Nature, 1996. **383**(6603): p. 787-93.
74. Sriram, S., et al., *Identification of T cell subsets and B lymphocytes in mouse brain experimental allergic encephalitis lesions.* J Immunol, 1982. **129**(4): p. 1649-51.
75. Ando, D.G., et al., *Encephalitogenic T cells in the B10.PL model of experimental allergic encephalomyelitis (EAE) are of the Th-1 lymphokine subtype.* Cell Immunol, 1989. **124**(1): p. 132-43.

76. Bettelli, E., et al., *Loss of T-bet, but not STAT1, prevents the development of experimental autoimmune encephalomyelitis.* J Exp Med, 2004. **200**(1): p. 79-87.
77. Traugott, U. and P. Lebon, *Interferon-gamma and Ia antigen are present on astrocytes in active chronic multiple sclerosis lesions.* J Neurol Sci, 1988. **84**(2-3): p. 257-64.
78. Panitch, H.S., et al., *Exacerbations of multiple sclerosis in patients treated with gamma interferon.* Lancet, 1987. **1**(8538): p. 893-5.
79. Comabella, M., et al., *Elevated interleukin-12 in progressive multiple sclerosis correlates with disease activity and is normalized by pulse cyclophosphamide therapy.* J Clin Invest, 1998. **102**(4): p. 671-8.
80. Becher, B., B.G. Durell, and R.J. Noelle, *Experimental autoimmune encephalitis and inflammation in the absence of interleukin-12.* J Clin Invest, 2002. **110**(4): p. 493-7.
81. Oppmann, B., et al., *Novel p19 protein engages IL-12p40 to form a cytokine, IL-23, with biological activities similar as well as distinct from IL-12.* Immunity, 2000. **13**(5): p. 715-25.
82. Cua, D.J., et al., *Interleukin-23 rather than interleukin-12 is the critical cytokine for autoimmune inflammation of the brain.* Nature, 2003. **421**(6924): p. 744-8.
83. Langrish, C.L., et al., *IL-23 drives a pathogenic T cell population that induces autoimmune inflammation.* J Exp Med, 2005. **201**(2): p. 233-40.
84. Bettelli, E., et al., *Reciprocal developmental pathways for the generation of pathogenic effector TH17 and regulatory T cells.* Nature, 2006. **441**(7090): p. 235-8.
85. Veldhoen, M., et al., *TGFbeta in the context of an inflammatory cytokine milieu supports de novo differentiation of IL-17-producing T cells.* Immunity, 2006. **24**(2): p. 179-89.
86. Mangan, P.R., et al., *Transforming growth factor-beta induces development of the T(H)17 lineage.* Nature, 2006. **441**(7090): p. 231-4.
87. Parham, C., et al., *A Receptor for the Heterodimeric Cytokine IL-23 Is Composed of IL-12Rβ1 and a Novel Cytokine Receptor Subunit, IL-23R.* 2002. **168**(11): p. 5699-5708.
88. Vaknin-Dembinsky, A., K. Balashov, and H.L. Weiner, *IL-23 is increased in dendritic cells in multiple sclerosis and down-regulation of IL-23 by antisense oligos increases dendritic cell IL-10 production.* J Immunol, 2006. **176**(12): p. 7768-74.
89. Matusevicius, D., et al., *Interleukin-17 mRNA expression in blood and CSF mononuclear cells is augmented in multiple sclerosis.* Mult Scler, 1999. **5**(2): p. 101-4.
90. Ishigame, H., et al., *Differential roles of interleukin-17A and -17F in host defense against mucoepithelial bacterial infection and allergic responses.* Immunity, 2009. **30**(1): p. 108-19.
91. Hofstetter, H.H., et al., *Therapeutic efficacy of IL-17 neutralization in murine experimental autoimmune encephalomyelitis.* Cellular Immunology, 2005. **237**(2): p. 123-130.
92. Jager, A., et al., *Th1, Th17, and Th9 effector cells induce experimental autoimmune encephalomyelitis with different pathological phenotypes.* J Immunol, 2009. **183**(11): p. 7169-77.

93. Housley, W.J., D. Pitt, and D.A. Hafler, *Biomarkers in multiple sclerosis.* Clin Immunol, 2015. **161**(1): p. 51-8.
94. Brandle, S.M., et al., *Distinct oligoclonal band antibodies in multiple sclerosis recognize ubiquitous self-proteins.* Proc Natl Acad Sci U S A, 2016. **113**(28): p. 7864-9.
95. Berger, T., et al., *Antimyelin antibodies as a predictor of clinically definite multiple sclerosis after a first demyelinating event.* N Engl J Med, 2003. **349**(2): p. 139-45.
96. Reindl, M., et al., *Antibodies against the myelin oligodendrocyte glycoprotein and the myelin basic protein in multiple sclerosis and other neurological diseases: a comparative study.* Brain, 1999. **122 (Pt 11)**: p. 2047-56.
97. Kuhle, J., et al., *Lack of association between antimyelin antibodies and progression to multiple sclerosis.* N Engl J Med, 2007. **356**(4): p. 371-8.
98. Keegan, M., et al., *Relation between humoral pathological changes in multiple sclerosis and response to therapeutic plasma exchange.* Lancet, 2005. **366**(9485): p. 579-82.
99. Lucchinetti, C., et al., *Heterogeneity of multiple sclerosis lesions: implications for the pathogenesis of demyelination.* Ann Neurol, 2000. **47**(6): p. 707-17.
100. Magliozzi, R., et al., *Meningeal B-cell follicles in secondary progressive multiple sclerosis associate with early onset of disease and severe cortical pathology.* Brain, 2007. **130**(Pt 4): p. 1089-104.
101. Peters, A., et al., *Th17 cells induce ectopic lymphoid follicles in central nervous system tissue inflammation.* Immunity, 2011. **35**(6): p. 986-96.
102. Serafini, B., et al., *Detection of ectopic B-cell follicles with germinal centers in the meninges of patients with secondary progressive multiple sclerosis.* Brain Pathol, 2004. **14**(2): p. 164-74.
103. Gelfand, J.M., B.A.C. Cree, and S.L. Hauser, *Ocrelizumab and Other CD20(+) B-Cell-Depleting Therapies in Multiple Sclerosis.* Neurotherapeutics, 2017. **14**(4): p. 835-841.
104. Lanzavecchia, A., *Antigen-specific interaction between T and B cells.* Nature, 1985. **314**(6011): p. 537-9.
105. Parker Harp, C.R., et al., *B cell antigen presentation is sufficient to drive neuroinflammation in an animal model of multiple sclerosis.* J Immunol, 2015. **194**(11): p. 5077-84.
106. Molnarfi, N., et al., *MHC class II–dependent B cell APC function is required for induction of CNS autoimmunity independent of myelin-specific antibodies.* The Journal of Experimental Medicine, 2013. **210**(13): p. 2921-2937.
107. Bar-Or, A., et al., *Abnormal B-cell cytokine responses a trigger of T-cell-mediated disease in MS?* Ann Neurol, 2010. **67**(4): p. 452-61.
108. Guerrier, T., et al., *Proinflammatory B-cell profile in the early phases of MS predicts an active disease.* Neurol Neuroimmunol Neuroinflamm, 2018. **5**(2): p. e431.
109. Duddy, M., et al., *Distinct Effector Cytokine Profiles of Memory and Naive Human B Cell Subsets and Implication in Multiple Sclerosis.* The Journal of Immunology, 2007. **178**(10): p. 6092-6099.
110. Barr, T.A., et al., *B cell depletion therapy ameliorates autoimmune disease through ablation of IL-6-producing B cells.* J Exp Med, 2012. **209**(5): p. 1001-10.

111. Harris, D.P., et al., *Regulation of IFN-gamma production by B effector 1 cells: essential roles for T-bet and the IFN-gamma receptor.* J Immunol, 2005. **174**(11): p. 6781-90.
112. Olalekan, S.A., et al., *B cells expressing IFN-gamma suppress Treg-cell differentiation and promote autoimmune experimental arthritis.* Eur J Immunol, 2015. **45**(4): p. 988-98.
113. Li, R., et al., *Proinflammatory GM-CSF-producing B cells in multiple sclerosis and B cell depletion therapy.* Sci Transl Med, 2015. **7**(310): p. 310ra166.
114. Fillatreau, S., et al., *B cells regulate autoimmunity by provision of IL-10.* Nat Immunol, 2002. **3**(10): p. 944-50.
115. Shen, P., et al., *IL-35-producing B cells are critical regulators of immunity during autoimmune and infectious diseases.* Nature, 2014. **507**(7492): p. 366-370.
116. Bjarnadottir, K., et al., *B cell-derived transforming growth factor-beta1 expression limits the induction phase of autoimmune neuroinflammation.* Sci Rep, 2016. **6**: p. 34594.
117. Duddy, M.E., A. Alter, and A. Bar-Or, *Distinct Profiles of Human B Cell Effector Cytokines: A Role in Immune Regulation?* 2004. **172**(6): p. 3422-3427.
118. du Plessis, W.J., et al., *The Functional Response of B Cells to Antigenic Stimulation: A Preliminary Report of Latent Tuberculosis.* PLOS ONE, 2016. **11**(4): p. e0152710.
119. Harris, D.P., et al., *Reciprocal regulation of polarized cytokine production by effector B and T cells.* Nat Immunol, 2000. **1**(6): p. 475-82.
120. Li, R., et al., *Cytokine-Defined B Cell Responses as Therapeutic Targets in Multiple Sclerosis.* Frontiers in Immunology, 2016. **6**(626).
121. Kobayashi, M., et al., *Identification and purification of natural killer cell stimulatory factor (NKSF), a cytokine with multiple biologic effects on human lymphocytes.* J Exp Med, 1989. **170**(3): p. 827-45.
122. Pflanz, S., et al., *IL-27, a heterodimeric cytokine composed of EBI3 and p28 protein, induces proliferation of naive CD4+ T cells.* Immunity, 2002. **16**(6): p. 779-90.
123. Awasthi, A., et al., *A dominant function for interleukin 27 in generating interleukin 10-producing anti-inflammatory T cells.* Nat Immunol, 2007. **8**(12): p. 1380-9.
124. Pot, C., et al., *Cutting edge: IL-27 induces the transcription factor c-Maf, cytokine IL-21, and the costimulatory receptor ICOS that coordinately act together to promote differentiation of IL-10-producing Tr1 cells.* J Immunol, 2009. **183**(2): p. 797-801.
125. Fitzgerald, D.C., et al., *Suppression of autoimmune inflammation of the central nervous system by interleukin 10 secreted by interleukin 27-stimulated T cells.* Nat Immunol, 2007. **8**(12): p. 1372-9.
126. Chong, W.P., et al., *IL-27p28 inhibits central nervous system autoimmunity by concurrently antagonizing Th1 and Th17 responses.* J Autoimmun, 2014. **50**: p. 12-22.
127. Diveu, C., et al., *IL-27 blocks RORc expression to inhibit lineage commitment of Th17 cells.* J Immunol, 2009. **182**(9): p. 5748-56.
128. Niedbala, W., et al., *IL-35 is a novel cytokine with therapeutic effects against collagen-induced arthritis through the expansion of regulatory T cells and suppression of Th17 cells.* Eur J Immunol, 2007. **37**(11): p. 3021-9.

129. Collison, L.W., et al., *The inhibitory cytokine IL-35 contributes to regulatory T-cell function.* Nature, 2007. **450**: p. 566.
130. Collison, L.W., et al., *IL-35-mediated induction of a potent regulatory T cell population.* Nat Immunol, 2010. **11**(12): p. 1093-101.
131. Wei, X.Q., et al., *The Role of the IL-12 Cytokine Family in Directing T-Cell Responses in Oral Candidosis.* Clin Dev Immunol, 2011. **2011**.
132. Wang, X., et al., *A novel IL-23p19/Ebi3 (IL-39) cytokine mediates inflammation in Lupus-like mice.* Eur J Immunol, 2016. **46**(6): p. 1343-50.
133. Wang, X., et al., *Interleukin (IL)-39 [IL-23p19/Epstein-Barr virus-induced 3 (Ebi3)] induces differentiation/expansion of neutrophils in lupus-prone mice.* Clin Exp Immunol, 2016. **186**(2): p. 144-156.
134. Espígol-Frigolé, G., et al., *Identification of IL-23p19 as an endothelial proinflammatory peptide that promotes gp130-STAT3 signaling.* Science Signaling, 2016. **9**(419): p. ra28-ra28.
135. Shen, F.W., et al., *Cloning of Ly-5 cDNA.* Proc Natl Acad Sci U S A, 1985. **82**(21): p. 7360-3.
136. Mombaerts, P., et al., *RAG-1-deficient mice have no mature B and T lymphocytes.* Cell, 1992. **68**(5): p. 869-77.
137. Platt, R.J., et al., *CRISPR-Cas9 knockin mice for genome editing and cancer modeling.* Cell, 2014. **159**(2): p. 440-55.
138. Farley, F.W., et al., *Widespread recombinase expression using FLPeR (Flipper) mice.* 2000. **28**(3-4): p. 106-110.
139. Pettitt, S.J., et al., *Agouti C57BL/6N embryonic stem cells for mouse genetic resources.* Nat Methods, 2009. **6**(7): p. 493-5.
140. Nojima, T., et al., *In-vitro derived germinal centre B cells differentially generate memory B or plasma cells in vivo.* Nat Commun, 2011. **2**: p. 465.
141. Pear, W.S., et al., *Production of high-titer helper-free retroviruses by transient transfection.* 1993. **90**(18): p. 8392-8396.
142. Perera, N.C., et al., *NSP4 is stored in azurophil granules and released by activated neutrophils as active endoprotease with restricted specificity.* J Immunol, 2013. **191**(5): p. 2700-7.
143. Niedel, J.E., L.J. Kuhn, and G.R. Vandenbark, *Phorbol diester receptor copurifies with protein kinase C.* Proceedings of the National Academy of Sciences of the United States of America, 1983. **80**(1): p. 36-40.
144. Castagna, M., et al., *Direct activation of calcium-activated, phospholipid-dependent protein kinase by tumor-promoting phorbol esters.* Journal of Biological Chemistry, 1982. **257**(13): p. 7847-7851.
145. Toeplitz, B.K., et al., *Structure of ionomycin - a novel diacidic polyether antibiotic having high affinity for calcium ions.* Journal of the American Chemical Society, 1979. **101**(12): p. 3344-3353.
146. Griffiths, G., P. Quinn, and G. Warren, *Dissection of the Golgi complex. I. Monensin inhibits the transport of viral membrane proteins from medial to trans Golgi cisternae in baby hamster kidney cells infected with Semliki Forest virus.* The Journal of cell biology, 1983. **96**(3): p. 835-850.
147. Zhang, G.F., A. Driouich, and L.A. Staehelin, *Monensin-induced redistribution of enzymes and products from Golgi stacks to swollen vesicles in plant cells.* Eur J Cell Biol, 1996. **71**(4): p. 332-40.

148. Wei, G. and W. Hong, *Detection of LacZ expression by FACS-Gal analysis.* Protocol Exchange, 2021.
149. Matsushita, T., et al., *BAFF inhibition attenuates fibrosis in scleroderma by modulating the regulatory and effector B cell balance.* Sci Adv, 2018. **4**(7): p. eaas9944.
150. Schneider, P., et al., *BAFF, a novel ligand of the tumor necrosis factor family, stimulates B cell growth.* The Journal of experimental medicine, 1999. **189**(11): p. 1747-1756.
151. Matsumoto, M., et al., *Interleukin-10-Producing Plasmablasts Exert Regulatory Function in Autoimmune Inflammation.* Immunity, 2014. **41**(6): p. 1040-1051.
152. Nolan, G.P., et al., *Fluorescence-activated cell analysis and sorting of viable mammalian cells based on beta-D-galactosidase activity after transduction of Escherichia coli lacZ.* Proc Natl Acad Sci U S A, 1988. **85**(8): p. 2603-7.
153. Goodnow, C.C., et al., *Altered immunoglobulin expression and functional silencing of self-reactive B lymphocytes in transgenic mice.* Nature, 1988. **334**(6184): p. 676-82.
154. Phan, T.G., et al., *B Cell Receptor–independent Stimuli Trigger Immunoglobulin (Ig) Class Switch Recombination and Production of IgG Autoantibodies by Anergic Self-Reactive B Cells.* Journal of Experimental Medicine, 2003. **197**(7): p. 845-860.
155. Erikson, J., et al., *Expression of anti-DNA immunoglobulin transgenes in non-autoimmune mice.* Nature, 1991. **349**(6307): p. 331-4.
156. Wellmann, U., A. Werner, and T.H. Winkler, *Altered selection processes of B lymphocytes in autoimmune NZB/W mice, despite intact central tolerance against DNA.* Eur J Immunol, 2001. **31**(9): p. 2800-10.
157. Kenny, J.J., et al., *Autoreactive B cells escape clonal deletion by expressing multiple antigen receptors.* J Immunol, 2000. **164**(8): p. 4111-9.
158. Palm, A.-K.E., et al., *Function and regulation of self-reactive marginal zone B cells in autoimmune arthritis.* Cellular & Molecular Immunology, 2015. **12**(4): p. 493-504.
159. Carnrot, C., et al., *Marginal zone B cells are naturally reactive to collagen type II and are involved in the initiation of the immune response in collagen-induced arthritis.* Cellular & Molecular Immunology, 2011. **8**(4): p. 296-304.
160. Wither, J.E., V. Roy, and L.A. Brennan, *Activated B Cells Express Increased Levels of Costimulatory Molecules in Young Autoimmune NZB and (NZB × NZW)F1 Mice.* Clinical Immunology, 2000. **94**(1): p. 51-63.
161. Grimaldi, C.M., D.J. Michael, and B. Diamond, *Cutting Edge: Expansion and Activation of A Population of Autoreactive Marginal Zone B Cells in a Model of Estrogen-Induced Lupus.* 2001. **167**(4): p. 1886-1890.
162. Wither, J.E., et al., *Colocalization of Expansion of the Splenic Marginal Zone Population with Abnormal B Cell Activation and Autoantibody Production in B6 Mice with an Introgressed New Zealand Black Chromosome 13 Interval.* 2005. **175**(7): p. 4309-4319.
163. Mariño, E., et al., *Marginal-Zone B-Cells of Nonobese Diabetic Mice Expand With Diabetes Onset, Invade the Pancreatic Lymph Nodes, and Present Autoantigen to Diabetogenic T-Cells.* 2008. **57**(2): p. 395-404.
164. Rolf, J., et al., *The Enlarged Population of Marginal Zone/CD1d^{high} B Lymphocytes in Nonobese Diabetic Mice Maps to Diabetes Susceptibility Region Idd11.* 2005. **174**(8): p. 4821-4827.

165. Daridon, C., et al., *Identification of transitional type II B cells in the salivary glands of patients with Sjögren's syndrome.* 2006. **54**(7): p. 2280-2288.
166. Segundo, C., et al., *Thyroid-Infiltrating B Lymphocytes in Graves' Disease are Related to Marginal Zone and Memory B Cell Compartments.* Thyroid, 2001. **11**(6): p. 525-530.
167. Oliver, A.M., F. Martin, and J.F. Kearney, *IgMhighCD21high lymphocytes enriched in the splenic marginal zone generate effector cells more rapidly than the bulk of follicular B cells.* J Immunol, 1999. **162**(12): p. 7198-207.
168. Zhou, Z., et al. *Autoreactive marginal zone B cells enter the follicles and interact with CD4+ T cells in lupus-prone mice*. BMC immunology, 2011. **12**, 7 DOI: 10.1186/1471-2172-12-7.
169. Palm, A.-K.E., H.C. Friedrich, and S. Kleinau, *Nodal marginal zone B cells in mice: a novel subset with dormant self-reactivity.* Scientific Reports, 2016. **6**: p. 27687.
170. Singh, N., et al., *Dysregulated Marginal Zone B Cell Compartment in a Mouse Model of Sjögren's Syndrome with Ocular Inflammation.* International Journal of Molecular Sciences, 2018. **19**(10).
171. Martin, F. and J.F. Kearney, *Marginal-zone B cells.* Nat Rev Immunol, 2002. **2**(5): p. 323-35.
172. Kinzel, S., et al., *Myelin-reactive antibodies initiate T cell-mediated CNS autoimmune disease by opsonization of endogenous antigen.* Acta Neuropathol, 2016. **132**(1): p. 43-58.
173. Flach, A.C., et al., *Autoantibody-boosted T-cell reactivation in the target organ triggers manifestation of autoimmune CNS disease.* Proc Natl Acad Sci U S A, 2016. **113**(12): p. 3323-8.
174. Shapiro-Shelef, M., et al., *Blimp-1 is required for the formation of immunoglobulin secreting plasma cells and pre-plasma memory B cells.* Immunity, 2003. **19**(4): p. 607-20.
175. Suematsu, S., et al., *IgG1 plasmacytosis in interleukin 6 transgenic mice.* 1989. **86**(19): p. 7547-7551.
176. Fattori, E., et al., *Development of Progressive Kidney Damage and Myeloma Kidney in Interleukin-6 Transgenic Mice.* Blood, 1994. **83**(9): p. 2570-2579.
177. Mufazalov, I.A., et al., *Cutting Edge: IL-6-Driven Immune Dysregulation Is Strictly Dependent on IL-6R alpha-Chain Expression.* J Immunol, 2020.
178. Heinrich, P.C., J.V. Castell, and T. Andus, *Interleukin-6 and the acute phase response.* Biochem J, 1990. **265**(3): p. 621-36.
179. Ishibashi, T., et al., *Interleukin-6 is a potent thrombopoietic factor in vivo in mice.* Blood, 1989. **74**(4): p. 1241-1244.
180. Nakahara, H., et al., *Anti-interleukin-6 receptor antibody therapy reduces vascular endothelial growth factor production in rheumatoid arthritis.* Arthritis and rheumatism, 2003. **48**(6): p. 1521-1529.
181. Hashizume, M., et al., *IL-6/sIL-6R trans-signalling, but not TNF-alpha induced angiogenesis in a HUVEC and synovial cell co-culture system.* Rheumatol Int, 2009. **29**(12): p. 1449-54.
182. Okada, M., et al., *IL-6/BSF-2 functions as a killer helper factor in the in vitro induction of cytotoxic T cells.* J Immunol, 1988. **141**(5): p. 1543-9.
183. Chomarat, P., et al., *IL-6 switches the differentiation of monocytes from dendritic cells to macrophages.* Nat Immunol, 2000. **1**(6): p. 510-4.

184. Tanaka, T., A. Ogata, and M. Narazaki, *Tocilizumab: An Updated Review of Its Use in the Treatment of Rheumatoid Arthritis and Its Application for Other Immune-Mediated Diseases.* Clinical Medicine Insights: Therapeutics, 2013. **5**: p. CMT.S9282.
185. Zhang, C., et al., *Safety and efficacy of tocilizumab versus azathioprine in highly relapsing neuromyelitis optica spectrum disorder (TANGO): an open-label, multicentre, randomised, phase 2 trial.* Lancet Neurol, 2020. **19**(5): p. 391-401.
186. Beauchemin, P. and R. Carruthers, *MS arising during Tocilizumab therapy for rheumatoid arthritis.* Mult Scler, 2016. **22**(2): p. 254-6.
187. Zheng, Z., et al., *IL-6 Promotes the Proliferation and Immunosuppressive Function of Myeloid-Derived Suppressor Cells via the MAPK Signaling Pathway in Bladder Cancer.* Biomed Res Int, 2021. **2021**: p. 5535578.
188. Cheng, L., et al., *Interleukin-6 Induces Gr-1+CD11b+ Myeloid Cells to Suppress CD8+ T Cell-Mediated Liver Injury in Mice.* PLOS ONE, 2011. **6**(3): p. e17631.
189. Tobin, R.P., et al., *IL-6 and IL-8 Are Linked With Myeloid-Derived Suppressor Cell Accumulation and Correlate With Poor Clinical Outcomes in Melanoma Patients.* Front Oncol, 2019. **9**: p. 1223.
190. März, P., et al., *Role of interleukin-6 and soluble IL-6 receptor in region-specific induction of astrocytic differentiation and neurotrophin expression.* Glia, 1999. **26**(3): p. 191-200.
191. Schönrock, L.M., G. Gawlowski, and W. Brück, *Interleukin-6 expression in human multiple sclerosis lesions.* Neuroscience Letters, 2000. **294**(1): p. 45-48.
192. Guery, J.C., et al., *Normal B cells fail to secrete interleukin-12.* Eur J Immunol, 1997. **27**(7): p. 1632-9.
193. Stumhofer, J.S., et al., *A role for IL-27p28 as an antagonist of gp130-mediated signaling.* 2010. **11**: p. 1119.
194. Mondal, S., et al., *IL-12 p40 monomer is different from other IL-12 family members to selectively inhibit IL-12Rβ1 internalization and suppress EAE.* Proc Natl Acad Sci U S A, 2020.
195. Cooper, A.M. and S.A. Khader, *IL-12p40: an inherently agonistic cytokine.* Trends Immunol, 2007. **28**(1): p. 33-8.
196. Khader, S.A., et al., *Interleukin 12p40 is required for dendritic cell migration and T cell priming after Mycobacterium tuberculosis infection.* J Exp Med, 2006. **203**(7): p. 1805-15.
197. Gately, M.K., et al., *Interleukin-12 antagonist activity of mouse interleukin-12 p40 homodimer in vitro and in vivo.* Ann N Y Acad Sci, 1996. **795**: p. 1-12.
198. Jinek, M., et al., *A Programmable Dual-RNA–Guided DNA Endonuclease in Adaptive Bacterial Immunity.* 2012. **337**(6096): p. 816-821.
199. Gasiunas, G., et al., *Cas9–crRNA ribonucleoprotein complex mediates specific DNA cleavage for adaptive immunity in bacteria.* 2012. **109**(39): p. E2579-E2586.
200. Reali, C., et al., *B cell rich meningeal inflammation associates with increased spinal cord pathology in multiple sclerosis.* Brain Pathol, 2020. **30**(4): p. 779-793.
201. Lucchinetti, C.F., et al., *Inflammatory cortical demyelination in early multiple sclerosis.* N Engl J Med, 2011. **365**(23): p. 2188-97.
202. Howell, O.W., et al., *Extensive grey matter pathology in the cerebellum in multiple sclerosis is linked to inflammation in the subarachnoid space.* Neuropathol Appl Neurobiol, 2015. **41**(6): p. 798-813.

203. Rojas, O.L., et al., *Recirculating Intestinal IgA-Producing Cells Regulate Neuroinflammation via IL-10.* Cell, 2019.
204. Mitsdörffer, M., et al., *Formation and immunomodulatory function of meningeal B-cell aggregates in progressive CNS autoimmunity.* Brain, 2021.
205. Shalapour, S., et al., *Immunosuppressive plasma cells impede T-cell-dependent immunogenic chemotherapy.* Nature, 2015. **521**(7550): p. 94-98.
206. Shalapour, S., et al., *Inflammation-induced IgA+ cells dismantle anti-liver cancer immunity.* Nature, 2017. **551**(7680): p. 340-345.
207. Lino, A.C., et al., *LAG-3 Inhibitory Receptor Expression Identifies Immunosuppressive Natural Regulatory Plasma Cells.* Immunity, 2018. **49**(1): p. 120-133.e9.
208. Sørensen, T.L., et al., *Multiple sclerosis: a study of CXCL10 and CXCR3 co-localization in the inflamed central nervous system.* J Neuroimmunol, 2002. **127**(1-2): p. 59-68.
209. Carter, S.L., et al., *Induction of the genes for Cxcl9 and Cxcl10 is dependent on IFN-gamma but shows differential cellular expression in experimental autoimmune encephalomyelitis and by astrocytes and microglia in vitro.* Glia, 2007. **55**(16): p. 1728-39.
210. Muehlinghaus, G., et al., *Regulation of CXCR3 and CXCR4 expression during terminal differentiation of memory B cells into plasma cells.* Blood, 2005. **105**(10): p. 3965-3971.
211. Narumi, S., et al., *Neutralization of IFN-inducible protein 10/CXCL10 exacerbates experimental autoimmune encephalomyelitis.* Eur J Immunol, 2002. **32**(6): p. 1784-91.
212. Klein, R.S., et al., *IFN-inducible protein 10/CXC chemokine ligand 10-independent induction of experimental autoimmune encephalomyelitis.* J Immunol, 2004. **172**(1): p. 550-9.
213. Patel, J.R., et al., *Astrocyte TNFR2 is required for CXCL12-mediated regulation of oligodendrocyte progenitor proliferation and differentiation within the adult CNS.* Acta Neuropathologica, 2012. **124**(6): p. 847-860.
214. Calderon, T.M., et al., *A role for CXCL12 (SDF-1alpha) in the pathogenesis of multiple sclerosis: regulation of CXCL12 expression in astrocytes by soluble myelin basic protein.* J Neuroimmunol, 2006. **177**(1-2): p. 27-39.
215. Hartung, H.P. and B.C. Kieseier, *Atacicept: targeting B cells in multiple sclerosis.* Ther Adv Neurol Disord, 2010. **3**(4): p. 205-16.
216. Qureshi, S.A.J.B., *Beta-lactamase: an ideal reporter system for monitoring gene expression in live eukaryotic cells.* 2007. **42 1**: p. 91-6.
217. Calado, D.P., et al., *Stochastic monoallelic expression of IL-10 in T cells.* Journal of immunology (Baltimore, Md. : 1950), 2006. **177**(8): p. 5358-5364.
218. Rivière, I., M.J. Sunshine, and D.R. Littman, *Regulation of IL-4 expression by activation of individual alleles.* Immunity, 1998. **9**(2): p. 217-28.
219. Holländer, G.A., et al., *Monoallelic expression of the interleukin-2 locus.* Science (New York, N.Y.), 1998. **279**(5359): p. 2118-2121.
220. Gonda, D.K., et al., *Universality and structure of the N-end rule.* The Journal of biological chemistry, 1989. **264**(28): p. 16700-16712.
221. Thakker, P., et al., *IL-23 is critical in the induction but not in the effector phase of experimental autoimmune encephalomyelitis.* J Immunol, 2007. **178**(4): p. 2589-98.

222. Hasegawa, H., et al., *IL-23p19 and CD5 antigen-like form a possible novel heterodimeric cytokine and contribute to experimental autoimmune encephalomyelitis development.* Sci Rep, 2021. **11**(1): p. 5266.
223. Berer, K., et al., *Commensal microbiota and myelin autoantigen cooperate to trigger autoimmune demyelination.* Nature, 2011. **479**(7374): p. 538-41.
224. Lee, Y.K., et al., *Proinflammatory T-cell responses to gut microbiota promote experimental autoimmune encephalomyelitis.* Proc Natl Acad Sci U S A, 2011. **108 Suppl 1**(Suppl 1): p. 4615-22.
225. Lee, E., et al., *Increased expression of interleukin 23 p19 and p40 in lesional skin of patients with psoriasis vulgaris.* The Journal of experimental medicine, 2004. **199**(1): p. 125-130.
226. Kinnebrew, M.A., et al., *Interleukin 23 production by intestinal CD103(+)CD11b(+) dendritic cells in response to bacterial flagellin enhances mucosal innate immune defense.* Immunity, 2012. **36**(2): p. 276-87.
227. Yona, S., et al., *Fate mapping reveals origins and dynamics of monocytes and tissue macrophages under homeostasis.* Immunity, 2013. **38**(1): p. 79-91.
228. O'Koren, E.G., R. Mathew, and D.R. Saban, *Fate mapping reveals that microglia and recruited monocyte-derived macrophages are definitively distinguishable by phenotype in the retina.* Sci Rep, 2016. **6**: p. 20636.

Affidavit

Eidesstattliche Versicherung

Thomann, Anna Sophie

Name, Vorname

Ich erkläre hiermit an Eides statt,

dass ich die vorliegende Dissertation mit dem Titel

The Role of Cytokine-producing B cells in Initiation and Regulation of EAE

selbständig verfasst, mich außer der angegebenen keiner weiteren Hilfsmittel bedient und alle Erkenntnisse, die aus dem Schrifttum ganz oder annähernd übernommen sind, als solche kenntlich gemacht und nach ihrer Herkunft unter Bezeichnung der Fundstelle einzeln nachgewiesen habe.

Ich erkläre des Weiteren, dass die hier vorgelegte Dissertation nicht in gleicher oder in ähnlicher Form bei einer anderen Stelle zur Erlangung eines akademischen Grades eingereicht wurde.

München, 01.06.2022

Ort, Datum

Anna Sophie Thomann

Unterschrift Doktorandin bzw. Doktorand